NEUROANATOMICAL LIMBIC CONNECTIONS OF THE LOCUS COERULEUS IN THE NONHUMAN PRIMATE

Dissertation

zur Erlangung des Grades eines

Doktors der Naturwissenschaften

der Mathematisch-Naturwissenschaftlichen Fakultät

und

der Medizinischen Fakultät

der Eberhard-Karls-Universität Tübingen

vorgelegt

von

María del Mar Ubero Martínez

aus Alicante, Spain

2016

Tag der mündlichen Prüfung: 04. 02. 2016

Dekan der Math.-Nat. Fakultät: Prof. Dr. W. Rosenstiel

Dekan der Medizinischen Fakultät: Prof. Dr. I. B. Autenrieth

1. Berichterstatter: Prof. Dr. Uwe Ilg

2. Berichterstatter: Prof. Dr. Ricardo Insausti

Prüfungskommission: Prof. Dr. Uwe Ilg

Prof. Dr. Ricardo Insausti

Dr. Henry Evrard

Prof. Dr. Mónica Muñoz

I hereby declare that I have produced the work entitled "Neuroanatomical Limbic Connections Of The Locus Coeruleus In The Nonhuman Primate", submitted for the award of a doctorate, on my own (without external help), have used only the sources and aids indicated and have marked passages included from other works, whether verbatim or in content, as such. I swear upon oath that these statements are true and that I have not concealed anything. I am aware that making a false declaration under oath is punishable by a term of imprisonment of up to three years or by a fine.

Tübingen, den ....

Datum / Date Unterschrift /Signature

The present dissertation has been accomplished under a framework of joint-supervision between the University of Tübingen/Max Planck Insitute (Tübingen, Germany) and the University of Castilla-La Mancha (Albacete, Spain).

EBERHARD KARLS
UNIVERSITÄT
TÜBINGEN

UCLM
UNIVERSIDAD DE CASTILLA-LA MANCHA

Tübingen, ..., 2015

Rector of the University of Castilla-La Mancha
.....
Prof. Dr. Miguel Ángel Collado Yurrita

Rector of the University of Tübingen
.....
Prof. Dr. Bernd Engler

Chairman of the doctorate
University of Castilla-La Mancha
.....
Prof. Dr. José María Ruiz Moreno

Chairman of the doctorate
University of Tübingen
.....
Prof. Dr. Matthias Bethge

Thesis supervisor
University of Castilla-La Mancha
.....
Prof. Dr. Ricardo Insausti Serrano

Thesis supervisor
University of Tübingen
.....
Prof. Dr. Uwe Ilg

Thesis supervisor
Max Planck Institute /
Centre for Integrative Neuroscience
Werner Reichardt
.....
Dr. Henry Evrard

Doctoral Student
.....
Ms. María del Mar Ubero Martínez

ACKNOWLEDGEMENT

Life is a journey created with many steps and decisions. We live by taking one step at a time, but we only get the sense of the kind of life that we are leading, through those moments stored into the long-term memory; our memories, our life. At this point, it is nice to look backwards in time and see how this adventure started and remember all the people who were part of it. I would like to express my gratitude to all of those who accompanied me along this journey.

This journey started thanks to Ricardo Insausti who gave me the opportunity to get into this fascinating world of Neuroscience and has supported me throughout the whole process. Muchas gracias de corazón Ricardo, por tu confianza y apoyo siempre, por enseñarme tanto y por abrirme la puerta a uno de mis sueños. Thanks to Nikos Logothetis for the magnificent opportunity to work in his group and for his continuous support to my work. Thanks to Henry Evrard for guiding me through these years of challenging situations, and for your constant support. I also would like to thank Uwe Ilg for his kind advice on my work; to Tina Lampe, and Horst Herbert for all the energy and time invested in making the CoTutelle agreement to work. I would like to give a sincere acknowledgement to Prof. J. Price and Prof. D. Amaral for kindly opening their door in the lab for me to study their valuable and treasured collection of cases. Without their kind help, this work could not have been accomplished.

Along this path, I found colleagues who became friends, and friends who became family. Some of these friends made the journey worth living and gave me reasons to keep stepping everyday.

I would like to give my most sincere acknowledgement to the Human Neuroanatomy Lab at UCLM. Mercedes, thanks for your impeccable and precious work, for all your help, and for turning the difficult days into bright ones. Emilio, you are that kind heart that always encouraged me and kept my spirits up. Thanks to Mar Arroyo for your help and for making those shared working moments more enjoyable. Alicia, you guided my first scientific work and taught me to give my first steps as a scientist. Thanks for your help and your contagious enthusiasm. Pilar, thanks for sharing your knowledge so altruistically; your help meant a lot to me and was the boost to get successful results through the tough world of the immunohistochemistry. I would also like to thank Mónica, a mentor and a friend, for being my “Estrella Polar” and guiding me along this journey. Your passion and enthusiasm have inspired my work and have given me the motivation and the strength to keep going. You taught me to overcome the difficulties with the right values and attitude, and to change an experimental problem into a new challenge to be achieved. Thanks for your valuable and

continuous input on my work. A special acknowledgement goes to Richard Morris for his kind advice, and because through the very interesting conversations we have held, I found the motivation to keep going.

I feel very grateful to Mª Carmen Lourdy too; your help was fundamental to make the arduous process of the CoTutelle and Thesis submission a bit smoother and easier. Thanks for your thousand "¡Ánimo chicas!, ¡Ya queda menos!". Isidro Medina, thanks for your predisposition to help and for reminding me which are the important things in life; and Marisa Ramos for opening your heart to me from the very beginning, I appreciate your friendship and care. Thanks also to Paqui Cortés for your great work and help with the Scanner. Mª José, Joaquín, Sandra, Guille, Marta, Gonzalo, Carlos, Ester and Jesús, it was great to have you around. I shared "lab-moments" with some of you, and moments of "charging the batteries with a coffee under the sun" with others; all treasured to me.

Later on, I lived part of this journey in Tübingen, where I met great colleagues. Thanks to the whole Department of Physiology of Cognitive Processes at the Max Planck Institute, especially to the "Neuroanatomy Group", a very important support to me during the writing of this Thesis. Thanks to Jenny for being so supportive and helpful. I would also like to thank the animal caretakers, the workshop, TAs, ITs, research technicians and vets for their amazing work. Thanks Ricardo Neves for helping with the localization of LC electrophysiologically; to Catherine Perrodin for being the sunshine in those cloudy days; and to Conchy, for being a great support and a friend. I would like to make a special mention to Diana, friend and "compañera de aventuras", for these four years of shared memories. I have learnt a lot by your side. I feel lucky to have shared with you experiment sessions, long scanning-nights at UCLM, SfN trips, the stays at UC Davis and WashU, and all the ensuing experiences and adventures.

And this work could not have been accomplished without the inestimable support of the friends and family who were by my side, even though we were thousand kilometers apart. There are many friends that I would like to thank, and I could make another thesis just on that. But I will shorten it by mentioning some of them.

Thanks, Pepa, for inspiring me and for being always there, through the years. Castaño, your steps showed me that everything is possible with effort and passion; "when there is a will, there is a way". Thanks Elena R, for the uncountable good moments lived together, in- and outside the lab. Your friendship and support mean a lot to me. And especial thanks to Mónica, "mi hermanilla" and best friend, who has been by my side every single day during this trip, beyond distance and time. Thanks for being part of my life, lighting up the days, and being a source of strength and love (∞∞∞).

Thanks to my family, especially to my parents who supported me all along the way, despite the fear of having their daughter taking flights to here and there so often, and despite the long absences. Thanks for your love and comprehension. And to my Aunts Begoña and Carmen for celebrating with me every little step (“Uuueee”). Also would love to give a huge thanks to my family in Barcelona, especially to my parents and siblings in law, who were beside me in every decision, supporting me unconditionally. And thanks to my German family, Hilde and Ingrid, for your love and care; and for those meals that you very generously prepared and left at my door, when I did not have time for anything else but write, and write, and write.

Finally, and most important, I would like to give an infinite thanks to my husband, without whom I could not have get this far in this journey. Thanks Edu, for loving me so unconditionally in Spain, Germany or the USA, no matter what. You have shown me that true love has no limits. Thanks for encouraging me to follow my dreams, and helping me to make them come true (even though that may mean to quit a permanent job in your home country, move to another country, and learn a new and totally unknown language to get a new job; and always smiling!). This work is dedicated to you. And get prepared for the new adventure! :)

CONTENTS

I. ZUSAMMENFASSUNG (German)

I. ZUSAMMENFASSUNG

Um die Rolle des *Locus Coeurleus* (LC) bei kognitiven Prozessen besser zu verstehen wurde in der vorliegenden Dissertation die neuroanatomische Organisation des LC im Primatenhirn, mit Fokus auf die Verbindungen des limbischen Systems, der hippocampalen Formation (HF), der Amygdala und des präfrontalen Cortex (PFC), untersucht.

Funktionale Studien an Nagetieren deuten darauf hin, dass der LC durch neuartige, saliente Reize aktiviert wird und direkt die Erinnerungsverarbeitung moduliert. Diese Modulation läuft vermutlich über Verbindungen zwischen dem LC und der HF, der Amygdala und dem PFC ab, welche eine wichtige Rolle bei höheren kognitiven Prozessen spielen. Trotz funktioneller Hinweise sind anatomische Daten, welche die Beteiligung des LC an der Verarbeitung von Erinnerungen belegen, sehr limitiert. Auch ist noch unbekannt ob und wie viele 'top-down' Eingänge der LC von der HF und dem PFC erhält.

Das Hauptziel dieser Arbeit war es, die Verbindungen zwischen dem LC und der HF, der Amygdala und des PFCs, welche die Grundlage zur Wahrnehmung sein könnten, im nicht-menschlichen Primatenhirn zu untersuchen. Neben hoch auflösender Kernspintomographie wurden Methoden wie neuronales Tract-Tracing, Histochemie und Immunohistochemie angewendet. Es wurde untersucht ob es (1) direkte Eingänge der HF zum LC gibt, (2) ob der PFC direkt zum LC projiziert, (3) welche architektonischen Gebiete zu diesen Projektionen beitragen, (4) ob es Verbindungen des Amygdaloiden Kernes, neben dem Zentralen Kern der Amygdala, gibt und (5) wie diese Verbindungen topographisch organisiert sind.

Diese detaillierten Kartierungen der neuronalen Verbindungen zwischen dem LC, der HF und dem PFC könnten zum Verständnis der Rolle des LCs bei der Modulation von höheren kognitiven Prozessen, wie zum Beispiel Entscheidungsfindungen und Erinnerungsverarbeitung, beitragen. Auch könnten sie eine Schlüsselrolle in dem Verständnis von Katecholamin-abhängigen Krankheiten (wie z.B. Depression, ADHS, Parkinson und Demenz) darstellen und die Entwicklung neuer Behandlungsmethoden ermöglichen.

II. ABSTRACT

II. ABSTRACT

The present doctoral dissertation concerns the neuroanatomical organization of the LC in the primate brain; and it is more specifically focused on the limbic connections of the HF, amygdala (Amy) and PFC with the LC in order to better understand the role that this nucleus may have in cognitive processes.

Rodent functional studies indicate that LC is activated by novel salient stimuli and directly modulate memory processing. This modulation likely involves connections between LC and the HF, Amy and PFC, which have a crucial role in higher cognitive processes. Despite the functional evidences, anatomical data supporting the implication of LC in the “memory pathways” is still very limited, and whether and to what extent HF and PFC send direct ‘top-down’ input to LC remains unknown.

The main goal of this project is to study the connections between LC and HF/Amy/PFC in the nonhuman primate that could undelie high cognitive processes. We use high-resolution MRI, neuronal tract tracing, histochemical and immunohistochemical methods to examine (1) whether there exist direct inputs from the HF to LC, (2) whether the PFC projects directly to LC, (3) which of the architectonic areas contribute to these projections, (4) whether there exist projections from the other amygdaloid nucleus beyond the central nucleus of the amygdala, and (5) the topography of these projections.

This detailed mapping of the neuronal interconnections between LC, HF and PFC could provide a novel insight on the anatomy underlying the role of LC in the modulation of higher cognitive processes such as decision making and memory processing, and a key step for the understanding of the catecholamine-related disorders (depression, attention deficit- hyperactivity, and dementia in Alzheimer’s and Parkinson’s diseases), and towards the development of appropriate treatments.

III. RESUMEN (Spanish)

III. RESUMEN (Spanish)

El presente trabajo de tesis doctoral trata de la organización neuroanatómica del *Locus coeruleus* en el cerebro del primate; se centra, más específicamente, en las conexiones límbicas (formación del hipocampo, amígdala, y la corteza prefrontal) con el *Locus coeruleus*, con el fin de comprender mejor el papel que éste núcleo puede tener en los procesos cognitivos.

Estudios funcionales desarrollados en roedores indican que el *Locus coeruleus* es activado por estímulos novedosos y modula directamente el procesamiento de la memoria. Esta modulación probablemente involucra conexiones del *Locus coeruleus* con la formación del hipocampo, complejo amigdalino, y corteza prefrontal, los cuales tienen un papel importante en los procesos cognitivos. Se desconoce si existe o no una proyección directa y descendente desde la formación del hipocampo y la corteza prefrontal hacia el *Locus coeruleus*; a pesar de las evidencias funcionales, los datos anatómicos que apoyan la implicación del *Locus coeruleus* en las vías de la memoria son muy escasos.

El objetivo principal de este trabajo es estudiar las connexiones anatómicas entre la formación del hipocampo y la corteza prefrontal con el *Locus coeruleus*, que subyacen los procesos cognitivos. Para ello, se emplean imágenes de resonancia magnética de alta resolución, trazadores neuronales, y técnicas histológicas e inmunohistoquímicas, para examinar (1) si existe proyección directa desde la formación del hipocampo al *Locus coeruleus*, (2) si existe proyección directa desde la corteza prefrontal al *Locus coeruleus*, (3) cuáles son las áreas arquitectónicas que contribuyen a esa proyección, (4) si existe proyección desde el complejo amigdalino, más allá del núcleo central de la amígdala, y (5) la topografía de estas proyecciones.

Esta topografía detallada de las interconexiones neuronales entre el *Locus coeruleus*, la formación del hipocampo y la corteza prefrontal podría proporcionar una nueva visión de las vías anatómicas subyacentes en la modulación de los procesos cognitivos superiores por el *Locus coeruleus*, tales como la toma de decisiones y procesamiento de la memoria. Además, los resultados derivados de este trabajo podrían proporcionar un paso clave para la comprensión de los trastornos relacionados con las vías catecolaminérgicas (depresión, déficit de

atención e hiperactividad y demencias de la enfermedad de Alzheimer y la enfermedad de Parkinson), que facilitarían el desarrollo de tratamientos adecuados.

IV. INTRODUCTION

IV. INTRODUCTION

1. Background

The first description of *Locus coeruleus* (LC) dates back to 1809 by Reil as a blue-black substance in the anterior floor of the human fourth ventricle (Reil, 1809). The pigmented area remained nameless until 1812 when the term '*Locus coeruleus*' was introduced (Wenzel and Wenzel, 1812). In 1955 Russell reviewed evidence for the potential involvement of LC in trigeminal sensory activity, visceral sensibility, and respiration (Russel, 1955).

The development of the Falck-Hillarp method (Falck et al., 1962), which involved exposing freeze-dried tissue sections to formaldehyde vapor resulting in the fluorescence of the monoamine-containing cells through the formation of tetrahydroisoquinoline derivatives, enabled to differentiate groups of neurons based upon their color. Cells in the substantia nigra and LC were found to exhibit an intense green fluorescence, while profiles of raphe nuclei appeared yellow. Dopaminergic and noradrenergic neurons were, therefore, classified under the A group designation (A1-A12), while serotonergic neurons were categorized in the B series (B1-B9).

Dahlström and Fuxe (1964) described the noradrenergic groups (A1-A7) and in 1983 Felten and Sladek described their pathways throughout the brain. The noradrenergic axons are distributed widely throughout the central nervous system, suggesting a prominent role in brain function and behavior.

The release of noradrenaline (NA) by the LC has a crucial role in brain-wide neuromodulation, taking part in attention, sleep-wake cycle, stress responses and sympathetic regulation, as well as higher cognitive processes such as learning, decision-making, goal-directed behavior, memory formation and retrieval. Alterations in the functions of LC may trigger psychiatric disorders and diseases including schizophrenia, autism, depression, attention deficit-hyperactivity disorder, and dementias in Alzheimer's and Parkinson's diseases.

The vast majority of our knowledge on the anatomical organization of LC and its connection with the hippocampal formation (HF), the amygdala, and the prefrontal cortex (PFC) is based on experiments undertaken in rodents. These experiments provide a basis for understanding how LC might modulate brain processes and behaviors in primates. However, the anatomy in rodents is not necessarily similar to

the anatomy in primates. One major difference between rodents and primates regarding the connectivity of LC is that, in the rodent, the nucleus paragigantocellularis and the prepositus hypoglossi are the two only structures targeting directly the core of LC (Aston-Jones et al., 1986), whereas in the primate, there are subcortical nuclei like the central nucleus of the amygdala (Price and Amaral, 1981), as well as cortical regions like the dorsolateral PFC (area 9) (Arnsten and Goldman-Rakic, 1984) that also project to the core of LC (see section 2 for the anatomy of LC).

The HF of the primates also differs from the rodents in its anatomy (see figure 2). A lateral view of the rodent brain reveals a C-shaped hippocampus with the top part of the C, namely dorsal or septal, critical for spatial processing, and a bottom part, ventral, or temporal, critical for object processing. In the primate brain, this C-shaped hippocampus unfolds in the longitudinal plane to take an elongated shape, whereby the dorsal rodent hippocampus corresponds to the caudal hippocampus in the primate and the ventral rodent hippocampus corresponds to the rostral or uncal part in the primate brain (Strange et al., 2014, Muñoz-López, 2015). In addition, another anatomical difference is that the entorhinal cortex in the rodents is divided into medial and lateral parts (although further divisions, parallel to the primate have been described (Insausti et al., 1997), while in the nonhuman primates it has been described to have up to seven subfields (Amaral et al., 1987).

Given all these evidence, together along with the lack of knowledge on direct LC afferents from the HF, the amygdala and the PFC, it is of great importance to undertake the present study in the nonhuman primate. The outcome might provide a new insight on the anatomy that underlies the role of LC in cognitive functions, and this might be a key step towards the development of appropriate treatments against disorders in which the NA-system might be involved.

2. The locus coeruleus

2.1. Anatomy

The majority of NA neurons are concentrated in LC, a small (0,5x3x3 mm^3 in the macaque monkey) well-delineated cluster of densely packed neurons, located in the brainstem, adjacent to the wall of the fourth ventricle (figure 1; for more anatomical

details, see figure 2). LC neurons contain and synthetize both NA and dopamine (DA) (figure 3).

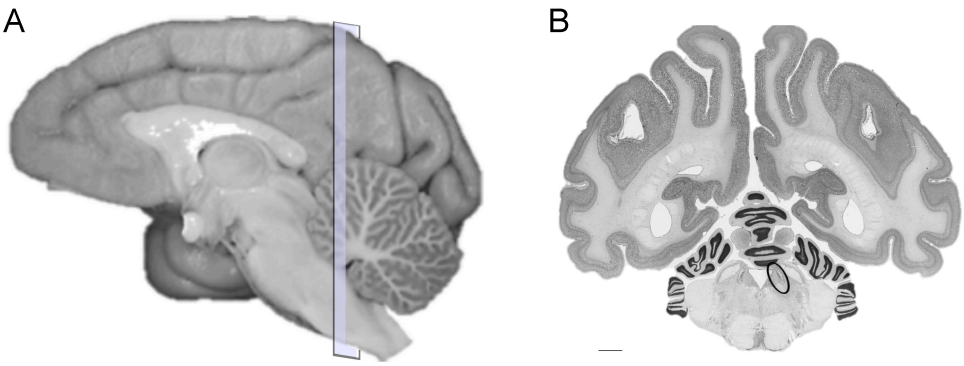

Figure 1. (A) Lateral view of the *Macaca fascicularis* brain. (B) Microphotograph of a coronal nissl-stained section containing LC (ellipse). Scale bar: 2mm.

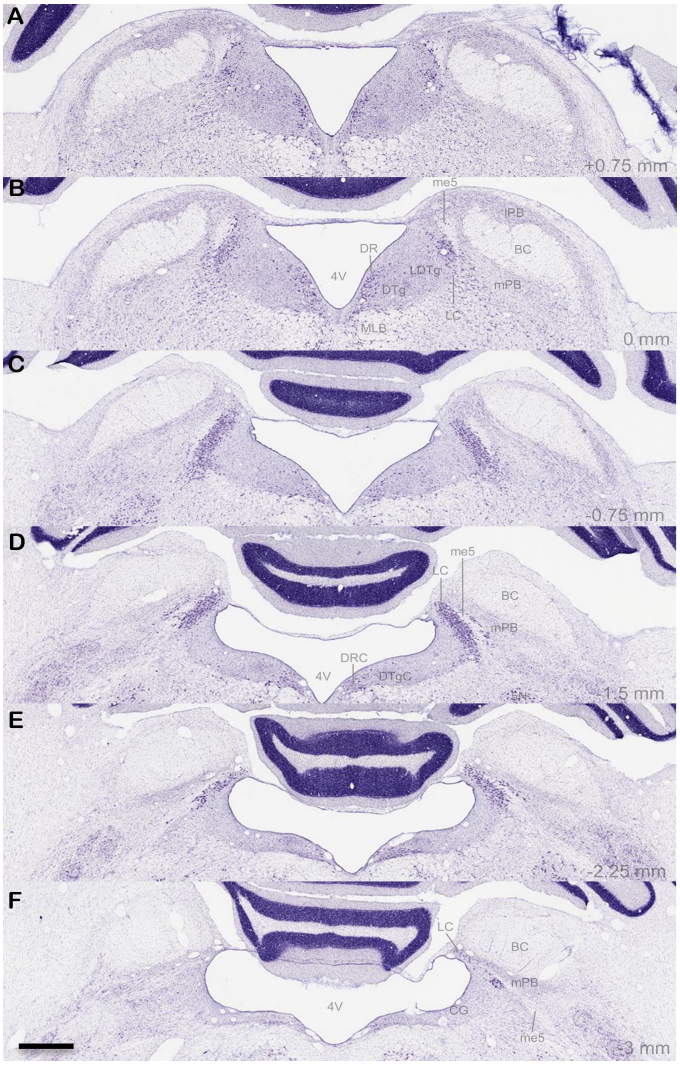

Figure 2. Microphotographs of coronal nissl-stained sections of the locus coeruleus from rostral (A) to caudal (F). Abbreviations: 4V, fourth ventricle; 4x, trochlear decussation; CGPn, cg pons; DRC, dorsal raphe caudal; DTg, dorsal tegmentum; LDTg, laterodorsal tegmentum; LC, locus coueruleus; me5, mesencephalic tract 5; Me5, mesencephalic nucleus 5; mlf,

medial longitudinal fascicle; MPB, medial parabrachial nucleus; scp, superior cerebelar peduncle. Scale bar: 1mm.

Anatomically, the LC is composed of a densely packed nuclear core and a surrounding noradrenergic process zone, which is asymmetrically distributed and contains mostly dendrites. These extranuclear dendrites extend preferentially into two distinct Peri-LC regions: the rostromedial and caudal juxtaependymal Peri-LC (Shipley et al., 1996). The core of LC is divided into dorsal and ventral parts, cytoarchitectonically well separated, since the cells in the dorsal division are more densely packed, and a majority of these cells in the dorsal division are aligned obliquely in a dorsomedial to ventrolateral orientation when viewed in the transverse plane.

Based on both DBH (dopamine-ß-hydroxylase) and TH (tyrosine hydroxylase) immunostaining, the limiting enzymes in the synthesis of NA and DA respectively, two major cell classes have been identified within the nucleus, the small fusiform cells that are found mainly in the dorsal portion of LC and the medium-sized multipolar cells that are mainly observed in the ventral portion of the nucleus.

LC projects throughout the cerebral cortex, hippocampus, thalamus, midbrain, brainstem, cerebellum and spinal cord (Aston-Jones et al., 1984; Foote et al., 1983), and provides the sole source of NA to neocortex and hippocampus, regions that are critical for higher cognitive processes (Berridge and Waterhouse, 2003). In turn, LC receives major direct input from the nucleus gigantocellularis and the prepositus hypoglossi both located in the anterior medulla. Furthermore, it receives also input from brainstem nuclei such as the periaqueductal gray, central gray, reticular formation, parabrachial nucleus and contralateral LC, regions involved in the control of basic behavior and autonomic functions. Minor afferents arise from other regions such as central nucleus of the amygdala, thalamus, hypothalamus, ventral tegmental area, raphe, and prefrontal cortex (Luppi et al., 1995).

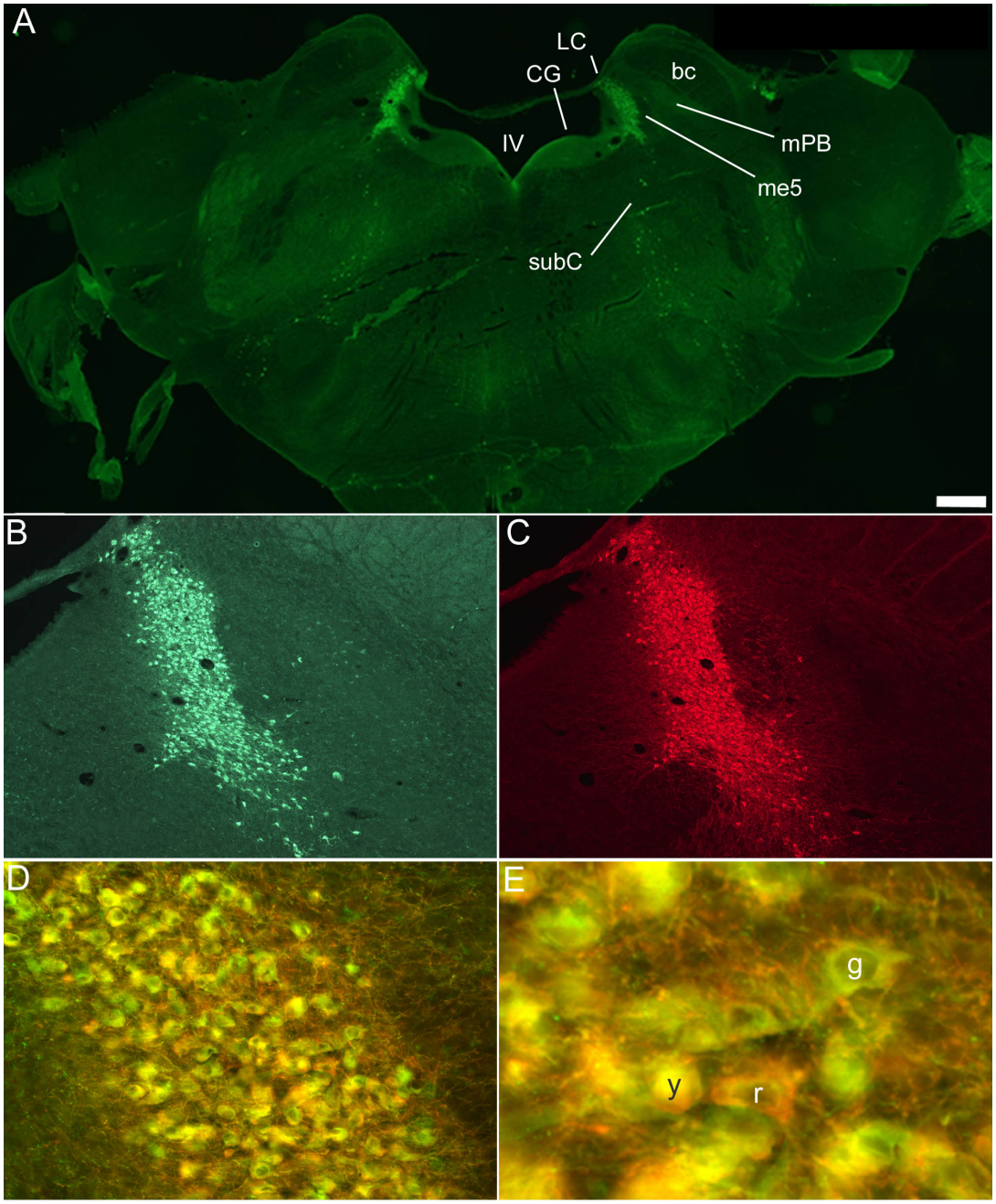

Figure 3. DBH and TH immune-localization in LC. (A) Low magnification overview of the localization of the DBH-positive cells in the pons of the *Macaca fascicularis*. (B-C) Medium magnification microphotographs of DBH- and TH-positive cells in LC, respectively. (D-E) High resolution and very high resolution of DBH- (green), TH- (red), and DBH+TH- (yellow) positive cells in LC. In (E), "g", "r" and "y" designate DBH-, TH- and DBH+TH-positive cells respectively. Abbreviations: IV, fourth ventricle; CG, central gray; LC, locus coueruleus; me5, mesencephalic tract 5; mPB, medial parabrachial nucleus; bc, brachium conjuntivum. Scale bar: 1mm (A), 260μm (B-C), 70μm (D) and 20μm (E).

2.2. Functional implications

A large body of literature implicates NA in cellular excitability, synaptic plasticity, long-term potentiation (LTP), attention, decision-making and behavioral flexibility (Harley, 1987; Aston-Jones and Cohen, 2005; Yu and Dayan, 2005; Bouret and Sara, 2005; Arnsten and Li, 2005; Robbins and Roberts, 2007; Harley, 2007). In addition, it is known that LC neurons fire at critical periods during learning, memory consolidation and retrieval, releasing NA in crucial forebrain regions that control attention, sensory and memory processing, and releasing both NA and dopamine (DA) in the dorsal hippocampus and medial prefrontal cortex (Devoto et al., 2005a; 2008; McGaugh and Roozendaal, 2008; Smith and Greene, 2012; Sara, 2012).

Electrophysiological studies in behaving monkeys pointed out that LC neurons fire in two distinct activity modes: *tonic* and *phasic* (for review see Aston-Jones et al., 2007). Phasic mode would facilitate sustained attention to maximize reward in a period of high opportunity (exploit). In contrast, tonic mode would result in disengagement from a task as reward and utility wanes in order to facilitate exploration of more rewarding options (explore).

The phasic mode is characterized as an overall decrease in baseline firing coupled with a burst of activity following presentation of a target stimulus but preceding a behavioral response. In contrast, tonic mode is associated with higher baseline LC impulse activity but little to no phasic response to stimuli or events. During the phasic mode of LC firing, performance on various cognitive tasks that require focused attention was facilitated in both monkeys (Usher et al., 1999; Rajkowski et al., 2004) and rats (Bouret and Sara, 2004). Periods of elevated tonic LC activity were also consistently associated with decreased phasic responsiveness of LC neurons to target stimuli. The phasic activation of LC neurons occurred selectively during epochs of intermediate tonic LC discharge and accurate behavioral performance. Moreover, phasic LC responses to target stimuli were also suppressed in the few instances when task performance continued during drowsiness and very low LC tonic activity. Therefore, phasic-evoked responses are closely related to intermediate tonic discharge levels of LC neurons and focused attentional performance (Aston-Jones et al., 2007).

Aston-Jones and colleagues described the existence of three modes of LC activity corresponding to different levels of performance on a task that require

focused attention. In the hypoactive mode (1), LC neurons exhibit very little activity either tonically or in response to task events. This mode is associated with drowsiness and inattention to the task or other external stimuli. In the phasic mode (2), LC cells exhibit phasic activation selectively for stimuli that are discriminated as targets but only a moderate level of tonic discharge. This mode of LC activity is consistently associated with accurate performance on the task with few errors and high visual fixation. In the tonic mode (3), LC cells fail to respond phasically to any task stimuli, but exhibit higher levels of ongoing tonic activity. This mode corresponds to poor performance on this task, with many errors of false alarm, less fixation and more scanning eye movements.

The dysregulation of LC activity may underlie certain cognitive disorders. Sustained hypertonic LC activity underlies attention-deficit/hyperactivity disorder (ADHD). Drugs that treat ADHD, including stimulants (such as methylphenidate) and clonidine, improve performance of subjects in an attentional task (Solano, 1998). These pharmaceutical agents decrease tonic activity in LC and facilitate a shift to the phasic discharge mode. On the other hand, in patients with autism, LC neurons are in a persistent hyperphasic mode that makes the individual to have difficulties in shifting attention to new stimuli (Aston-Jones et al., 2007). Furthermore, chronically hyperactive LC system may give rise to some symptoms of manic-depressive disorder, including sleeplessness, and impulsivity (Siever and Davis, 1985). On the other hand, chronically decreased LC function may be associated with limited emotionality and flat affect, a common characteristic of a subpopulation of depressed patients. It is noteworthy in this regard that alterations in receptors and biochemical parameters of LC neurons have been reported in brains of suicide victims (Biegon and Fieldust, 1992; Ordway et al., 1994; Ordway et al., 1994b; Widdowson et al., 1992). In addition, several studies have found reduced numbers of LC neurons in patients suffering from dementia associated with Parkinson´s or Alzheimer´s diseases (Chan-Palay, 1991; 1993; German et al., 1992; Hoogendijk et al., 1995; Zweig et al., 1993).

3. Hippocampal formation

3.1. Anatomy

In humans and nonhuman primates, the HF is located in the medial temporal lobe and is composed (figure 4) by the dentate gyrus (DG), the hippocampus proper (CA1, CA2 and CA3), entorhinal cortex (EC), subiculum, presubiculum and parasubiculum.

The *dentate gyrus* in primates is a trilaminar region, C-shaped in transverse sections, and it is ventral and laterally separated from the subiculum and CA1, CA2 and CA3 by the fissure of the hippocampus. The main layer of the dentate gyrus is the granular layer. It is mainly populated by a single type of neurons (granular cells), which send their dendrites to the molecular layer. The polymorphic layer, also called the hilus of the dentate gyrus, is complex and has brought a lot of controversy between different authors. Some of them consider this layer as a part of the dentate gyrus (Amaral, 1978; Amaral e Insausti, 1990; Insausti y Amaral, 2004) and some others as a field of the hippocampus proper called CA4 (Lorente de Nó, 1934).

The *hippocampus proper* has a similar cytoarchitectonic organization in both non-human and human primates, and it is divided into three fields: CA1, CA2 and CA3 according to Amaral and Insausti (1990). They are subdivided from the ventricular surface to the hippocampal fissure into six layers (Duvernoy, 1998): *Alveus, Stratum Oriens, Stratum Piramidale, Stratum Lucidum, Stratum Radiatum, and Stratum Lacunosum-moleculare*.

The *subiculum*, *presubiculum* and *parasubiculum* are transition areas between the hippocampus and entorhinal cortex. The subiculum is located rostrally, while the parasubiculum is located adjacent to the posterior parahippocampal cortex. The subiculum has three layers named as molecular, pyramidal and polymorphic; whereas presubiculum and parasubiculum are organized in two layers, molecular (layer I) and cellular (layer II) of densely packed cells.

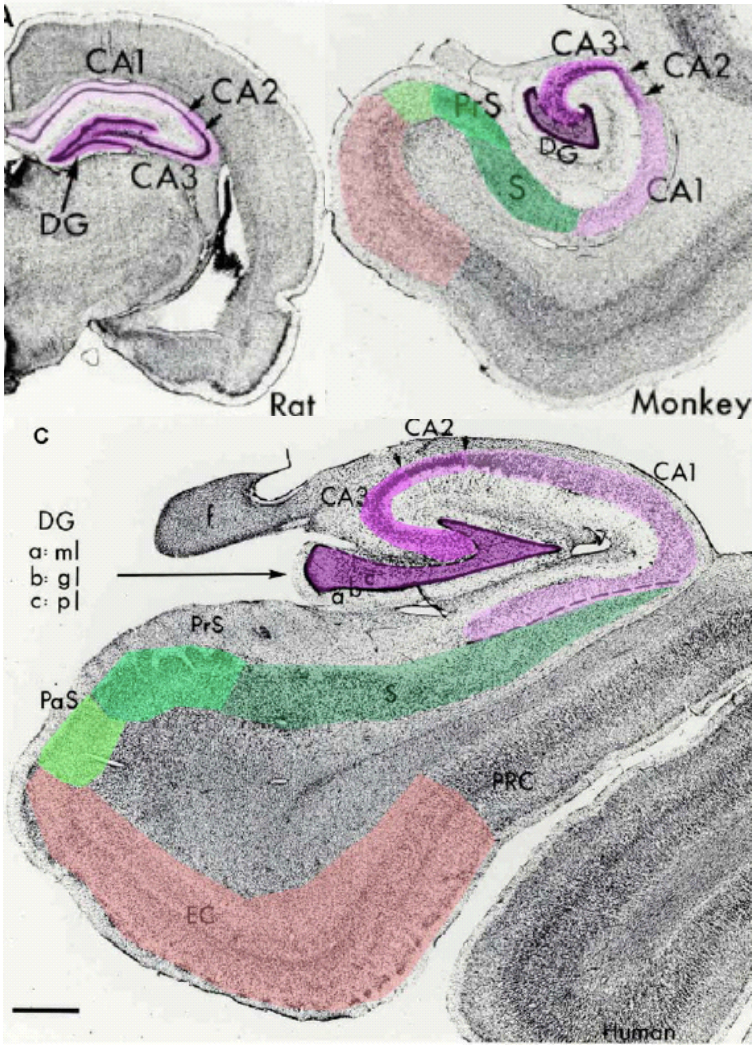

Figure 4. Microphotograph of coronal nissl-stained sections of the hippocampal formation in the rat (A), monkey (B), and human (C). Pink: Hippocampus proper; green: subicular complex; red: entorhinal cortex. Courtesy of Dr. Mohedano-Moriano. Scale bar: 1mm.

The *entorhinal cortex* in the primate is divided in 7 subfields (olfactory entorhinal subfield [Eo], rostral entorhinal subfield [Er], intermediate entorhinal subfield [Ei], lateral rostral entorhinal subfield [Elr], lateral caudal entorhinal subfield [Elc], caudal entorhinal subfield [Ec] and caudal limiting entorhinal subfield [Ecl]) according to the laminar and columnar cytoarchitecture along the rostrocaudal and mediolateral axis (Amaral et al., 1987), in such a way that the organization of its cells in layers and columns is higher at the caudal levels.

The HF structures are grouped together based on their proximity, function and their particular connectivity characterized by unidirectional projections (Amaral and

Insausti, 1990; Amaral and Witter, 1995; Insausti and Amaral, 2004). The polysensory information from the neocortex reaches the dentate gyrus through the layer II of the entorhinal cortex through the perforant pathway, the main input to the hippocampus (Witter et al. 1989). This pathway perforates the subiculum and synapses the dendrites of the granule cells located in the dentate gyrus. Furthermore, the axons of the pyramidal cells in layer III of the entorhinal cortex project to the subiculum and CA1 (Amaral and Witter 1989; Amaral and Insausti 1990; Witter, 1993; Kobayashi and Amaral 1999). The mossy fibers of dentate gyrus make synapsis with the dendrites of CA3 pyramidal cells. CA3 axons send projections to the CA1 (Schaffer collaterals) area. Subsequently, CA1 projects densely to subiculum and to the deep layers of the entorhinal cortex. And subiculum sends projections to the presubiculum and parasubiculum, which project to layer V of the entorhinal cortex (Rosene and Van Hoesen 1987; Amaral and Insausti 1990; Kobayashi and Amaral 1999).

3.2. Functional implications

The hippocampal formation has a critical function in memory processing (Squire y Zola-Morgan, 1991). In humans, lesions restricted to CA1/subiculum or bilateral hippocampal volume reductions of over 30% are enough to cause severe amnesia, including both episodic and spatial memory impairment (Rempel-Clower, 1996; Vargha-Khadem et al., 2007).

Furthermore, altered synaptic circuitry or “wiring” within the hippocampal formation and its extrinsic connections underlie diseases such as schizophrenia (Amaral and Insausti 1990; Duvernoy 1998), epilepsy (Schwartzkroin, 1994; Jöels, 2009), drug addiction (Everitt and Robbins, 2005), and Alzheimer’s disease (Hyman et al., 1984; West, 1993).

4. Amygdala

4.1. Anatomy

The amygdala is located in the medial temporal lobe, adjacent to the hippocampus. It is a complex structure that comprises different nuclei distinguished on the basis of the cytoarchitecture, histochemistry, and its connectivity (Krettek and Price, 1978; Amaral et al., 1992; Alheid et al., 1995; McDonald, 1998; Pitkänen,

2000). These studies reveal that while there are many similarities between species, there are also clear differences in the organization and the relative sizes of the different amygdaloid nuclei.

The monkey amygdaloid complex (figure 5) is formed by the *deep nuclei* that include the lateral nucleus (divided into dorsal, dorsal intermediate, ventral intermediate, and ventral divisions), the basal nucleus (divided into magnocellular, intermediate, and parvicellular divisions), the accessory basal nucleus (partitioned into magnocellular, parvicellular, and ventromedial divisions), and the paralaminar nucleus. The *superficial areas* include the anterior cortical nucleus, the medial nucleus, the nucleus of the lateral olfactory tract, the periamygdaliod cortex (PAC-divided into five subregions: oral division [PACo], cortices 1–3 [PAC1, PAC2, PAC3], and sulcal division [PACs]), and the posterior cortical nucleus. The *remaining areas* consist of the anterior amygdaloid area, the central nucleus (divided into lateral and medial subdivisions), the amygdalohippocampal area (which has dorsal and ventral divisions), and the intercalated nuclei (Price et al, 1987; Amaral et al. 1992; Pitkänen and Amaral, 1998).

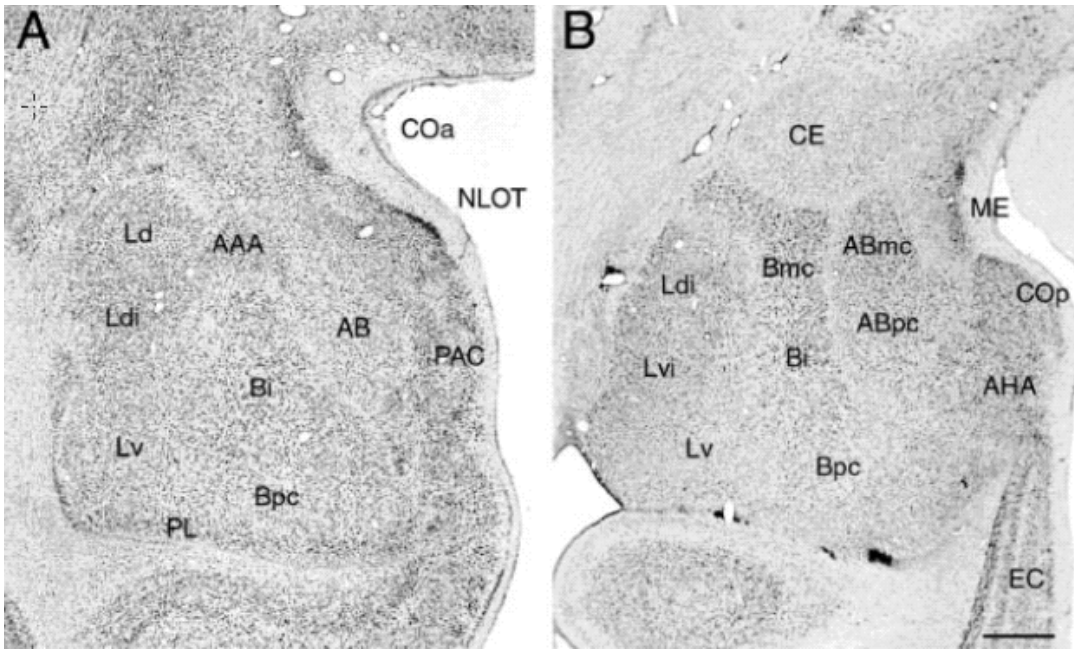

Figure 5. Microphotographs of coronal nissl-stained sections of the Amygdala in the monkey, (A) rostral, and (B) caudal. Abbreciations: AAA: anterior amygdaloid area; AB: accessory basal nucleus; ABmc: accessory basal, magnocelular division; ABpc: accessory basal, parvocelular division; Bi: basal nucleus, intermediate division; Bpc: basal nucleus, parvocelular division; Bmc: basal nucleus, magnocelular division; CE: central nucleus; COa: cortical nucleus, anterior division; COp: cortical nucleus, posterior division; L: lateral nucleus; Ld: lateral nucleus, dorsal division; Ldi: lateral nucleus, dorsal intermediate

division; Lv: lateral nucleus, ventral division; ME: medial nucleus; PAC: periamygdaline cortex; PL: paralaminar nucleus. Scale bar: 1mm. (Stefanacci and Amaral, 2000).

The amygdala is characterized by widespread connections. Anatomical tract tracing studies have shown that these nuclei have extensive intrinsic (Pitkänen and Amaral, 1998) and extrinsic (De Olmos, 1972; Pitkänen et al., 2002; Price and Amaral, 1981; Amaral and Price, 1984; Price, 2003; Freese and Amaral, 2005) connections with cortical and subcortical structures such as hypothalamus, thalamus, septum, accumbens, periaqueductal gray, reticular formation, parabrachial nucleus, spinal cord, parahippocampal gyrus, cingulum, piriform cortex and orbitofrontal cortex. In turn, the lateral nucleus is the major recipient of sensory information from sensory association cortices (Price et al., 1987; Amaral et al., 1992).

4.2. Functional implications

The amygdala is well known to play an important role in Pavlovian fear conditioning and inhibitory avoidance (Kapp et al., 1979; McGaugh et al., 1996; LeDoux, 2000). It has also been implicated in diverse behavioral functions such as emotional learning (Applegate et al., 1982; Pascoe and Kapp, 1985), regulation of attentional processes (Gallagher and Holland, 1994; Holland and Gallagher, 1999), long-term memory processing in concert with the hippocampal formation (Mishkin, 1978), and retrieval of memory encoded in an emotional context (Sterpenich et al., 2006).

Damasio and colleagues have studied a patient, S.M., who appears to have rather complete bilateral damage to the amygdala with relatively little involvement of surrounding structures (Adolphs et al., 1995, 1998, 1999). Despite the complete absence of the amygdala, the patient did not demonstrate significant social pathology and appears to have a remarkably normal daily life. She was impaired, however, in her ability to judge facial emotions. While she could reliably interpret happy faces, she had difficulty in seeing fear in a face. Moreover, she was markedly impaired in attributing “trustworthiness” to an individual on the basis of facial appearance. These findings are consistent with the notion that the amygdala evaluates the environment for potential danger (Amaral, 2003).

5. Prefrontal cortex

5.1. Anatomy and function

The prefrontal cortex is a large and heterogeneous structure that is divided into several networks that have distinct roles (figure 6).

The *orbital (OPFC) network* is connected to several sensory-related cortical areas, such as the olfactory and taste cortex, visual-related areas in the inferior temporal gyrus, and somatic sensory-related areas in the insula and frontoparietal operculum (Carmichael and Price, 1995; Ongur and Price, 2000; Saleem et al., 2008). This network appears to integrate multimodal sensory information, especially related to food, and to be involved in assessment of stimuli in terms of reward and/or aversion, and their relative "value" in relation to other stimuli (Öngür and Price 2000; Padoa-Schioppa and Assad, 2006; Rudebeck and Murray 2011a, b). The *medial (MPFC) network* has few sensory inputs, but has substantial outputs to visceral control areas in the hypothalamus and brainstem (An et al., 1998; Öngür et al., 1998). It is also interconnected with a well-defined cortical circuit involving the anterior and posterior cingulate cortex (Saleem et al., 2008b), as well as limbic structures, including the amygdala, hippocampus, and entorhinal cortex. This network is related to modulation of visceral function in relation to emotion, and is critically involved in mood disorders (Drevets et al., 1997, 1998; Mayberg et al., 1999, 2005; Price and Drevets, 2012).

In the lateral part of the prefrontal cortex (LPFC), there are also indications that relatively restricted regions have distinct functions. Thus, in monkeys the *ventrolateral prefrontal cortex (VLPFC),* below the principal sulcus, has been related to the assessment and convergence of sensory information, including the processing of faces, visual association, and integration of species-specific face and vocal stimuli, and has also been thought to be involved in object working memory and memory retrieval (Wilson et al., 1993; O´Scalaidhe et al., 1997; Asaad et al., 1998; Levy and Goldman-Rakic 2000; Passingham et al., 2000; Cadoret and Petrides, 2007; Tsao et al., 2008b; Romanski 2012). The *dorsal prefrontal cortex (DPFC)* above the principal sulcus has been thought to be involved in self-centered functions, including behaviors that depend on the previous actions or feelings of the individual (Petrides 2005). Finally, the *caudolateral prefrontal cortex (CLPFC)*, the region around the arcuate sulcus, and parts of the caudal principal sulcus has been related to eye

movements (frontal eye field), attention, shape selectivity, and working memory for spatial position (Bruce and Goldberg, 1985; Bruce et al., 1985; Gamlin and Yoon, 2000; Tehovnik et al., 2000; Schall 2004; Peng et al., 2008; Amiez and Petrides 2009; Monosov and Thompson, 2009; Zhou and Desimone, 2011).

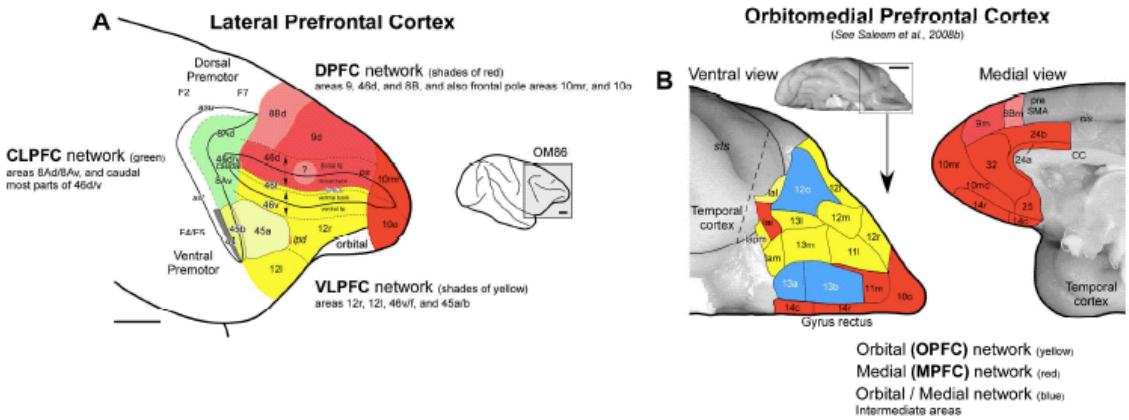

Figure 6. Subdivisions of the prefrontal cortex in different networks.
(Modified from Saleem et al., 2014).

6. State of the Art

Recent physiological studies in rodents pointed out that, beyond the NA, LC terminals also release DA in the hippocampus and the medial PFC (Devoto et al., 2005a, 2008; Devoto and Flore, 2006). Posteriorly, Smith and Greene (2012) suggested that NA-LC fibers might be the primary source of DA release in hippocampus instead of the ventral tegmental area (VTA), since there is an anatomical mismatch between the distribution of the VTA terminals in the hippocampus and the distribution of the D1-receptors, which are critical for encoding and persistence of episodic memories in hippocampus (O'Carroll et al., 2006; Bethus et al., 2010). D1-receptors are distributed mainly in the dorsal hippocampus where LC sends its terminals, while the VTA sends projections to the ventral hippocampus.

In addition, Devoto and colleagues inhibited the mesocorticolimbic pathway arising from VTA, by injecting 6-hydroxydopamine (6-OHDA), and observed the subsequent dramatic reduction in the concentration of extracellular DA in the striatum, although the levels in the cortex barely changed (Devoto et al., 2008). Therefore, they hypothesized that the majority of the extracellular DA released in the cortex, unlike the accumbens, originates from NA-terminals.

There might exist the possibility of an indirect, LC-mediated activation of VTA or substantia nigra terminals; however, there is in fact some evidence demonstrating that burst-type electrical or chemical stimulation of LC produces a long-lasting inhibition in VTA (Grenhoff et al., 1993; Paladini and Williams, 2004). The influence of LC on midbrain DA-neurons could be important in behavioural situations involving novelty and reward.

The evidence of the co-release of DA and NA by LC terminals confers to LC a major role in the neuromodulation of certain cognitive processes. This fact opens a new insight for LC implication in the regulation of the brain-wide activity, not only through the NA system but also in a wider extent through the DA system.

The projections of LC are widely distributed throughout the central nervous system, and they provide the sole source of NA to neocortex and hippocampus. In turn LC receives inputs from many subcortical structures (Arnsten and Goldman-Rakic, 1984; Price and Amaral, 1981), whilst the only cortical input reported so far in the primate arises from few specific regions of the PFC (Arnsten and Goldman-Rakic, 1984, Freedman et al., 2000; Chiba et al., 2001; Aston-Jones et al., 2007).

Of particular interest are the connections of LC with the hippocampal formation, amygdala, prefrontal and anterior insular cortex through which LC participates in the modulation of cognitive processes such as decision-making and memory processing (Aston-Jones and Cohen, 2005; Aston-Jones et al., 2007; Lemon et al., 2009; Lim et al., 2010).

Functional studies in rats and monkeys showed that LC has an important role in memory processing such as long-term memory and working memory (Ramos et al., 2005; Eschenko and Sara, 2008; Roozendaal et al, 2007). Prior functional studies demonstrated that LC is activated with novel salient stimuli (Aston-Jones et al., 1994; Sara et al., 1994; Vankov et al., 1995) and novelty detection is accompanied by increased hippocampal noradrenergic activity driven by enhanced firing of LC (Sara et al. 1994; Kitchigina et al. 1997).

One hypothesis is that novelty signals originating in the HF could activate LC, and subsequently LC could release DA and NA in the hippocampus (Smith and Greene, 2012) promoting long-term potentiation (LTP) and memory consolidation. However, there are few anatomical data supporting the existence of these 'memory pathways'.

The existence of inputs from LC to the entorhinal cortex and the hippocampus has been reported in prior studies (Amaral and Cowan, 1980; Insausti et al., 1987). However, the topographical organization of LC terminals within these regions and whether there exist a direct top-down projection from the HF remains unknown.

The PFC also plays an important role in long-term memory (Blumenfeld and Ranganath, 2007; Muñoz and Morris, 2009), and working memory (Miller, 2013). The available anatomical knowledge on the connections between LC and PFC in macaques is also poor. There are only few tract-tracing studies in monkeys focused on only a subset of PFC areas (Gatter and Powell, 1977; Arnsten and Goldman-Rakic, 1984; Freedman et al., 2000; Chiba et al., 2001; Aston-Jones et al., 2007). An overall view of the projections to LC from the different areas of the PFC is still lacking. Like for HF, the top-down input from the PFC to LC is barely known.

Elucidating the anatomy underlying the role of LC in higher cognitive processes is of great importance. The detailed mapping of the neuronal interconnections between LC, HF, Amy and PFC could provide a novel insight on the anatomy and functional organization underlying the role of LC in the modulation of higher cognitive processes such as decision making and memory processing, and a key step for the understanding of the catecholamine-related disorders (depression, attention deficit-

hyperactivity, and Alzheimer's and Parkinson's diseases), and towards the development of appropriate treatments.

7. References

Adolphs R, Tranel D, Damasio H, Damasio AR (1995). Fear and the human amygdala. J. Neurosci. 15: 5879-5891. 32.

Adolphs R, Tranel D, Damasio AR (1998). The human amygdala in social judgment. Nature 393: 470-474. 33.

Adolphs R, Tranel D, Hamann S, et al. (1999). Recognition of facial emotion in nine individuals with bilateral amygdala damage. Neuropsychol 37: 1111–1117.

Alheid GF, De Olmos J, Beltramino CA (1995). Amygdala and extended amygdala. In: The Rat Nervous System, edited by Paxinos G. Orlando, FL: Academic, 1995, p. 495–578.

Amaral DG (2003). The amygdala, social behaviour and danger detection. Ann NY Acad Sci 1000: 337-347.

Amaral DG, Insausti R (1990). Hippocampal formation. In: The Human Nervous System (Paxinos G, ed), pp 711-755. San Diego.

Amaral DG, Insausti R, Cowan WM (1987). The entorhinal cortex of the monkey: I. Cytoarchitectonic organization. J Comp Neurol 264: 326-355.

Amaral DG, Price JL (1984). Amygdalo-cortical projections in the monkey (*Macaca fascicularis*). J Comp Neurol 230(4): 465-96.

Amaral DG, Price JL, Pitkänen A, Carmichael ST (1992). Anatomical organization of the primate amygdaloid complex. In: Aggleton J, editor. The amygdala: neurobiological aspects of emotion, memory, and mental dysfunction. New York: Wiley-Liss Publishers. pp. 1-66.

Amaral DG, Witter MP (1989). The three-dimensional organisation of the hippocampal formation: a review of anatomical data. Neurosci 31(3): 571-591.

Amaral DG, Witter MP (1995). Hippocampal formation. In: The Rat Nervous System (Paxinos G, ed), pp 443-492. San Diego: Academic Press.

Amiez C, Petrides M (2009). Anatomical organization of the eye fields in the human and non-human primate frontal cortex. Prog Neurobiol 89: 220-230.

An X, Bandler R, Ongur D, Price JL (1998). Prefrontal cortical projections to longitudinal columns in the midbrain periaqueductal gray in macaque monkeys. J Comp Neurol 401: 455-479.

Applegate CD, Frysinger RC, Kapp BS, Gallagher M (1982). Multiple unit activity recorded from amygdala central nucleus during pavlovian heart rate conditioning in rabbit. Brain Res 238: 457-462.

Arnsten AF, Goldman-Rakic PS (1984). Selective prefrontal cortical projections to the region of the locus coeruleus and raphe nuclei in the rhesus monkey. Brain Res 306(1-2):9-18.

Arnsten AF, Li BM (2005). Neurobiology of executive functions: catecholamine influences on prefrontal cortical functions. Biol. Psychiatry 57: 1377-1384.

Asaad WF, Rainer G, Miller EK (1998). Neural activity in the primate prefrontal cortex during associative learning. Neuron 21: 1399-1407.

Aston-Jones G, Cohen JD (2005). An integrative theory of locus coeruleus-norepinephrine function: adaptive gain and optimal performance. Annu Rev Neurosci 28: 403-50.

Aston-Jones G, Ennis M, Pieribone VA, Nickell WT, Shipley MT (1986). The brain nucleus locus coeruleus: restricted afferent control of a broad efferent network. Sci 234: 734-737.

Aston-Jones G, Iba M, Clayton E, Rajkowski J, Cohen J (2007). The locus coeruleus and regulation of behavioral flexibility and attention: clinical implications. In Brain Norepinephrine: Neurobiology and Therapeutics, ed. Ordway GA, Schwartz MA and Frazer A. Cambridge University Press. Pp 136-235.

Berridge CW, Waterhouse BD (2003). The locus coeruleus-noradrenergic system: modulation of behavioral state and state-dependent cognitive processes. Brain Res Rev 42: 33-84.

Bethus I, Tse D, Morris RG (2010). Dopamine and memory: modulation of the persistence of memory for novel hippocampal NMDA receptor dependent paired associates. J Neurosci 30: 1610-1618.

Biegon A, Fieldust S (1992). Reduced tyrosine hydroxylase immunoreactivity in locus coeruleus of suicide victims. Synapse 10: 79-82.

Blumenfeld RS, Ranganath C (2007). Prefrontal cortex and long-term memory encoding: an integrative review of findings from neuropsychology and neuroimaging. Neuroscientist 13: 280-291.

Bouret S, Sara SJ (2004). Reward expectation, orientation of attention and locus coeruleus-medial frontal cortex interplay during learning. Eur. J. Neurosci. 20: 791-802.

Bouret S, Sara SJ (2005). Network reset: a simplified overarching theory of locus coeruleus noradrenaline function. Trends Neurosci 28: 574-582.

Bruce, CJ, Goldberg ME (1985). Primate frontal eye fields. I. Single neurons discharging before saccades. J. Neurophysiol 53: 603-635.

Bruce CJ, Goldberg ME, Bushnell MC, Stanton, GB (1985). Primate frontal eye fields. II. Physiological and anatomical correlates of electrically evoked eye movements. J. Neurophysiol 54: 714-734.

Cadoret G, Petrides M (2007). Ventrolateral prefrontal neuronal activity related to active controlled memory retrieval in nonhuman primates. Cere Cortex 17: i27-i40.

Carmichael ST, Price JL (1995). Sensory and premotor connections of the orbital and medial prefrontal cortex of macaque monkeys. J Comp Neurol 363: 642-664.

Chan-Palay V (1991). Alterations in the locus coeruleus in dementias of Alzheimer´s and Parkinson´s disease. Prog Brain Res 88: 625-630.

Chan-Palay V (1993). Depression and dementia in Parkinson´s disease. Catecholamine changes in the locus coeruleus, a basis for therapy. Adv Neuorl 60: 438-446.

Chiba T, Kayahara T, Nakano K (2001). Efferent projections of infralimbic and prelimbic areas of the medial prefrontal cortex in the Japanese monkey, *Macaca fuscata*. Brain Res 888: 83–101.

Dahlström A, Fuxe K (1964). Localization of monoamines in the lower brain stem. Experientia 20: 398-399.

De Olmos JS (1972). The amygdaloid projections field in the rat as studied by the cupric-silver method. In: The neurobiology of the amygdala, edited by Elefheriou BE. New York: Plenum, pp. 145-204.

Devoto P, Flore G. 2006. On the origin of cortical dopamine: is it a cotransmitter in noradrenergic neurons? Curr Neuropharmacol 4: 115-125.

Devoto P, Flore G, Saba P, Castelli MP, Piras AP, Luesu W, Viaggi MC, Ennas MG, Gessa GL (2008). 6-Hydroxydopamine lesion in the ventral tegmental area fails to reduce extracellular dopamine in the cerebral cortex. J Neurosci Res 86: 1647-1658.

Devoto P, Flore G, Saba P, Fá M, Gessa GL (2005a). Co-release of noradrenaline and dopamine in the cerebral cortex elicited by single train and repeated train stimulation of the locus coeruleus. BMC Neuroscience 6:31

Drevets WC, Price JL, Simpson JR, Todd RD, Reich T, Vannier M, Raichle ME (1997). Subgenual prefrontal cortex abnormalities in mood disorders. Nature 386: 824-827.

Drevets WC, Ongur D, Price JL (1998). Neuroimaging abnormalities in the subgenual prefrontal cortex: implications for the pathophysiology of familial mood disorders. Mol Psychiatry 3: 220-226.

Duvernoy HM (1998). The human hippocampus. Functional anatomy, vascularization and serial sections with MRI, 2nd edition. Springer, Berlin.

Eschenko O, Sara SJ (2008). Learning-dependent, transient increase of activity in noradrenergic neurons of locus coeruleus during slow wave sleep in the rat: brain stem-cortex interplay for memory consolidation?. Cerebral Cortex 18: 2596-2603.

Everitt BJ, Robbins TW (2005). Neural systems of reinforcement for drug addiction: from actions to habits to compulsion. Nature Neurosci 8(11): 1481-1489.

Falck B, Hillarp NA, Tieme G, Torp A (1962). Fluorescence of catecholamines and related compounds condensed with formaldehyde. J Histochem Cytochem 10: 348-354.

Felten DL, Sladek JR (1983). Monoamine distribution in primate brain V. Monoaminergic nuclei: anatomy, pathways and local organization. Brain Res Bull 10: 171-284

Foote SL, Bloom FE, Aston-Jones G (1983). Nucleus locus coeruleus: new evidence of anatomical and physiological specifity. Physiol Rev 63: 844-914.

Freedman LJ, Insel TR, Smith Y (2000). Subcortical projections of area 25 (subgenual cortex) pf the macaque monkey. J Comp Neurol 421: 172-188.

Freese JL, Amaral DG (2005). The organization of projections from the amygdala to visual cortical areas TE and V1 in the Macaque monkey. J Comp Neurol 486: 295-317.

Gallagher M, Holland PC (1994). The amygdala complex: multiple roles in associative learning and attention. Prog Natl Acad Sci USA 91: 11771-11776.

Gamlin PD, Yoon K (2000). An area for vergence eye movement in primate frontal cortex. Nature 407: 1003-1007.

Gatter KC, Powell TP (1977). The projection of the locus coeruleus upon the neocortex in the macaque monkey. Neurosci 2: 441-445.

German DC, Manaye KF, White CLD, et al. (1992). Disease-specific patterns of locus coeruleus cell loss. Ann Neurol 32: 667-676.

Grenhoff J, Nisell M, Ferré S, Aston-Jones G, Svensson TH (1993). Noradrenergic modulation of midbrain dopamine cell firing elicited by stimulation of the locus coeruleus in the rat. J Neural Transm 93: 11-25.

Harley CW (1987). A role for norepinephrine in arousal, emotion and learning: limbic modulation by norepinephrine and the Kety hypothesis. Prog. Neuropsychopharmacol. Biol. Psychiatry 11: 419-458.

Harley CW (2007). Norepinephrine and the dentate gyrus. Prog. Brain Res. 163: 299-318.

Holland PC, Gallagher M (1999). Amygdala circuitry in attentional and representational processes. Trends Cogn Sci 3: 65-73.

Hoogendijk WJ, Pool CW, Troost D, van Zwieten E, Swaab DF (1995). Image analyzer-assisted morphometry of the locus coeruleus in Alzheimer´s disease, Parkinson´s disease and amyotrophic lateral sclerosis. Brain 118: 131-143.

Hyman BJ, Van Hoesen GW, Damasio AR, Barnes CL (1984). Alzheimer's disease: Cell specific pathology isolates in the hippocampal formation. Sci 225: 121-122.

Insausti R, Amaral DG (2004). Hippocampal Formation. In Paxinos G, Mai JK, The Human Nervous System. Chapter 23, pp. 871-914. Elsevier Academic Press.

Insausti R, Amaral DG, Cowan WM (1987). The entorhinal cortex of the monkey: III. Subcortical afferents. J Comp Neurol 264: 396-408.

Insausti R, Herrero MT, Witter MP (1997). Entorhinal cortex of the rat: cytoarchitectonic subdivisions and the origin and distribution of cortical efferents. Hippocampus 7(2): 146-183.

Jöels, M. (2009), Stress, the hippocampus, and epilepsy. Epilepsia. 50: 586-597.

Kapp BS, Frysinger RC, Gallagher M, Haselton JR (1979). Amygdala central nucleus lessions: effect on heart rate condicioning in the rabbit. Physiol Behav 23: 1109-1117.

Kitchigina V, Vankov A, Harley C, Sara SJ (1997). Novelty-elicited, noradrenaline-dependent enhancement of excitability in the dentate gyrus. Eur J Neurosci 9: 41-47.

Kobayashi Y, Amaral DG (1999). Chemical neuroanatomy of hippocampal formation and the perirhinal and parahippocampal cortices. In: The Primate Nervous System, Part III (Bloom FE, Björklund A, Hökfelt T, eds), pp 285-401. Amsterdam: Elsevier.

Krettek JE, Price JL (1978). A description of the amygdaloid complex in the rat and cat with observations on intra-amygdaloid axonal connections. J Comp Neurol 178: 255–280.

Lemon N, Aydin-Abidin S, Funke K, Manahan-Vaughan D (2009). Locus coeruleus activation facilitates memory encoding and induces hippocampal LTD that depends on ß-adrenergic receptor activation. Cerebral Cortex 19: 2827-2837.

LeDoux JE (2000). Emotion circuits in the brain. Annu Rev Neurosci 23: 155-184.

Levy R, Goldman-Rakic PS (2000). Segregation of working memory functions within the dorsolateral prefrontal cortex. Exp Brain Res 133: 23-32.

Lim EP, Tan CH, Jay TM, Dawe GS (2010). Locus coeruleus stimulation and noradrenergic modulation of hippocampo-prefrontal cortex long-term potentiation. Int J Neuropsychopharmacol. 13(9): 1219-1231.

Luppi PH, Aston-Jones G, Akaoka H, Chouvets G, Jouvet M (1995). Afferent projections to the rat locus coeruleus demonstrated by retrograde and anterograde tracing with cholera-toxin b subunit and *Phaseolus vulgaris leucoagglutinin*. Neurosci 65(1): 119-160.

Mayberg HS, Liotti M, Brannan SK, McGinnis S, Mahurin RK, Jerabek PA, Silva JA, Tekell JL, Martin CC, Lancaster JL, Fox PT (1999). Reciprocal limbic-cortical function and negative mood: converging PET findings in depression and normal sadness. Am J Psychiatry 156: 675-682.

Mayberg HS, Lozano AM, Voon V, McNeely HE, Seminowicz D, Hamani C, Schwalb JM, Kennedy SH (2005). Deep brain stimulation for treatmen resistant depression. Neuron 45: 651-660.

McDonald AJ (1998). Cortical pathways to the mammalian amygdala. Prog Brain Res 55: 257-332.

McGaugh JL, Cahill L, Rozendaal B (1996). Involvement of the amygdala in memory storage: interactions with other brain systems. Prog Natl Acad Sci USA 93: 13508-13514.

McGaugh JL, Roozendaal B (2008). Drug enhancement of memory consolidation: historical perspective and neurobiological implications. Psychopharmacol 202: 3-14.

Miller EK (2013). The “working” of working memory. Dialogues Clin Neurosci 15: 411-418.

Mishkin M (1978). Memory in monkeys severely impaired by combined but not by separate removal of amygdala and hippocampus. Nature 273: 297-298.

Monosov IE, Thompson KG (2009). Frontal eye field activity enhances object identification during covert visual search. J Neurophysiol 102: 3656-3672.

Muñoz-López M (2015). Past, Present, and Future in Hippocampal Formation and Memory Research. Hippocampus 25:726–730.

Muñoz M, Morris RGM (2009). Episodic Memory: Assessment in Animals. In: Squire LR (ed.) Encyclopedia of Neuroscience, volume 3, pp. 1173-1182. Oxford: Academic Press.

O’Carroll CM, Martin SJ, Sandin J, Frenguelli B, Morris RG (2006). Dopaminergic modulation of the persistence of one-trial hippocampus dependent memory. Learn Mem 13: 760-769.

Ongur D, Price JL (2000). The organization of networks within the orbital and medial prefrontal cortex of rats, monkeys and humans. Cereb Cortex 10: 206-219.

Ordway GA, Smith KS, Haycock JW (1994). Elevated tyroxine hydroxylase in the locus coeruleus of suicide victims. J Neurochem 62: 680-685.

Ordway GA, Widdowson PS, Smith KS, Halaris A (1994b). Agonist binding to alpha 2-adrenoceptors is elevated in the locus coeruleus from victims of suicide. J Neurochem 63: 617-624.

O’Scalaidhe SP, Wilson FA, Goldman-Rakic PS (1997). Areal segregation of face processing neurons in prefrontal cortex. Science 278: 1135-1138.

Padoa-Schioppa C, Assad JA (2006). Neurons in the orbitofrontal cortex encode economic value. Nature 441: 223-226.

Paladini CA, Williams JT (2004). Noradrenergic inhibition of midbrain dopamine neurons. J Neurosci 24(19): 4568-4575.

Pascoe JP, Kapp BS (1985). Electrophysiological characteristics of amygdaloid central nucleus neurons in the awake rabbit. Brain Res Bull 14: 331-338.

Passingham RE, Toni I, Rushworth MF (2000). Specialisation within the prefrontal cortex: the ventral prefrontal cortex and associative learning. Exp Brain Res 133: 103-113.

Peng X, Sereno ME, Silva AK, Lehky SR, Sereno AB (2008). Shape selectivity in primate frontal eye field. J Neurophysiol 100: 796-814.

Petrides M (2005). Lateral prefrontal cortex: architectonic and functional organization. Philos Trans R Soc Lond B Biol Sci 360: 781-795.

Pitkänen A (2000). Connectivity of the rat amygdaloid complex. In: The Amygdala: A Functional Analysis, edited by Aggleton JP. Oxford, UK: Oxford Univ. Press, 2000, p. 31–115.

Pitkänen A, Amaral DG (1998). Organization of the intrinsic connections of the monkey amygdaloid complex: projections originating in the lateral nucleus. J Comp Neurol 398: 431-458.

Pitkänen A, Kelly JL, Amaral DG (2002). Projections From the Lateral, Basal, and Accessory Basal Nuclei of the Amygdala to the Entorhinal Cortex in the Macaque Monkey. Hippocampus 12: 186-205.

Price JL (2003). Comparative aspects of amygdala connectivity. Ann NY Acad Sci 985: 50-58.

Price JL, Amaral DG (1981). An autoradiographic study of the projections of the central nucleus of the monkey amygdala. J Neurosci 1(11): 1242-1259.

Price JL, Drevets WC (2012). Neural circuits underlying the pathophysiology of mood disorders. Trends Cogn Sci 16: 61-71.

Price JL, Russchen FT, Amaral DG (1987). The limbic region. II: the amygdaloid complex. In Bjorklund A, Hokfelt T, Swanson LW (eds), Handbook of Chemical Neuroanatomy, Vol. 5, Integrated Systems of the CNS, Part I. Elsevier Science, Amsterdam. pp. 279-388.

Rajkowski J, Majczynski H, Clayton EC, Aston-Jones G (2004). Activation of monkey locus coeruleus neurons varies with difficulty and behavioural performance in a target detection task. J Neurophysiol 92(1): 361-371.

Ramos BP, Colgan L, Nou E, Ovadia S, Wilson SR, Arnsten AF (2005). The beta-1 adrenergic antagonist, betaxolol, improves working memory performance in rats and monkeys. Biol Psychiatry 58: 894-900.

Reil JC (1809). Untersuchungenüber den Bau des grossen Gehirns im Meschen. Arch Physiol 9: 136-524.

Rempel-Clower NL, Zola SM, Squire LR, Amaral DG (1996). Three cases of enduring memory impairment after bilateral damage limited to the hippocampal formation. J Neurosci 16: 5233-5255.

Robbins TW, Roberts AC (2007). Differential regulation of fronto-executive function by the monoamines and acetylcholine. Cereb. Cortex 17: i151-i160.

Romanski LM (2012). Integration of faces and vocalizations in ventral prefrontal cortex: implications for the evolution of audiovisual speech. Proc Natl Acad Sci USA 109: 10717-10724.

Roozendaal B, Lengvilas R, McGaugh JL, Civelli O, Reinscheid RK (2007). Orphanin FQ/nociception interacts with the basolateral amygdala noradrenergic system in memory consolidation. Learn Mem 14: 29-35.

Rosene DL, Van Hoesen G (1987). Hippocampal formation of the primate brain. Cereb cortex 6: 345-455.

Rudebeck PH, Murray EA (2011a). Balkanizing the primate orbitofrontal cortex: distinct subregions for comparing and contrasting values. Ann N Y Acad Sci 1239: 1-13.

Rudebeck PH, Murray EA (2011b). Dissociable effects of subtotal lesions within the macaque orbital prefrontal cortex on reward-guided behavior. J Neurosci 31: 10569-10578.

Russel GV (1955). The nucleus locus coeruleus (dorsolateralis tegmenti). Texas Rep Biol Med 13: 939-988.

Saleem KS, Kondo H, Price JL. 2008. Complementary circuits connecting the orbital and medial prefrontal networks with the temporal, insular, and opercular cortex in the macaque monkey. Journal of Comparative Neurology 506(4):659-693.

Saleem KS, Miller B, Price JL (2014). Subdivisions and connectional networks of the lateral prefrontal cortex in the macaque monkey. J Comp Neurol 522: 1641-1690.

Sara SJ (2012). The locus coeruleus and noradrenergic modulation of cognition. Nat Rev Neurosci 10: 211-223.

Sara SJ, Vankov A, Herve A (1994). Locus coeruleus-evoked responses in behaving rats: a clue to the role of noradrenaline in memory. Brain Res Bull 35: 457-465.

Schwartzkroin PA (1994). Role of the hippocampus in epilepsy. Hippocampus 4(3): 239-242.

Shipley MT, Fu L, Ennis M, Liu WL, Aston-Jones G (1996). Dendrites of locus coeruleus neurons extend preferentially into two pericoerulear zones. J Comp Neurol 365: 56-68.

Siever LJ, Davis KL (1985). Overview: toward a dysregulation hypothesis of depression. Am J Psychiatry 142: 1017-1031.

Smith CC, Greene RW (2012). CNS dopamine transmission mediated by noradrenergic innervation. J Neurosci 32(18): 6072-6080.

Solano MV (1998). Neuropsychopharmacological mechanisms of stimulant drugs action in attention-deficit hyperactivity disorder: a review and integration. Behav Brain Res 94: 127-152.

Squire LR, Zola-Morgan S (1991). The medial temporal lobe memory system. Science 253: 1380-1386.

Stefanacci L, Amaral DG (2000). Topographic organization of cortical inputs to the lateral nucleus of the macaque monkey amygdala: a retrograde tracing study. J of Comp Neurol 421: 52–79.

Sterpenich V, D'Argembeau A, Desseilles M, Balteau E, Albouy G, Vandewalle G, Degueldre C, Luxen A, Collette F, Maquet P (2006). The locus coeruleus is involved in the successful retrieval of emotional memories in humans. J Neurosci 26: 7416:7423.

Strange BA, Witter MP, Lein ES, Moser EI (2014). Functional organization of the hippocampal longitudinal axis. Nat Rev Neurosci 15: 655-669.

Tehovnik EJ, Sommer MA, Chou IH, Slocum WM, Schiller PH (2000). Eye fields in the frontal lobes of primates. Brain Res Rev 32: 413-48.

Tsao DY, Schweers N, Moeller S, Freiwald WA (2008b). Patches of face-selective cortex in the macaque frontal lobe. Nat Neurosci 11: 877-879.

Usher M, Cohen JD, Servan-Schreiber D et al. (1999). The role of locus coeruleus in the regulation of cognitive performance. Sci 283: 549-554.

Vankov A, Hervé-Minvielle A, Sara SJ (1995). Response to novelty and its rapid habituation in locus coeruleus neurons of freely exploring rat. Eur J Neurosci 7: 1180-1187.

Vargha-Khadem F, Gadian DG, Watkins KE, Connelly A, Van Paesschen W, Mishkin M (1997). Differential effects of early hippocampal pathology on episodic and semantic memory. Sci 277: 376-380.

Wenzel J, Wenzel C (1812). De Penitiori Structura Cerebri Hominis et Brutorum. Tübingen.

West MJ (1993). Regionally specific loss of neurons in the aging human hippocampus. Neurobiol Aging 14(4): 287-293.

Widdowson PS, Orsway GA, Halaris A (1992). Reduced neuropeptide Y concentrations in suicide brain. J Neurochem 59: 73-80.

Wilson FA, O'Scalaidhe SP, Goldman-Rakic PS (1993). Dissociation of object and spatial processing domains in primate prefrontal cortex. Science 260: 1955-1958.

Witter MP (1993). Organization of the entorhinal-hippocampal system: a review of current anatomical data. Hippocampus 3: 33-44.

Witter MP, Van Hoesen GW, Amaral DG (1989). Topographical organization of the entorhinal projection to the dentate gyrus of the monkey. J Neurosci 9: 216-228.

Yu AJ, Dayan P (2005). Uncertainty, neuromodulation, and attention. Neuron 46: 681-692.

Zhou H, Desimone R. (2011). Feature-based attention in the frontal eye field and area V4 during visual search. Neuron 70: 1205-17.

Zweig RM, Cardillo JE, Cohen M, Giere S, Hedreen JC (1993). The locus coeruleus and dementia in Parkinson´s disease. Neurology 43: 986-991.

V. STATEMENT OF CONTRIBUTIONS

V. STATEMENT OF CONTRIBUTIONS

All the projects presented were carried out under the joint supervision of Dr. Henry Evrard by the Max Planck Institute (University of Tübingen, Germany) and Prof. Dr. Ricardo Insausti by the University of Castilla-La Mancha (Spain).

Additional collaboration was established with Prof. Joseph Price at the Washington University (St. Louis, USA) and Prof. David Amaral at the MIND Institute (UC Davis, California, USA).

1. **Hippocampal formation and amygdaloid projections to the *Locus coeruleus* in the nonhuman primate.**

The following persons collaborated in this project and are listed in alphabetic order (with the exception of the first author).

Ubero M*: First author. Conception. Acquisition of the data. Analysis of the data. Interpretation of the results. Writing the manuscript.

Amaral D: Acquisition of the data.

Evrard H: Conception. Acquisition of the data. Interpretation of the results. Writing the manuscript.

Hernández D: Conception, acquisition of the data.

Insausti R: Acquisition of the data. Interpretation of the results. Writing the manuscript.

Logothetis N: Acquisition of the data.

2. **Cortical Afferents to the *Locus Coeruleus* in the *Macaca fascicularis* Monkey.**

The following persons collaborated in this project and are listed in alphabetic order (with the exception of the first author).

Ubero M*: First author. Conception. Acquisition of the data. Analysis of the data. Interpretation of the results. Writing the manuscript.

Evrard H: Conception. Acquisition of the data. Interpretation of the results. Writing the manuscript.

Hernández D: Conception, acquisition of the data.

Insausti R: Acquisition of the data. Interpretation of the results. Writing the manuscript.

Logothetis N: Acquisition of the data.

Price J: Acquisition of the data.

3. **Heterogeneous prefrontal projections to the midbrain ventral tegmental area in the macaque monkey.**

The following persons collaborated in this project and are listed in alphabetic order (with the exception of the first author).

Hernández D: First author. Conception. Acquisition of the data. Analysis of the data. Interpretation of the results. Writing the manuscript.

Evrard H: Conception. Acquisition of the data. Interpretation of the results. Writing the manuscript.

Insausti R: Acquisition of the data. Interpretation of the results. Writing the manuscript.

Logothetis N: Acquisition of the data.

Price J: Acquisition of the data.

Ubero M: Conception, acquisition of the data.

4. **Heterogeneous Hippocampal formation and Amygdala projections to the ventral tegmental area in the macaque monkey.**

The following persons collaborated in this project and are listed in alphabetic order (with the exception of the first author).

Hernández D: First author. Conception. Acquisition of the data. Analysis of the data. Interpretation of the results. Writing the manuscript.

Amaral D: Acquisition of the data.

Evrard H: Conception. Acquisition of the data. Interpretation of the results. Writing the manuscript.

Insausti R: Acquisition of the data. Interpretation of the results. Writing the manuscript.

Logothetis N: Acquisition of the data.

Ubero M: Conception, acquisition of the data.

VI. RESULTS

CHAPTER 1. Hippocampal formation and amygdaloid projections to the *Locus coeruleus* in the nonhuman primate

ABSTRACT

The *Locus coeruleus* (LC) modulates the limbic system through direct projections to the hippocampal formation (HF) and amygdala (Amy) that in turn, regulate noradrenergic activity necessary for memory processing. Whether this regulation courses through direct projections or through indirect connections is unknown. Only the central nucleus of the amygdala has been reported to target directly and regulate the activity of LC. Here, we examine whether such modulation of the HF and Amy could be relayed by direct afferents to LC. Deposits of biotin-dextran amine, *Phaseolus vulgaris* leucoagglutinin or tritiated aminoacids in the dentate gyrus, hippocampus (CA1-3), entorhinal cortex, and subiculum, as well as in different deep nuclei of the amygdaloid complex, resulted in anterograde labeling that was analyzed. Overall, deposits in the subiculum resulted in the highest number of labeled fibers and presumably synaptic terminals in LC, particularly localized throughout the entire rostrocaudal extent of the lateral portion of the nucleus. Injections placed in the entorhinal cortex produced labeling, but the deposit spread into the amygdala and a differential analysis suggests that the labeling produced with injections centered in EC actually likely originate in the Amy. Injections in CA1-3 or dentate gyrus did not produce any labeling. Within the amygdala, only the injections made in the basal and the paralaminar nuclei produced labeling in the lateral portion of LC, similar to the labeling produced after deposits into the subiculum. Prior studies showed that both subiculum and the basal nucleus of the amygdala receive projections from LC. The present study shows that these projections are bidirectional in primates and that the spatial distribution of both subiculum and amygdala overlaps within the lateral portion of locus coeruleus, suggesting a role for LC in memory processing under emotional context.

INTRODUCTION

The noradrenergic (NA) system has been shown to be involved in memory processing (Roullet and Sara 1998; Tronel et al., 2004; McGaugh and Roozendaal, 2008), as well as synaptic plasticity in the hippocampus and amygdala (Tully and

Bolshakov, 2010). The majority of the NA neurons are allocated in the brainstem, the most important of which is the *Locus coeruleus* (LC), which fires at critical periods during learning, off-line memory consolidation and retrieval (Sara, 2009).

LC phasically responds to novel salient stimuli arising from ascending sensory afferents (Aston-Jones and Bloom, 1981) and modulates the limbic system, and in particular the HF and Amy through direct projections (Jones and Moore, 1977; Bowden et al., 1978; Fallon et al., 1978; Amaral and Cowan, 1980; Loughlin et al., 1986; Insausti et al., 1987; Wilcox and Unnerstall, 1990). Those, in turn might regulate the noradrenergic activity necessary for memory processing. Whether this regulation courses through direct or through indirect connections is largely unknown.

There is no anatomical data demonstrating the existence of direct inputs from the HF to LC. In fact, there are studies in both rodents and primates indicating that the only cortical region showing direct projections to the LC is the prefrontal cortex (PFC) (Cedarbaum and Aghajanian, 1978; Arnsten and Golman-Rakic, 1984; Luppi et al., 1995; Freedman et al., 2000; Chiba et al., 2001; Aston-Jones and Cohen, 2005; Lu et al., 2012). Regarding the amygdaloid complex, only the central nucleus of the amygdala (CeA) has been shown to send a rather strong projection to LC in both rodents and monkeys (Price and Amaral, 1981; Ennis et al., 1991; Luppi et al., 1995). No evidence for other amygdala nuclei projections to the LC exists, to the best of our knowledge.

However, functional studies indicate that HF and Amy might project to the LC and, therefore, regulate the activity of NA-LC under certain conditions. Pharmacological studies in rodents revealed that, after a learning experience, there is a time window during which the NA system is activated to reinforce long-term memory processing (Sara et al., 1999; Tronel et al., 2004). On the other hand, the Amy might also improve the retrieval of emotional memories by modulating central arousal by the LC (Davis and Whalen, 2001). Furthermore, functional MRI demonstrated that both Amy and LC are functionally connected during the successful retrieval of memories that were encoded in an emotional context (Sterpenich et al., 2006).

In this study, we used anterograde tract-tracing in the macaque monkey to test whether HF and Amy project directly to LC, and to examine the topographical organization of these projections.

MATERIALS AND METHODS

Subjects

The present data were obtained from 55 young adult *Macaca fascicularis* monkeys (mean weight 3.3 kg, range 2.5–4.5 kg), which had been prepared and used in previous studies (Pitkänen and Amaral, 1998; Bonda, 2000; Pitkänen et al., 2002; Freese and Amaral, 2005; Mohedano-Moriano et al., 2015). The cases were reexamined and the connections with LC analyzed. In addition, anterograde tracers were injected into different subfields of the EC in 3 more monkeys.

All procedures were carried out under an approved University of California-Davis Institutional Animal Care and Use Protocol, and strictly adhered to National Institutes of Health policies on primate animal subjects. Likewise, experiments were conducted according to the guideline of the European Community on welfare of research animals (directive 86/609/EEC) and the supervision and approval of the Ethical Committee of Animal Research of the University of Castilla-La Mancha (UCLM), Spain.

Surgery and tracer injection

Animals were tranquilized with an initial intramuscular dose of ketamine HCl (8 mg/Kg), fitted with a tracheal cannula, and brought to a surgical level of anesthesia with isoflurane. All surgeries were performed under sterile conditions, and the animal's heart rate, respiration, temperature, and blood oxygenation were monitored throughout the procedure. The animal was placed in a Kopf stereotaxic apparatus; a midline incision was made, and a small burr hole was drilled in the skull at a position appropriate for the injection of tracer. The coordinates were based on the atlas of Szabo and Cowan (1984). The dorsoventral coordinate for the injection was determined by recording extracellular unit activity along the injection trajectory, as described previously (Amaral and Price, 1984). Postoperatively, the monkeys received analgesics as needed and prophylactic doses of antibiotics.

Different anterograde tracers were injected in the hippocampal formation and

the deep amygdala nuclei. The tracer *Phaseolus vulgaris* leucoagglutin (PHA-L) was iontophoretically injected as a 2.5% solution of in 0.1 M sodium phosphate buffer, pH 7.4 (5-μA pulsed DC current, 7 seconds on and 7 seconds off, for 40–45 minutes). The ^{3}H-aminoacid injections contained an equal amount of ^{3}H-leucine and ^{3}H-proline (L-[4-5-3H] leucine; L-[2, 3-3H] proline, respectively, New England Nuclear, Dupont, DE, USA), vacuum evaporated and reconstituted to a final concentration of 100 μC/μl (see Insausti and Amaral, 2008 for details). Injections of biotin dextran amine (BDA, 10.000 MW, lysine fixable, 10%, Molecular Probes, Eugen, OR, USA) were injected either by iontophoresis (Freese and Amaral, 2005) or by pressure (Muñoz and Insausti 2005; Mohedano-Moriano et al., 2008)

To avoid spread of tracer along the pipette track, the micropipette was left in place for 30 minutes after the injection was finished.

Perfusion and histological processing

After a 2-week survival period, the animals were the animals were anesthetized with ketamine (10 mg/kg, i.m.), followed by sodium pentobarbital (25–30 mg/kg, i.v.), and transcardially perfused with 0.5 L of cold 1% paraformaldehyde in 0.1 M phosphate buffer followed by 7.0 L of cold 4% paraformaldehyde in 0.1 M phosphate buffer. The brain was blocked stereotaxically, postfixed for 6 hours in 4% paraformaldehyde, and then cryoprotected in 10% glycerol and 2% dimethyl sulfoxide (DMSO) in 0.1 M phosphate buffer (pH 7.4) for 24 hours, then 20% glycerol, 2% DMSO in 0.1 M phosphate buffer for 72 hours. Blocks were subsequently sectioned or stored at –80ºC until they were sectioned into either 30 or 50 μm sections in the coronal plane on a microtome where the stage was frozen with dry ice. After rinses in phosphate buffer, the sections were mounted onto acid cleaned, gelatin-coated slides and stained by the Nissl method with 0.25% thionin. BDA and PHA-L was processed directly with the avidin-biotin-peroxidase method (ABC Elite Kit, Vector, Burlingame, CA).

Data analysis and illustrations

The spatial distribution of labeled terminals was analyzed with an epifluorescence microscope coupled to a computerized charting system (MD-Plot, Datametrics, Minnesota, USA), and each labeled fiber was plotted as a single dot. Subcortical boundaries and other landmarks were added to these plots by camera

lucida drawings of adjacent Nissl-stained sections.

The relative strength or densities of connections was evaluated, although factors such as differences between tracers in transport levels, injection volumes and location of each injection precluded the estimation of absolute values. LC labeling was analyzed bilaterally in coronal sections, and maps were prepared to visualize the spatial distribution and density of the terminal fields across the rostrocaudal extension of the nucleus. Only those fibers contained presumed synaptic buttons or varicosities were represented in the maps.

Nomenclature

Hippocampal formation. The hippocampal formation includes the, dentate gyrus, hippocampus, subiculum, presubiculum, parasubiculum and entorhinal cortex (Insausti and amaral, 2012). The entorhinal cortex was divided into seven subfields according to the nomenclature of Amaral et al. (1987): olfactory entorhinal subfield (Eo), rostral entorhinal subfield (Er), intermediate entorhinal subfield (Ei), lateral rostral entorhinal subfield (Elr), lateral caudal entorhinal subfield (Elc), caudal entorhinal subfield (Ec) and caudal limiting entorhinal subfield (Ecl).

Amygdaloid complex. In this study, we used the nomenclature of Price et al. (1987); Amaral et al. (1992) and Pitkänen & Amaral (1998) for the monkey amygdaloid complex with slight modifications. The deep nuclei of the amygdala consist of the lateral nucleus (dorsal, dorsal intermediate, ventral intermediate, and ventral divisions), the basal nucleus (magnocellular, intermediate, and parvicellular divisions), the accessory basal nucleus (magnocellular, parvicellular and ventromedial divisions) and the paralaminar nucleus.

Locus coeruleus. Anatomically, the LC is composed of a densely packed group of neurons (nuclear core) and a surrounding peripheral zone with more loosely packed neurons (figure 1), which is asymmetrically distributed and contains mostly dendrites. The core of LC is divided into dorsal and ventral parts cytoarchitectonically distinct, since the cells in the dorsal division are more densely packed and a majority of these cells in the dorsal division are aligned obliquely in a dorsomedial to ventrolateral orientation when viewed in the coronal plane of the brain. The less dense part of LC core starts in the rostral pole of LC, and extends caudally, mainly

ventral to the more densely packed part; at midlevel of the rostrocaudal extent, the less dense part spreads both medially, where some sparse medium-size cells are interspersed into the laterodorsal tegmentum, and laterally beyond the mesencephalic tract of the fifth cranial nerve.

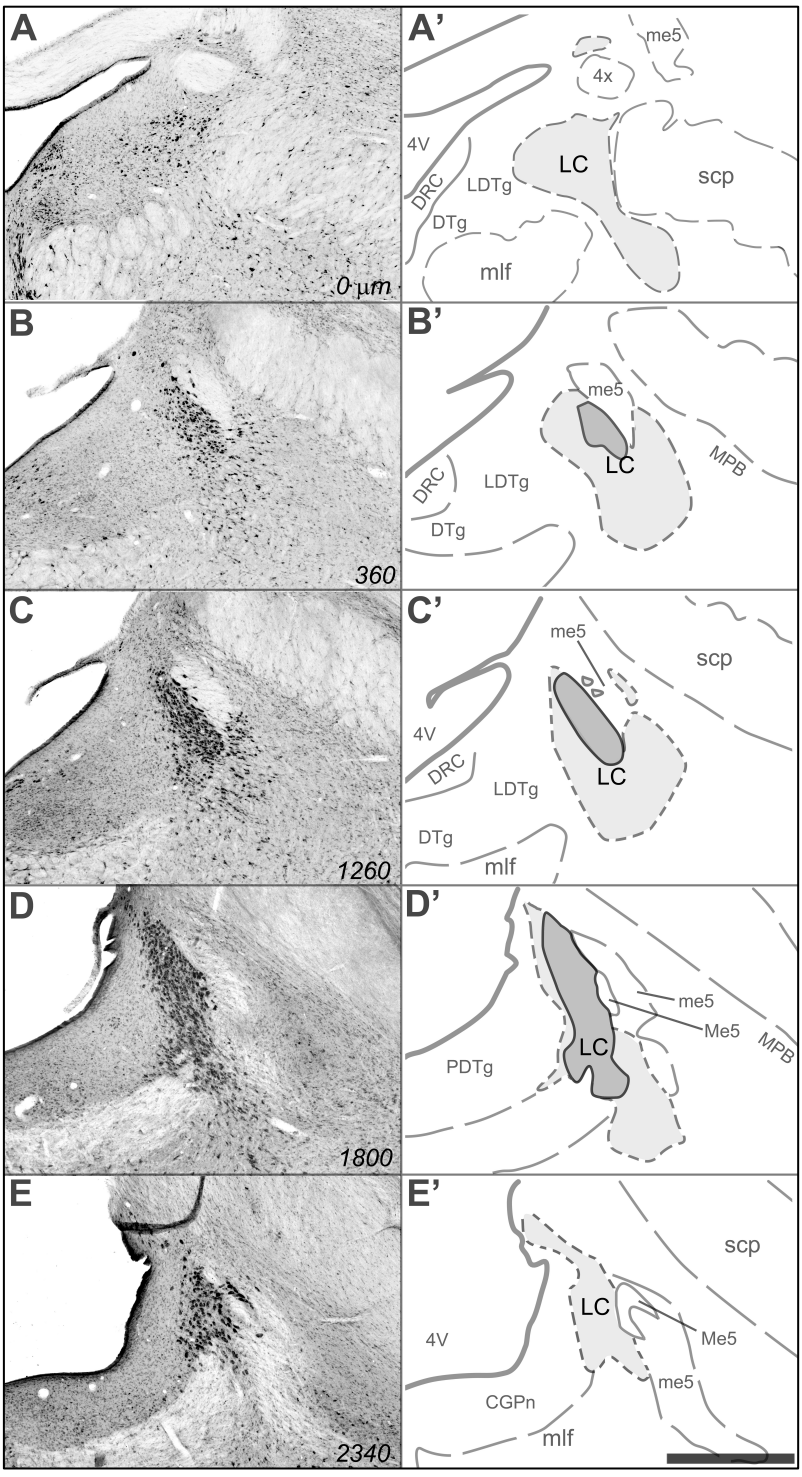

Figure 1. Cytoarchitecture. Coronal sections of LC in the monkey from rostral (A) to caudal (E), and the corresponding drawing (A'-E'). Abbreviations: 4V, fourth ventricle; 4x, trochlear decussation; CGPn, cg pons; DRC, dorsal raphe caudal; DTg, dorsal tegmentum; LDTg, laterodorsal tegmentum; LC, locus coueruleus; me5, mesencephalic tract 5; Me5, mesencephalic nucleus 5; mlf, medial longitudinal fascicle; MPB, medial parabrachial nucleus; scp, superior cerebelar peduncle. Scale bar: 1mm.

RESULTS

Injection sites

Table 1 presents the list of cases, the tracer injected in each case and the location of the injection site. We analyzed the labeling obtained from 71 injections (Table 1) that included DG (n=13), CA1 (n=5), CA2 (n=2), CA3 (n=7), Subiculum/Presubiculum (n=4), EC (n=17) and Amygdala (n=35). Figures 2, 3 and 4 show the collation of all these injections sites onto standard maps of the hippocampus, entorhinal cortex, and amygdaloid complex, respectively.

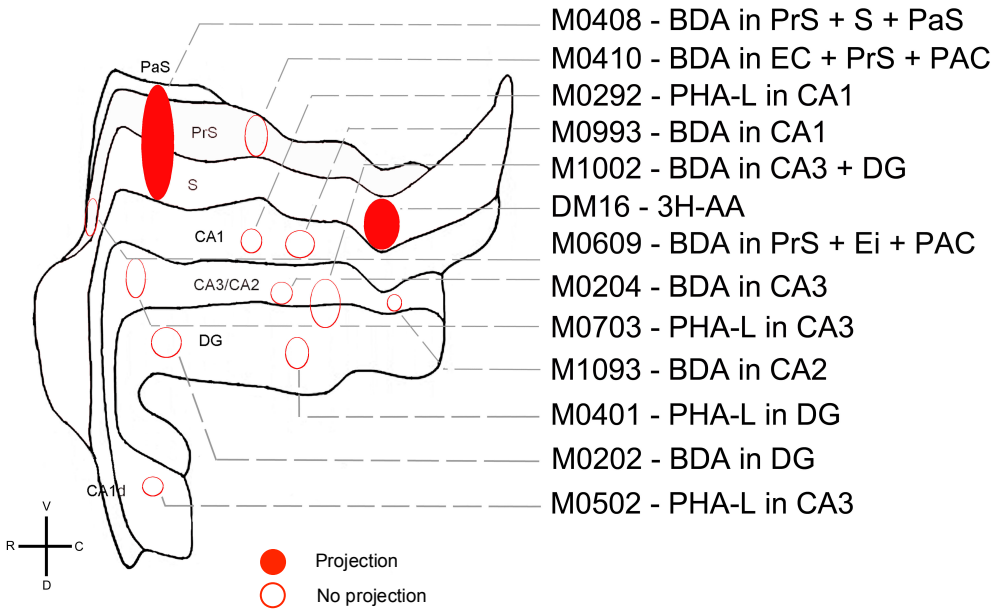

Figure 2. Flat map of the hippocampus, subiculum, presubiculum and parasubiculum.The circles represent the injection sites. Filled circle: project; empty circle: do not project.

Figures 5A-B and 6A-B show examples of injection sites in subiculum and amygdala, respectively. PHA-L and BDA injection sites were identified under both dark and bright field (Fig. 5 and 6) illumination; ^{3}H-aminoacid injection site was identified under dark field illumination (not illustrated).

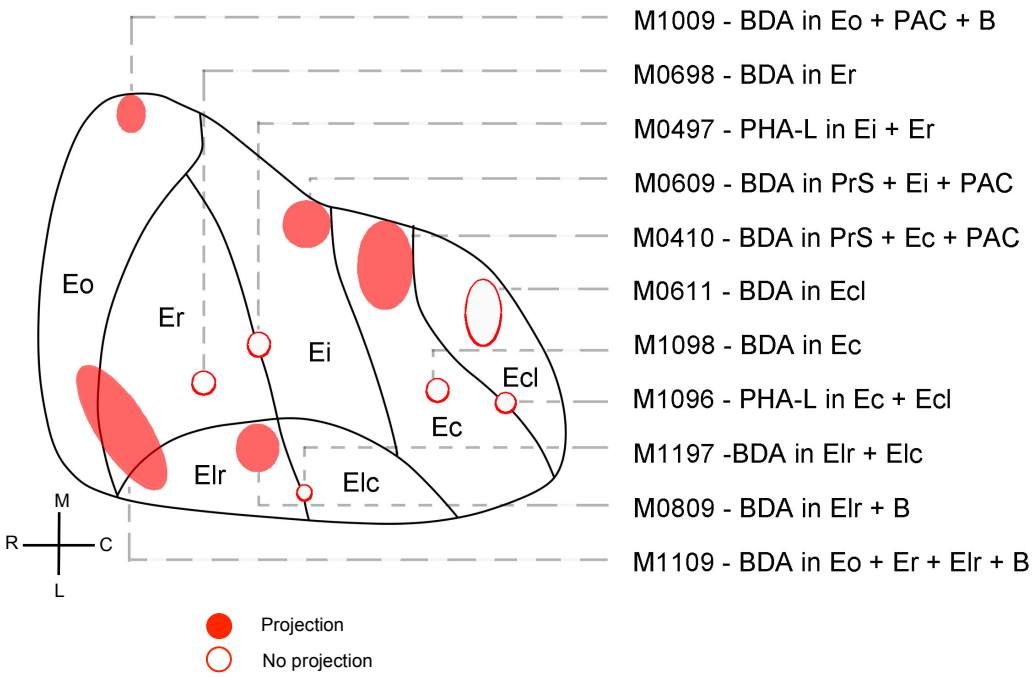

Figure 3. Unfolded map of the entorhinal cortex. The circles represent the injection sites.

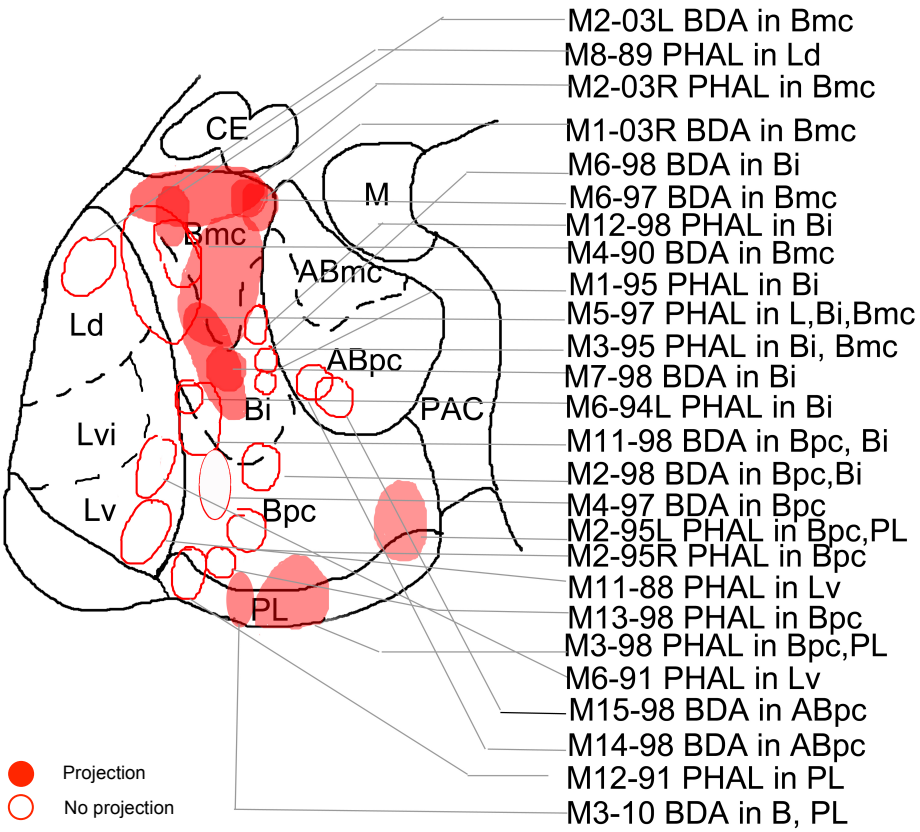

Figure 4. Bidimensional map representing the location of the injection sites in the amygdaloid complex. The circles represent the injection sites.

Due to differences in the amount of the tracer injected and variations in tracer uptake, the injection sites varied in shape and size. The injections of BDA injected by pressure were usually bigger than those injected iontophoretically, where the injections were well restricted to a small region.

The BDA injected by pressure in the EC involved layers I-VI. The tracer did not extend to the white matter in any of the cases, but in some of them the Amy was involved along the tract (See Table 1). The pressure injections of BDA in the Amy were also bigger and the diffusion area usually spread to contiguous nuclei within the Amy. Finally, the iontophoretic injections of BDA and PHA-L in the HF or Amy involved just a small group of cells in a restricted portion, and the layers involved in the EC varied among the different cases.

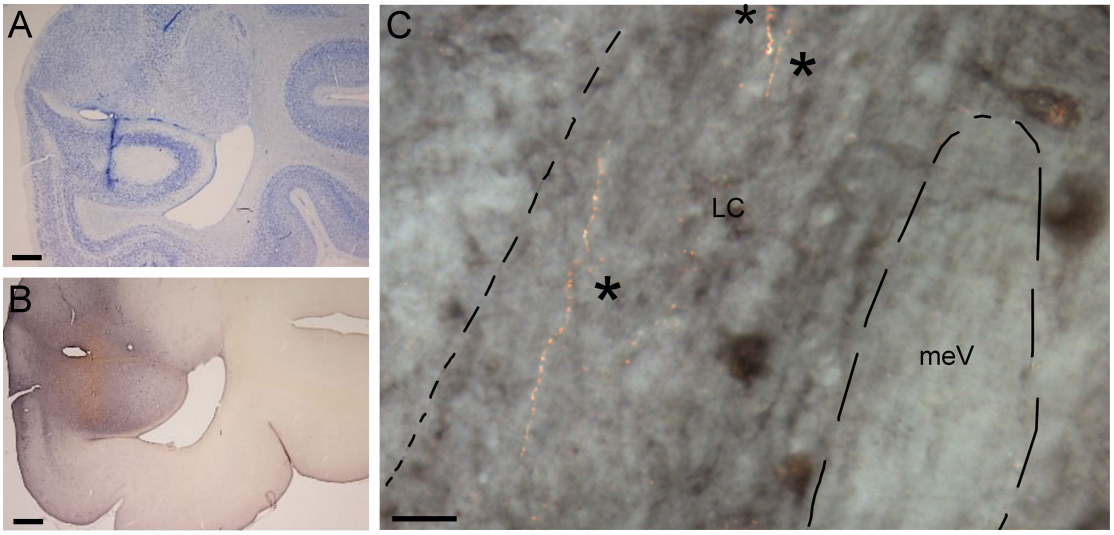

Figure 5. Photomicrographs of coronal section of the injection site in subiculum (M04-08). A. Nissl. B, BDA. C, Darkfield photomicrograph of anterograde labeling in LC. Asterisks indicate labeled fiber. Scale bar: 100μm (A and B), 20μm (C). For abbreviations see legend of figure 1.

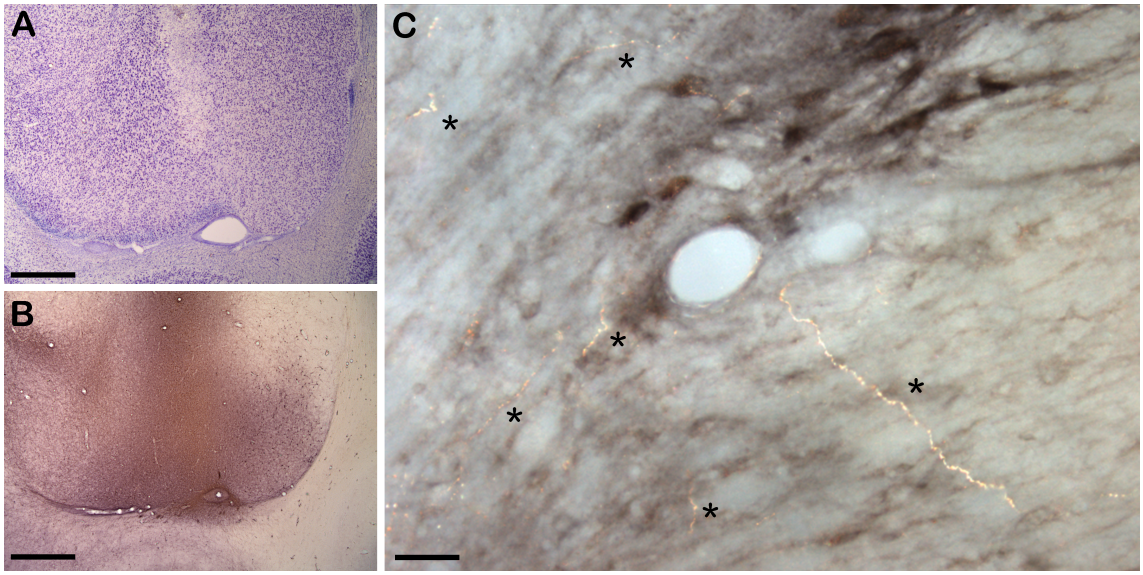

Figure 6. Photomicrographs of coronal section of the injection site in the basal nucleus of the amygdala (M03-10). A. Nissl. B, BDA. C, Darkfield photomicrograph of anterograde labeling in LC. Asterisks indicate labeled fiber. For bbreviations see legend of figure 1. Scale bar: 100μm (A and B), 20μm (C).

TABLE 1. Anterograde tracer injections in the hippocampal formation[1] and the amygdala[1]. + Symbol refers to the presence of labeled fibers (> 1), - symbol refers to the absence of labeling (<1).

			INJECTION SITE																							
			HIPPOCAMPAL FORMATION													AMYGDALA										
				Hippocampus			Subicular Complex			Entorhinal Cortex						Lateral			Basal			Accesory Basal	Paralaminar			
	CASE	TRACER	DG	CA1	CA2	CA3	Sub	PrS	PaS	Eo	Er	Ei	Elr	Elc	Ec	Ecl	Ld	Lvi	Lv	Bmc	Bi	Bpc	ABpc	PL	PAC	AHA	Labeling
1	M01-02	PHA-L	■																								-
2	M02-02	PHA-L	■																								-
3	M02-02	BDA	■																								-
4	M03-02	PHA-L	■																								-
5	M04-01	BDA	■																								-
6	M04-01	PHA-L	■																								-
7	M04-02	PHA-L	■																								-
8	M04-02	BDA	■																								-
9	M10-02	PHA-L	■																								-
10	M11-92	PHA-L	■																								-
11	M02-04	PHA-L	■	■																							-
12	M09-03	BDA	■			■																					-
13	M10-02	BDA	■			■																					-
14	M02-92	PHA-L		■																							-
15	M09-93	BDA		■																							-
16	M14-03	BDA		■																							-
17	M28-92	PHA-L		■	■																						-
18	M10-93	BDA			■																						-
19	M07-03	BDA				■																					-
20	M9-92	PHA-L				■																					-
21	M05-02	PHA-L				■																					-
22	M07-03	PHA-L				■																					-
23	M02-04	BDA				■																					-
24	DM16	3H-AA					■																				+
25	M04-08	BDA					■	■	■																		+
26	M06-09	BDA						■				■													■		-
27	M04-10	BDA						■							■											■	+
28	M12-98	BDA									■																-
29	M3-98	BDA									■																-
30	M12-97	PHA-L										■															-
31	M02-97	PHA-L													■	■											-
32	M11-97	BDA											■	■													-
33	M10-87	3H-AA											■														+
34	M10-96	PHA-L													■	■											-
35	M10-98	BDA													■												-
36	M06-11	BDA														■											-
37	M04-97	PHA-L									■	■															-
38	M06-98	BDA									■																-
39	M10-09	BDA								■												■	■		■		+
40	M08-09	BDA											■								■	■	■	■			+
41	M03-10	BDA																		■	■	■		■			+
42	M11-09	BDA								■	■		■								■	■					+
43	M4-90	BDA																		■							-
44	M8-89	PHA-L															■										-
45	M11-88	PHA-L																	■								-
46	M6-91	PHA-L																	■								-
47	M12-91	PHA-L																						■			-
48	M1-95	PHA-L																			■						-
49	M2-95L	PHA-L																				■		■			+
50	M2-95R	PHA-L																				■					+
51	M3-95	PHA-L																		■	■						+
52	M4-97	BDA																				■					-
53	M5-97	PHA-L																■	■	■	■						-
54	M6-97	BDA																		■							+
55	M6-94L	PHA-L																			■						-
56	M3-98	PHA-L																				■		■			+
57	M2-98	BDA																			■	■					-
58	M6-98	BDA																			■						-
59	M11-98	BDA																			■	■					-
60	M7-98	BDA																			■						+
61	M13-98	PHA-L																				■					-
62	M14-98	BDA																					■				-
63	M15-98	BDA																					■				-
64	M12-98	PHA-L																		■							+
65	M1-03R	BDA																		■							+
66	M1-03L	PHA-L																		■	■						+
67	M2-03R	PHA-L																		■							+
68	M2-03L	BDA																		■							+
69	M14-97	BDA																					■				-
70	M6-98	PHA-L																				■					+
71	M12-98	PHA-L																		■							+

[1]For abbreviations, see list.

Limbic afferents to the *Locus coeruleus*

The anterogradely labeled fibers had a sinuous shape with a high number of varicosities (figures 5C, and 6C), mainly distributed in the ipsilateral hemisphere; however there was scarce labeling also into the contralateral hemisphere that did not represent more than the 5% of the total labeled fibers.

Figures 8 and 9 show the plots of anterograde labeling in sets of coronal sections through LC. Overall, the subiculum and the basal magnocellular nucleus of the amygdala deposits resulted in the heaviest labeling in the core of LC. The majority of the terminal fields were located in the sparse part of the core, although in some cases (e.g. M02-03R, M02-03L, M04-08, M08-09, M03-10) the labeled fibers were present also in the densest part of nucleus. Overall, the most of the labeling was located in the rostrolateral portion of LC, although in some cases a sparse labeling was observed in the medial portion of the LC at caudal levels of the nucleus. Moreover, not all the injections produced labeling in LC.

Hippocampal Formation

The subiculum was the region of the HF that projected most heavily to the LC. Injections in DG and hippocampal fields (CA3, CA2 and CA1) did not produce any labeling. The deposits in EC labeled axons in LC, although in some cases some nuclei of the Amy were involved, and the resulting labeling in LC could have been also originated in the diffusion zone of the deposit.

Subiculum

The data obtained from the analysis of two injections in Sub (figure 2), one with BDA (M04-08; figure 8G) and one with 3H-AA (DM16; not shown but see Table 1), revealed a strong input to LC. The injection of 3H-AA, showed a moderate concentration of silver-aggregates in the lateral part of the ipsilateral nucleus. The BDA injection also showed that the terminal fields in LC were distributed ipsilaterally, and adopted the form of long fibers running longitudinally to the coronal plane and mainly localized within the lateral portion of the core of LC, close to the mesencephalic tract of the fifth cranial nerve. Even though there were fibers throughout the whole rostrocaudal extension of the nucleus, most of them were innervating the rostral levels.

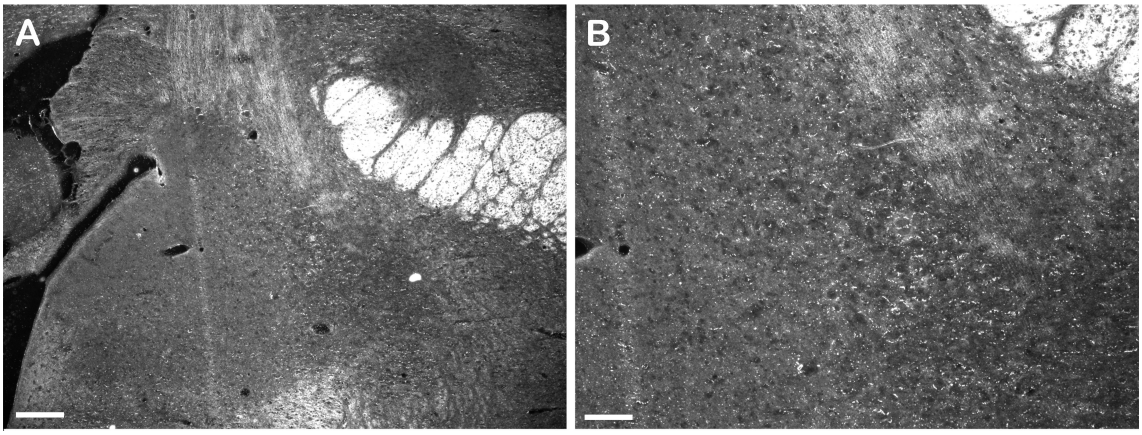

Figure 7. Darkfield photomicrographs of a coronal section showing 3H-AA labeling in the lateral part of the *Locus coeruleus* (case DM16). Scale bar: 100μm (A), 20μm (B)

Presubiculum

Three injections included the PrS (cases M04-08, M06-09, and M04-10; see figure 2). The case M06-09 had an injection of BDA that involved the PrS, Ei and PAC and no labeled axons were found in the LC (Fig. 8D). Therefore, it seems that the PrS does not project directly to LC. In the case M04-10, the BDA injection targeted PrS, EC and AHA and produced moderate to sparse labeling within the ipsilateral core of LC (Fig. 8F). However, some axons also reached the core of the contralateral LC. Since neither PrS nor EC (see below) seemed to send projections, it is likely that the labeling seen in LC could arise in AHA. The case M04-08 has been described above (Fig. 8G).

Dentate Gyrus and Hippocampus

The thirteen injections at different levels of the DG were very small, and involved only a limited number of cells in the most of the cases (not shown in Figs. 7 and 8; but see Table 1). Since no labeled fibers were found in the LC, neither in the periphery nor in the core, there was strong indication that they did not project to LC. Likewise, CA fields, CA3, CA2 and CA1 did not send projections to the LC, since none of the fourteen injections of either BDA or PHA-L made iontophoretically in CA3, CA2 and CA1 fields showed labeling (see Table 1).

Entorhinal Cortex

A total of sixteen injections in different subfields of the entorhinal cortex were analyzed (see Table 1). Eleven out of sixteen injections were located in a specific subfield of the EC without involvement of other brain structures. The result of these

deposits of anterograde tracer either in Eo, Er, Ei, Ec or Ecl was negative as no labeled axons were found (Table 1). However, the injection of 3H-AA in Elr (case M1087) showed moderate to light density of silver deposit in the rostroventral part of the LC (Table 1).

Furthermore, five more BDA injections in EC were analyzed. In these cases, either the deposit or the periphery of the injection site spread to neighboring amygdalar nuclei, and thereby it is likely the labeling obtained arised in the Amy rather than in EC (see below).

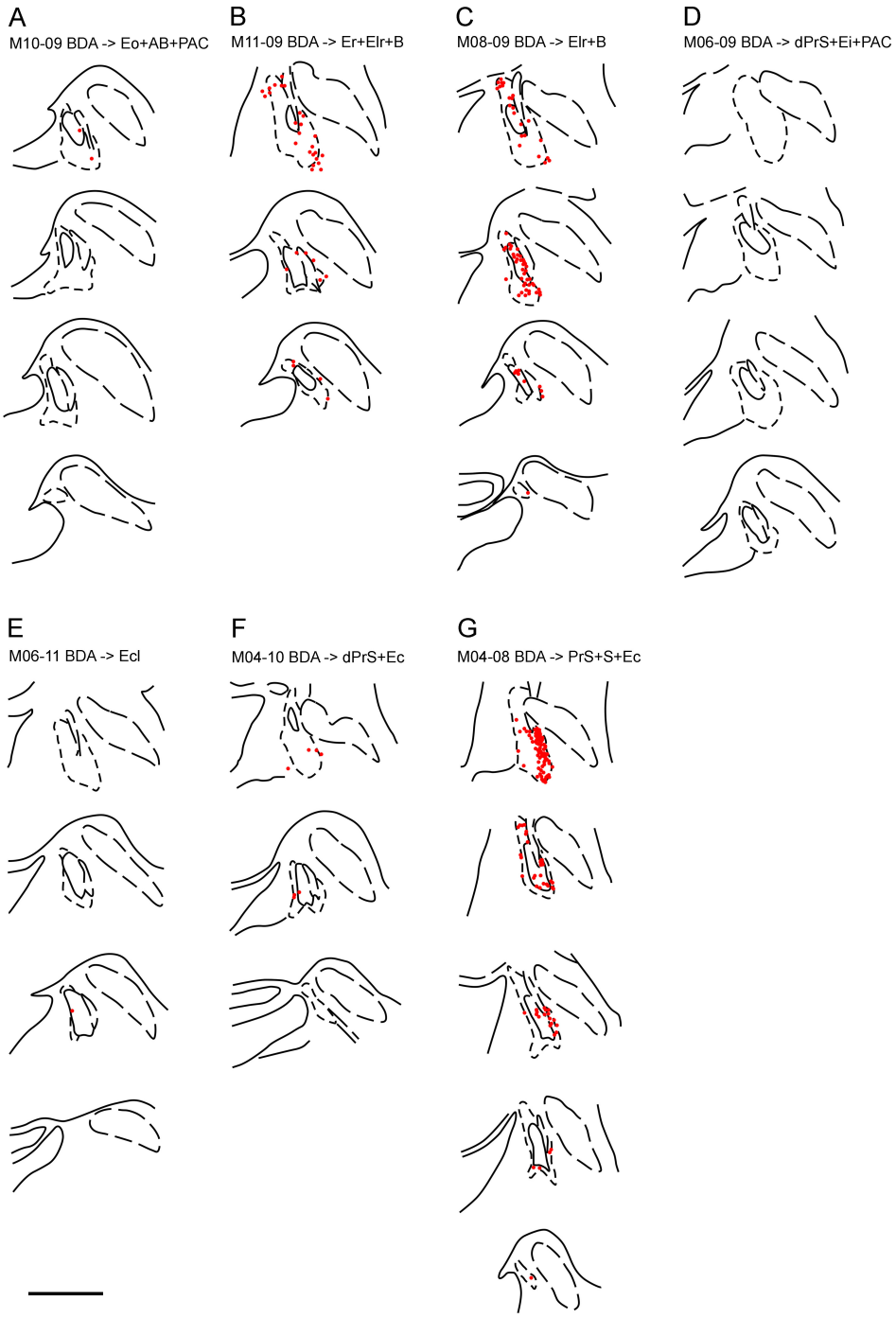

Figure 8. Drawings depicting the labeling obtained in the *Locus coeruleus* after injections of anterograde tracers in the hippocampal formation and the amygdala. Each red dot represents 1 labeled fiber. Scale bar: 2mm.

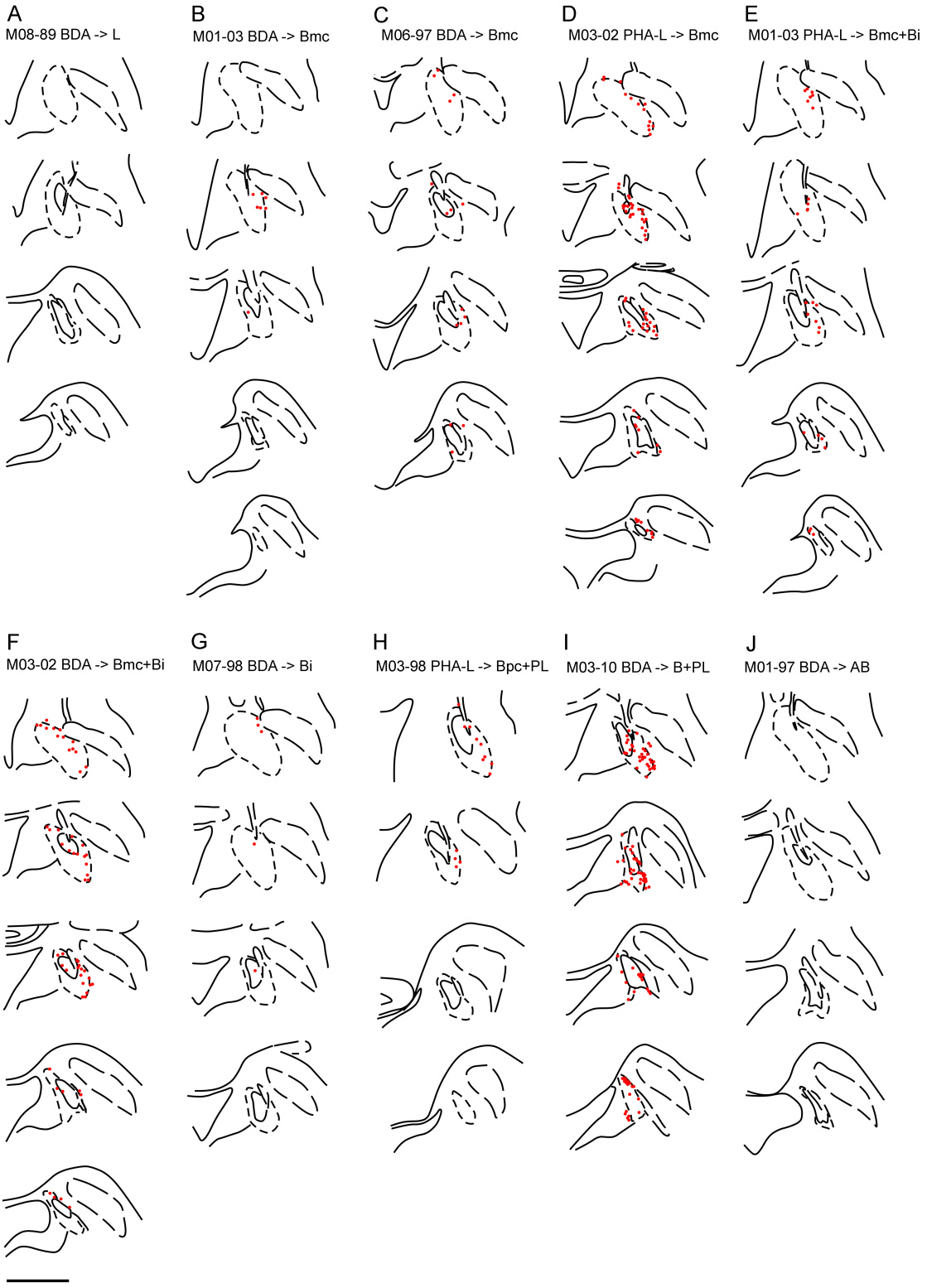

Figure 9. Continuation

Amygdaloid Complex

The data obtained from the analysis of 35 injections in different deep amygdaloid nuclei as well as PAC and AHA, showed that there is a complex organization of subpopulations of cells projecting to the LC. Injections in the same nucleus but involving different divisions often resulted in opposite results. For example, in both cases M6-97 (BDA; Fig. 9C) and M4-90 (BDA; not shown but see Table 1) the injection was located in Bmc; however only the first one showed labeling in LC. Therefore, it seemed that the projections of the Amy to LC could be originated in a subset of neurons.

Overall, the basal nucleus of the amygdala sends the densest inputs to LC, followed by the PL. Only some small regions in the Bi and Bpc send projections to LC. In contrast, injections in the lateral nucleus or the PAC did not show any labeling within LC.

The basal magnocellular and the paralaminar nuclei send their projections manly to the lateral part of the ipsilateral LC, and the density of fibers decreases from rostral to caudal levels of LC.

Lateral Nucleus

Four cases with injections of PHA-L in different divisions of the lateral nucleus (Ld, Lvi and Lv) did not reveal any labeled fiber, neither in the core of LC nor the periphery (M8-89, M11-88, M6-91, and M5-97. See Table 1). Therefore, it is likely that the lateral nucleus of the amygdala does not project to LC.

Basal Nucleus

In the present results, the major output from the amygdala to LC arises in the Bmc, although certain injections in Bi or Bpc also produced some labeling. These nuclei project preferentially to the rostrolateral portion of the core, but some scattered fibers are also present at caudal levels.

Within the Bmc, almost all of the deposits projected to the core of LC (e.g. M01-03, M06-97, M03-02, Fig. 9D; See figures 9B, 9C and 9D respectively). There is only one injection that did not produce labeling (M4-90. See Table 1), and was located close to Ld and Bi. On the contrary, only two injections in Bi out of 8 produced

labeling in LC, and one of them also involved the Bmc (see M7-98 and M3-95 in Table 1).

Paralaminar Nucleus

The PL nucleus was included in the injection site of six experiments. In five cases, the injection site included also the basal nucleus, mainly the Bpv and the ventral part of Bi (see Table 1). The analysis of these five cases showed labeling in the core of LC, with the fibers distributing along the entire longitudinal extension of the nucleus, the majority of them in the core. However, the density of these projections in LC decreased from rostral to caudal, so that the caudal pole contained a scarce amount of fibers. The labeling was stronger in the cases where the injection was bigger, such as M08-09 (Fig. 8C) and M03-10 (Fig. 9I). Only one case (M12-91; not shown, see Table 1) out of the six did not show any labeling in LC. In this case, the injection size was small and localized very close to the lateral nucleus of the amygdala.

Accessory Basal Nucleus

Four cases with injections of BDA in the AB were analyzed. In three of them, the injections were small and strictly restricted to the ABpc (cases M14-97, M14-98, M15-98; see Table 1). No labeled axons were found neither in the core nor the periphery of LC. In one case (M10-09; Fig. 8A), the injection involved ABmc, ABpc, Bpc, PAC and Eo, and resulted in scarce labeling in the rostral part of the core. It is likely that this light labeling arose in Bpc.

DISCUSSION

The present study shows the existence of a direct input from the subiculum to the locus coeruleus. In addition, the present results demonstrate that, beyond the central nucleus, the Amy targets the LC directly through the basal and the paralaminar nuclei. It seems that these projections originate in specific groups of cells with an irregular distribution. Moreover, all the projecting cell groups innervate the core of LC, while some of them project directly to the densest part of the nucleus, what is suggestive of a direct and a presumably powerful modulatory influence on LC activity. Interestingly, the spatial distribution of the labeled fibers in LC is very similar

for both the Sub and Amy, since the labeling was preferentially distributed along the lateral portion of the nucleus, mostly at rostral levels.

Methodological considerations

The BDA as anterograde tracer specifically labeled axons and terminal arborizations with varicosities. Although many of the subsequent fibers were very thin and difficult to identify, they could be observed at higher magnification even if they were scattered. Dark-field illumination also helped with the observation of these thin fibers.

The size of the injection site could also be a limiting factor concerning the quantitative analysis. For example, most of the PHA-L injections in the EC were very small and confined to a reduced group of cells, while some BDA injections were considerably bigger and extended to adjacent regions.

The anatomical shape of the LC and adjacent structures represented in the drawings varied from animal to animal, depending on the size of the animal and angulation of the plane of section of the brain. However, neither the variation in shape across animals nor the variation in the plane of section altered the finding.

Hippocampal formation input to the *Locus coeruleus*

Although there are no previous anatomical reports on the existence of direct projection from the HF to LC, the present study shows that the subiculum targets directly the core of the nucleus and that these afferents are specifically distributed throughout the rostrolateral part of LC. The entorhinal cortex might also contribute with a small input, although more experiments would be needed to demonstrate it.

Despite the lack of the anatomical evidence in the literature regarding these projections, there are functional studies suggesting that the HF might influence LC activity under certain conditions. The neurons in LC are responsive to salient stimuli of various modalities (Aston-Jones et al., 1986, 1994) and this selective responsiveness of LC neurons to cognitively important stimuli points to a functional link between higher brain areas and the LC (Gibbs et al., 2010). The activation of LC leads to the release of NA in terminal fields, as well as in the somato-dendritic area of LC neurons (Singewald et al., 1994; Singewald and Philippu, 1998; Gulyas et al., 2010) and influence the functional state of LC cells to subsequent stimuli (Bouret and

Sara, 2005). NA release in the LC modulates memory formation and consolidation (Gibbs et al., 2010).

Furthermore, it has been demonstrated that both N-methyl-D-aspartate (NMDA) and a-amino-3-hydroxy-5- methyl-4-isoxazolepropionic acid (AMPA) of glutamatergic receptors are present in LC, and that LC neurons are phasically activated by glutamatergic input (Jodo and Aston-Jones, 1997; Jodo et al., 1998), what is followed by the release of noradrenaline (NA) onto its targets.

The subiculum represents the principal outflow of the HF (Swanson et al., 1978) and provides massive, topographically organized innervation to limbic cortices, nucleus accumbens, lateral septum, bed nucleus of the stria terminalis, preoptic area, hypothalamus, central gray region and medulla (Canteras and Swanson, 1992; Köhler, 1990), although projections to LC have not been described. The subiculum efferent terminals are glutamatergic (Blaha et al., 1997; Floresco et al, 2001; Lisman and Grace, 2005), and therefore it is likely that the subicular input to LC described in this work may activate the nucleus.

Amygdala input to the *Locus coeruleus*

The retrograde tracer horseradish peroxidase (HRP) was initially used to demonstrate brain regions that project to LC in the rodent (Cedarbaum and Aghajanian, 1978; Clavier, 1979; Aston-Jones et al., 1986; Luppi et al., 1995). These early studies suggested that only the CeA innervates LC. Anterograde tract-tracing studies corroborated the results obtained with the retrograde tracers. Aston-Jones et al (1986) injected WGA-HRP into the CeA of the rodent and found labeled axon processes into the dorsolateral peri-LC area but not within the nuclear boundaries. This might be a major difference between rodents and primates, since our results show that the amygdala innervates the core of the LC, mainly in its rostrolateral extension.

Previous studies in monkeys (Price and Amaral, 1981) demonstrated that the Amygdala targets the core of LC and this is in accordance with our data. They described moderate labeling mainly located in the ventral portion of the nucleus arising specifically in the CeA. Our results show variations in the distribution of the labeled axons depending on the location of the injection site; however, the overall labeling was concentrated in the lateral part of the nucleus, mainly at rostral levels. It

might be possible that the CeA sends projections to the ventral part of LC while the basal nucleus of the amygdala specifically projects to the lateral portion.

In addition, our data demonstrate that the CeA is not the only amygdaloid nucleus projecting to LC, as labeled fibers were obtained after injections in Bmc, and certain portions of the PL and Bpc. This work shows that the projection system of the amygdala is quite complex, and that might exist subsets of cells specialized in their outputs, since injections located close to each other within the same nucleus reported totally different results (See Fig. 4, 8 and 9).

On the other hand, The PAC seems not to send inputs to LC, since a big injection of BDA (M06-09; Fig. 8D) that involved PAC, Ei and PrS did not produce any labeling in neither the core nor the periphery of LC. One more case was analyzed (M10-09; Fig. 8A), where the injection involved the Bpc and scattered fibers were found in one slice in the rostral LC. It is likely that this scarce labeling originated in the Bpc rather than the PAC.

Only one experiment involved AHA as injection site (M04-10; Fig. 8F). This injection also extended to the PrS and Ec. Several cases mentioned earlier with deposits in the on PrS and Ec, clearly showed that these structures do not contribute to the labeling obtained in LC; therefore it is likely that the labeling found in this case may arise in AHA. The density is moderate to light and the labeled axons are scattered distributed along the core of LC, with no specific topographic organization. More injections would be needed in order to establish the contribution that AHA might have in the input to LC.

Functional interpretation

Notably, whereas prior rodent studies proposed that basolateral amygdala regulates LC indirectly through CeA (Bouret et al., 2003), the present tracing data indicates that the primate Bmc can directly regulate LC. Although it is unclear whether the converging hippocampo- and amygdalo-coerulean projections identified here are functionally related. Prior evidence from nonhuman and human studies suggests that both could have a role in memory processing (Sara, 2010). Novelty detection is accompanied by increased hippocampal noradrenergic activity, driven by enhanced firing of LC (Sara et al. 1994; Kitchigina et al. 1997). This activation of LC activity under novelty conditions might be mediated by the direct input that Sub sends

to the core of the nucleus. In turn LC might provide the saliency signal required to promote hippocampal encoding of relevant novel information through changes in synaptic strength (Lemon et al., 2009). Accordingly, the direct projections from the basal nucleus of the amygdala to LC could contribute in restoring central arousal states that promote emotional memory consolidation (Sterpenich et al. 2006).

REFERENCES

Amaral DG, Cowan WM (1980). Subcortical afferents to the hippocampal formation in the monkey. J Comp Neurol 189: 573-91.

Amaral DG, Price JL (1984). Amygdalo-cortical projections in the monkey (*Macaca fascicularis*). J Comp Neurol 230(4): 465-96.

Amaral DG, Price JL, Pitkänen A, Carmichael ST (1992). Anatomical organization of the primate amygdaloid complex. In: Aggleton J, editor. The amygdala: neurobiological aspects of emotion, memory, and mental dysfunction. New York: Wiley-Liss Publishers. pp. 1-66.

Arnsten AF, Goldman-Rakic PS (1984). Selective prefrontal cortical projections to the region of the locus coeruleus and raphe nuclei in the rhesus monkey. Brain Res 306(1-2):9-18.

Aston-Jones G, Bloom FE (1981). Norepinephrine-containing locus coeruleus neurons in behaving rats exhibit pronounced responses to non-noxious environmental stimuli. J Neurosci 1(8):887-900.

Aston-Jones G, Ennis M, Pieribone VA, Nickell WT, Shipley MT (1986). The brain nucleus locus coeruleus: restricted afferent control of a broad efferent network. Sci 234: 734-737.

Aston-Jones G, Rajkowski J, Kubiak P, Alexinsky T (1994). Locus coeruleus neurons in monkey are selectively activated by attended cues in a vigilance task. J Neurosci 14(7):4467-4480.

Blaha CD, Yang CR, Floresco SB, Barr AM, Phillips AG (1997). Stimulation of the ventral subiculum of the hippocampus evokes glutamate receptor-mediated changes in dopamine efflux in the rat nucleus accumbens.

Bonda E (2000). Organization of connections of the basal and accessory basal nuclei in the monkey amygdala. Eur J Neurosci 12: 1971-1992.

Bouret S, Duvel A, Onat S, Sara SJ (2003). Phasic activation of locus coeruleus by the central nucleus of the amygdala. J Neurosci 23(8): 3491-3497.

Bouret S, Sara SJ (2005). Network reset: a simplified overarching theory of locus coeruleus noradrenaline function. Trends Neurosci 28: 574-582.

Bowden DM, Graman DC, Poynter WD (1978). An autoradiographic, semistereotaxic mapping of major projections from locus coeruleus and adjacent nuclei in *Macaca mulatta.* Brain Res 145: 257-276.

Canteras NS, Swanson LW (1992). Projections of the ventral subiculum to the amygdala, septum, and hypothalamus: a PHAL anterograde tract-tracing study in the rat. J Comp Neurol 324: 180-194.

Cedarbaum JM, Aghajanian GK (1978). Afferent projections to the rat locus coeruleus as determined by a retrograde tracing technique. J Comp Neur 178: 1-16.

Chiba T, Kayahara T, Nakano K (2001). Efferent projections of infralimbic and prelimbic areas of the medial prefrontal cortex in the Japanese monkey, *Macaca fuscata*. Brain Res 888: 83–101.

Clavier RM (1979). Afferent projections to the self-stimulation regions of the dorsal pons, including the locus coeruleus, in the rat as demonstrated by the horseradish peroxidase technique. Brain Res Bull 4: 497-504.

Davis M, Whalen PJ (2001). The amygdala: vigilace and emotion. Mol Psychiatry 6: 13-34.

Ennis M, Behbehani M, Shipley MT, Van Bockstaele EJ, Aston-Jones G (1991). Projections from the periaqueductal grey to the rostromedial pericoerulear region and nucleus locus coeruleus: new evidence of anatomical and physiological specifity. Physiol Rev 63: 844-914.

Fallon JH, Koziel DA, Moore RY (1978). Catecholamine innervation of the basal forebrain. II. Amygdalasuprahinal cortex and entorhinal cortex. J Comp Neurol 180: 509-532.

Floresco SB, Todd CL, Grace AA (2001). Glutamatergic afferents from the hippocampus to the nucleus accumbens regulate activity of ventral tegmental area dopamine neurons. J Neurosci 21(13): 4915-4922.

Freedman LJ, Insel TR, Smith Y (2000). Subcortical projections of area 25 (subgenual cortex) pf the macaque monkey. J Comp Neurol 421: 172-188.

Freese JL, Amaral DG (2005). The organization of projections from the amygdala to visual cortical areas TE and V1 in the Macaque monkey. J Comp Neurol 486: 295-317.

Gibbs ME, Hutchinson DS, Summers RJ (2010). Noradrenaline release in the locus coeruleus modulates memory formation and consolidation; roles for α- and β-adrenergic receptors. Neurosci 170: 1209-1222.

Gulyas B, Brockschnieder D, Nag S, Pavlova E, Kasa P, Beliczai Z, et al (2010). The norepinephrine transporter (NET) radioligand (S,S)- [18F]FMeNER-D2 shows significant decreases in NET density in the human brain in Alzheimer's disease: a post-mortem autoradio- graphic study. Neurochem Int 56: 789-798.

Insausti R, Amaral DG (2008). Entorhinal cortex of the monkey: IV. Topographical and laminar organization of cortical afferents. J Comp Neurol 509(6):608-641.

Insausti R, Amaral DG (2012). Hippocampal formation. In Mai JK, Paxinos G (Eds.), Atlas of the Human Brain (Third Edition), Elsevier Academic Press, London (2012), pp. 896–942.

Insausti R, Amaral DG, Cowan WM (1987). The entorhinal cortex of the monkey: III. Subcortical afferents. J Comp Neurol 264: 396-408.

Jodo E, Aston-Jones G (1997). Activation of locus coeruleus by prefrontal cortex is mediated by excitatory amino acid inputs. Brain Res 768(1-2): 327-32.

Jodo E, Chiang C, Aston-Jones G (1998). Potent excitatory influence of prefrontal cortex activity on noradrenergic locus coeruleus neurons. Neurosci 83(1): 63-79.

Jones BE, Moore RY (1977). Ascending projections of the locus coeruleus in the rat. II Autoradiographic study. Brain Res 127: 25-53.

Kitchigina V, Vankov A, Harley C, Sara SJ (1997). Novelty-elicited, noradrenaline-dependent enhancement of excitability in the dentate gyrus. Eur J Neurosci 9: 41-47.

Köhler C (1990). Subicular projections to the hypothalamus and brainstem: some novel aspects revealed in the rat by the anterograde *Phaseolus vulgaris* leukoagglutinin (PHA-L) tracing method. Prog Brain Res 83: 59-69.

Lemon N, Aydin-Abidin S, Funke K, Manahan-Vaughan D (2009). Locus coeruleus activation facilitates memory encoding and induces hippocampal LTD that depends on ß-adrenergic receptor activation. Cerebral Cortex 19: 2827-2837.

Lisman JE, Grace AA (2005). The Hippocampal-VTA Loop: Controlling the Entry of Information into Long-Term Memory. Neuron 46(5): 703-713.

Loughlin SE, Foote SL, Bloom FE (1986). efferent projections of nucleus locus coeruleus: topographic organization of cells of origin demonstrated by three-dimensional reconstruction. Neurosci 18(2): 291-306.

Lu Y, Simpson KL, Weaver KJ, Lin RCS (2012). Differential distribution patterns from medial prefrontal cortex and dorsal raphe to the locus coeruleus in rats. Anat Rec 295: 1192-1201.

Luppi PH, Aston-Jones G, Akaoka H, Chouvets G, Jouvet M (1995). Afferent projections to the rat locus coeruleus demonstrated by retrograde and anterograde tracing with cholera-toxin b subunit and *Phaseolus vulgaris leucoagglutinin*. Neurosci 65(1): 119-160.

McGaugh JL, Roozendaal B (2008). Drug enhancement of memory consolidation: historical perspective and neurobiological implications. Psychopharmacol 202: 3-14.

Mohedano-Moriano A, Martinez-Marcos A, Pro-Sistiaga P, Blaizot X, Arroyo-Jimenez MM, Marcos P, Artacho-Pérula E, Insausti R (2008). Convergence of unimodal and polymodal sensory input to the entorhinal cortex in the *fascicularis* monkey. Neurosci 151: 255-71.

Mohedano-Moriano A, Muñoz-López M, Sanz-Arigita E, Pró-Sistiaga P, Martínez-Marcos A, Legidos-Garcia ME, Insausti AM, Cebada-Sánchez S, Arroyo-Jiménez MM, Marcos P, Artacho-Pérula E, Insausti R (2015). Prefrontal cortex afferents to the anterior temporal lobe in the Macaca fascicularis monkey. J Comp Neurol 523: 2570–2598.

Muñoz M, Insausti R (2005). Cortical efferents of the entorhinal cortex and the adjacent parahippocampal region in the monkey (Macaca fascicularis). Eur J Neurosci 22: 1368-88.

Pitkänen A, Amaral DG (1998). Organization of the intrinsic connections of the monkey amygdaloid complex: projections originating in the lateral nucleus. J Comp Neurol 398: 431-458.

Pitkänen A, Kelly JL, Amaral DG (2002). Projections From the Lateral, Basal, and Accessory Basal Nuclei of the Amygdala to the Entorhinal Cortex in the Macaque Monkey. Hippocampus 12: 186-205.

Price JL, Amaral DG (1981). An autoradiographic study of the projections of the central nucleus of the monkey amygdala. J Neurosci 1(11): 1242-1259.

Price JL, Russchen FT, Amaral DG (1987). The limbic region. II: the amygdaloid complex. In Bjorklund A, Hokfelt T, Swanson LW (eds), Handbook of Chemical Neuroanatomy, Vol. 5, Integrated Systems of the CNS, Part I. Elsevier Science, Amsterdam. pp. 279-388.

Roullet P, Sara SJ (1998). Consolidation of memory after its reactivation: involvement of β-noradrenergic receptors in the late phase. Neural Plast 6: 63-68.

Sara SJ (2009). The locus coeruleus and noradrenergic modulation of cognition. Nat Rev Neurosci 10(3): 211-23.

Sara S.J, Roullet P, Przybyslawski J (1999). Consolidation of memory for odor-reward association: β-adrenergic receptor involvement in the late phase. Learn Mem 6: 88-96.

Sara SJ, Vankov A, Herve A (1994). Locus coeruleus-evoked responses in behaving rats: a clue to the role of noradrenaline in memory. Brain Res Bull 35: 457-465.

Singewald N, Philippu A (1998). Release of neurotransmitters in the locus coeruleus. Prog Neurobiol 56: 237-267.

Singewald N, Schneider C, Pfitscher A, Philippu A (1994). In vivo release of catecholamines in the locus coeruleus. Naunyn Schmiedebergs Arch Pharmacol 350: 339-345.

Sterpenich V, D'Argembeau A, Desseilles M, Balteau E, Albouy G, Vandewalle G, Degueldre C, Luxen A, Collette F, Maquet P (2006). The locus coeruleus is involved in the successful retrieval of emotional memories in humans. J Neurosci 26: 7416:7423.

Swanson LW, Wyss JM, Cowan WM (1978). An autoradiographic study of the organization of intrahippocampal association pathways in the rat. J Comp Neurol 181: 681-715.

Szabo J, Cowan WM (1984). A stereotaxic atlas of the brain of the cynomolgus monkey (*Macaca fascicularis*). J Comp Neurol 222: 265-300.

Tronel S, Feenstra MG, Sara SJ (2004). Noradrenergic action in prefrontal cortex in the late stage of memory consolidation. Learn Mem 11: 453-458.

Tully K, Bolshakov VY (2010). Emotional enhancement of memory: how norepinephrine enables synaptic plasticity. Mol Brain 3(15): 1-9.

Wilcox BJ, Unnerstall JR (1990). Identification of a subpopulation of neuropeptide Y-containing locus coeruleus neurons that project to the entorhinal cortex. Synapse 6: 284-291.

CHAPTER 2. Heterogeneous cortical projections to the *Locus coeruleus* in the macaque monkey

ABSTRACT

Functional studies in rodents have demonstrated that the *Locus coeruleus* (LC) is activated directly by the prefrontal cortex; however, the anatomical related pathways are poorly understood. In this work, we examined the projections from the prefrontal cortex and anterior insular cortex to the *Locus coeruleus* (LC) in the macaque monkey. Anterograde tracers were injected in several distinct prefrontal and insular areas. All the studied areas reported labeling in LC, and the density of this labeling varied depending on the location of the injection site. Overall, injections placed in agranular or dysgranular areas produced a stronger labeling compared to those injections involving granular areas. Thereby, Injections in the agranular insular area (Iam) produced a very strong labeling in the core of LC, followed by injections placed in the medial part of the orbital prefrontal cortex (13b, 13l) and the medial prefrontal cortex (32, 24 and 25). In contrast, injections in granular areas of the orbital prefrontal cortex (11m and 11l) and the dorsolateral cortex (46d, 46v) produced sparse labeling. An exception was the granular area 9 that gave rise to a strong labeling compared to other granular areas. In most cases, the anterograde labeling occurred in the rostral part of the LC; however, injections in area 13 produced labeling throughout the rostrocaudal extent of LC. These data demonstrate a direct top-down input to LC from agranular/dysgranular limbic areas in the prefrontal and insular cortex. These connections might underlie the areal-specific role of high cognitive, motivational, and emotional processes in the control of LC activity.

INTRODUCTION

The noradrenergic system has an important role in brainwide neuromodulation, taking part in sleep-wake cycle, sympathetic regulation, neural plasticity and drug abuse, as well as higher cognitive processes such as decision-making and memory processing. The majority of noradrenergic neurons are concentrated in LC that provides the sole source of noradrenaline (NA) to the neocortex and hippocampus (Berridge and Waterhouse, 2003). Substantial evidence indicates that NA exerts a potent modulatory influence on prefrontal cortex (PFC) functions, such as attention,

working memory and decision-making (Aston-Jones et al., 2000; Kerns et al., 2004; Milstein et al., 2007; Ramos and Arnsten, 2007) by acting on different adrenoreceptors (Lim et al., 2010). These connections are important in the evaluation of the contextual relevance and emotional valence of novel stimuli in order to promote the adaptive responses by the medial prefrontal cortex (MPFC) (Radley et al., 2008). In turn, the PFC modulates LC activity through both NMDA and non-NMDA receptors (Jodo and Aston-Jones, 1997). Functional studies in rodents demonstrate that the MPFC phasically activates LC neurons either directly or through indirect connections, and that MPFC also provides a resting tonic excitatory influence on LC activity, since the inactivation of the MPFC suppresses LC firing (Jodo et al., 1998). Thus, the activity of the PFC on the regulation of cognitive and emotional processing influences LC function. Moreover, Aston-Jones et al. (2007) showed that LC neurons responses are driven by decision processes rather than by sensory or motor activities per se, and that this decision-related activation of LC serves to facilitate behavioral responses. All these functional evidences reinforce the idea that LC is involved in the modulation of higher cognitive processes (Jodo et al., 1998; Bush et al., 2000; Radley et al., 2008).

Anatomical data support the possibility of the existence of direct PFC projections to LC, although the vast majority of our knowledge is based on studies made in rodents. These data show that the PFC directly innervates the rostromedial dendritic peri-LC zone (Zhu and Aston-Jones, 1996; Luppi et al., 1996; Lu et al., 2012). Few studies have been undertaken in the primate claiming that only certain architectonic areas in the PFC (see discussion) project directly to the core of LC (Arnsten and Goldman-Rakic, 1984; Freedman et al., 2000; Rajkowski et al., 2000; Chiba et al., 2001; Zhu et al., 2004).

In the present work, we investigate which specific architectonic areas directly terminate on the LC and whether these projections present a particular distribution within the nucleus.

MATERIALS AND METHODS

Subjects

The present data were obtained from 20 adult cynomolgus macaques (*Macaca fascicularis,* 3-8 kg) in three different laboratories (USA, Price; Spain, Insausti, and Germany, Evrard). All monkeys from the Price's lab and some monkeys from the Insausti's lab were prepared and used in the context of prior tract-tracing studies (Carmichael and Price, 1995b, a, 1996; Kondo et al., 2003; Insausti and Amaral, 2008; Saleem et al., 2008; Mohedano-Moriano et al., 2015). The cases were examined and analyzed in relation to the connections with the LC.

The animals were treated according to the guidelines of the American Physiological Society, the NIH and the European Parliament and Council Directive 2010/63/EU on the protection of animals used for experimental and other scientific purposes. All animal protocols were reviewed and approved by the Animal Studies Committee of Washington University, St.-Louis, USA, the Ethical Committee of Animal Research of the University of Castilla-La-Mancha (UCLM), Spain, or the German authorities (*Regierungspräsidium*).

Tracer injection

All tracer injections were made during aseptic surgery under general anesthesia. Prior to surgery, each monkey was anesthetized (see below) and placed in an MRI-compatible stereotaxic frame. An MRI scan (T1 MPRAGE 3D image, with 0.8 or 1.0 mm isometric voxels) was then obtained by using a 1.5 T scanner, using a receive-only or volume coil placed over the top of the head of the animal. Stereotaxic coordinates for each desired injection site in the PFC that was specific for each individual animal were derived from the MR images. These individual-specific coordinates were compared with coordinates from the atlas of Szabo and Cowan (1984). Electrophysiological recording was used to further refine the coordinates for deep injections (see below). For the surgery (also for MRI), anesthesia was induced by intramuscular injection of ketamine (10 mg/kg) and xylazine (0.67 mg/kg). The animals were then intubated, and surgical anesthesia was initiated with a gaseous mixture of oxygen, nitrous oxide, and halothane or isofluorane. Once anesthesia was established, the animals were placed in a stereotaxic apparatus, and the scalp was

incised. Craniotomies were made in the skull at the sites indicated by the stereotaxic coordinates. In certain cases were the injection site was located in deep cortical layers of OMPFC, a tungsten electrode was used in order to determinate the depth of the base of the brain (Saleem et al., 2008). After surgery, a long-lasting analgesic, buprenorphine (0.1 mg/kg, i.m.), was given as the animal was brought out of anesthesia.

Aqueous solutions of the anterograde tracer biotinylated dextran amine [BDA; Molecular Probes, Eugene, OR; 10%]), and two bidirectional tracers (Fluoro Ruby [FR; Molecular Probes, 5% or 10%], and Lucifer Yellow [LY; Molecular Probes, 5% or 10%]) were injected in different portions of the PFC. The injections were made through micropipettes where the tracer was delivered with an air pressure system (Saleem et al., 2008). The volume of tracers injected varied between 0.1 to 1.2 µl, depending on the sensitivity of tracers. To avoid spread of tracer into areas along the pipette track, the micropipette was left in place for 30 minutes after the injection was finished. With this procedure, there was little spread of tracer into the overlying cortex or white matter.

Perfusion and histological processing

After a survival period of 2 weeks, the animals were anesthetized with ketamine (10 mg/kg, i.m.), followed by sodium pentobarbital (25–30 mg/kg, i.v.), and perfused with a pH shift fixation method as described by Carmichael and Price (1994), with slight modifications (Saleem et al., 2008). In this method, the animals were first perfused transcardially with warm heparinized saline, followed by a sequence of cold 4% paraformaldehyde in 0.1M sodium acetate buffer (pH 6.5), then 4% paraformaldehyde in 0.1M borate buffer (pH 9.5), and finally 4% paraformaldehyde and 10% sucrose in borate buffer. The brain was blocked sterotaxically, removed, photographed, and then placed in 20% and than transferred to 30% sucrose in 0.1 M phosphate buffer (pH 7.2–7.4) at 4ºC. After 3-4 days, the brain blocks were frozen in dry ice and isopentane, and cut coronally at 50µm thickness on a sliding microtome. An alternating series of sections was processed for each tracer, usually one section out of 10 in each series, with 500µm intervals between adjacent sections. BDA was processed directly with the avidin-biotin-peroxidase method. The other tracers FR, and LY, were processed immunohistochemically with an avidin-biotin-horseradish

peroxidase method (Carmichael et al., 1994). For these tracers, the sections were first processed to block the biotin from the injected BDA (Avidin-Biotin Blocking Kit; Vector, Burlingame Burlingame, CA) and then incubated for 3–3.5 days in the primary antibody (anti-tetramethylrhodamine [for FR] and anti-LY: Molecular Probes; Nos. A-6397 and A-5750; 1:1,000). The sections were then processed with the appropriate biotinylated secondary antibody and avidin-biotin staining kit (Vector) with diaminobenzidene as the chromogen (for other details see Saleem et al., 2008). The immunostaining was enhanced with a silver/gold intensification method, which made the labeled axons and cells visible with dark field illumination (Carmichael and Price, 1994). Additional series of adjacent sections were processed with Nissl staining for cytoarchitectonic study.

Data analysis and illustrations

The spatial distribution of labeled terminals was analyzed with an epifluorescence microscope coupled to a computerized charting system (MD-Plot, Datametrics, Minnesota, USA), and each labeled fiber was plotted as a single point. Subcortical boundaries and other landmarks were added to these plots by camera lucida drawings of adjacent Nissl-stained sections. The relative strength or densities of connections was evaluated; however, the absolute values were not determined due to factors such as differences between tracers in transport efficacy, injection volumes and location of each injection. LC labeling was analyzed bilaterally, and maps were prepared to visualize the distribution and density of the terminal fields.

Nomenclature

Subdivisions of the PFC were determined according to prior architectonic and tract-tracing studies that subdivided the entire PFC into 23 architectonic areas, and the anterior insula into 7 architectonic areas (Carmichael and Price, 1994; Evrard et al., 2014). The core of LC was subdivided into a central region of high cellular density and a region with sparser cellular density, as described in *Chapter 1* (Figure 1).

RESULTS

Injection sites in the prefrontal cortex

In most cases the injection site was confined to the cortical grey matter and included layers III and/or V. They all had a dense central 'core' around the tip of the micropipette penetration track and a more diffuse 'halo' extending for approximately 100 to 300 µm around the core. Figure 1 shows an example of injection site from case M02-15 with an injection of FR in area 12.

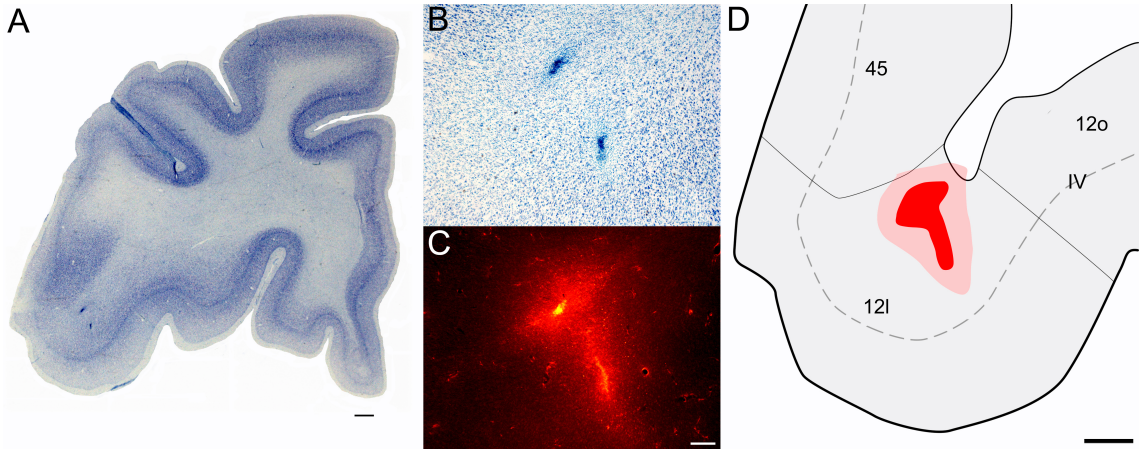

Figure 1. Location of the injection site in Case M02-15. A, Low-magnification photomicrograph of a Nissl-stained coronal section of the prefrontal cortex (*Macaca fascicularis*); B and C, Higher-magnification photomicrograph of contiguous sections mounted for nissl and fluorescence respectively. D, Representation of the injection site over the corresponding cytoarchitectonic areas.

A total of 28 injections of anterograde or bidirectional tracers were made in several distinct architectonic areas in the agranular insula anterior to the limen, and in the orbital, medial and lateral PFC. In light of the finding reported here (see below), the cases are ordered throughout the text according to the degree of granularity of the injected areas: agranular insula areas (Iam, Iamp, Iai, Ial), dysgranular cingulate areas (24, 25 and 32), dysgranular orbital and medial PFC areas (13b, 13l, 12r), granular orbital and medial PFC areas (12m, 12o, 11m, 11l, 10m, 10o), and granular lateral PFC areas (12l, 46 and 9).

Figure 2 depicts the injection sites collated all together in a standard unfolded map of PFC. The round and ellipsoidal shapes represent both the 'core' and 'halo' of each injection site. Injections were made in the left or the right side of PFC in different cases, but in Figure 2 all are illustrated in left PFC for consistency.

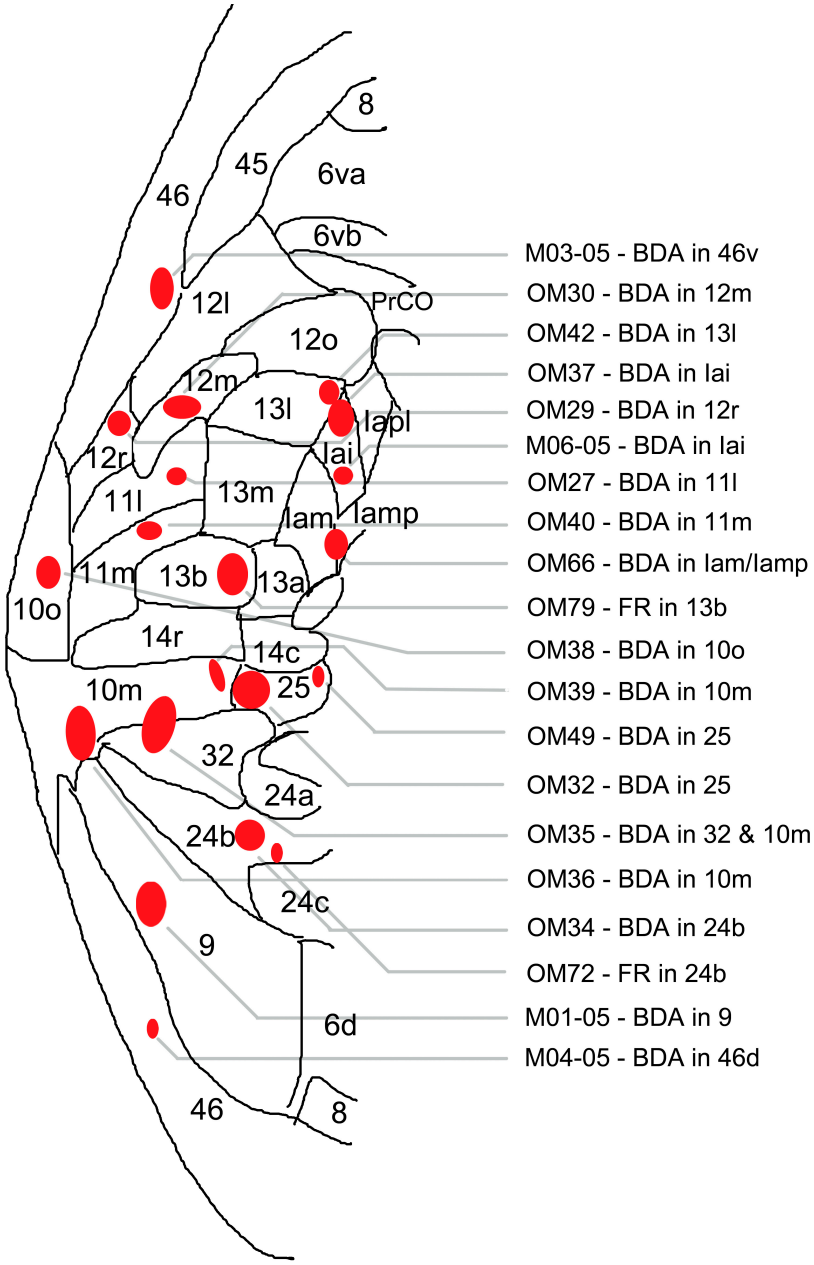

Figure 2. Unfolded map showing the location of the injection sites in the prefrontal cortex and anterior insular cortex.

Three injections were made in the anterior insula. One large injection of BDA filled all the layers of Iam and Iamp (OM66). Two smaller injections of BDA were confined to the deep layers of Iai (OM37) or Ial (M06-05), respectively.

Six injections were made in dysgranular MPFC areas. Most injections were confined to one area including two injections in area 24b (OM32-FR and OM34) and two injections in area 25 (OM32-BDA, and OM49-BDA). Among the injections in area 25, in case OM32, the injection had a medium size and involved all the layers,

whereas in case OM49 the injection was small and limited to deep layers (IV-VI). One injection in area 32 spread to area 10m (OM35) but a differential analysis of anterograde labeling in LC indicates that most, if not all the labeling from that injection arose from area 32. Five injections were made in the rostral pole of PFC, in distinct subdivisions of area 10 with two injections in area 10mr (OM69 and OM36), one injection in area 10m (OM39) and one injection in area 10o (OM38).

Six injections were made in the orbital PFC. These injections included one injection in area 13b (OM79), two injections in area 13l (OM28 and OM42), one injection in area 11m (OM40) and one in area 11l (OM27), one injection in area 12r (OM29), one in area 12m (OM30), and one in area 12l (M02-15).

Finally, four injections were made in the lateral PFC with one injection in area 9 (M01-05), 2 injections in area 46v (M03-05) and one injection in area 46d (M04-05).

Anterograde labeling in *Locus coeruleus*

Most of the injections reported here produced anterograde labeling in LC. Figure 3A and B show photomicrographs of representative anterograde labeling in LC. The labeled fibers were sinuous, and displayed varicosities. The majority of the terminal fields reached the sparse periphery of the core of LC, although in some cases (see below) the labeled fibers were present also in the dense core. The labeling was distributed mainly in the ipsilateral LC with only about 5% of labeling present in contralateral LC. The highest density of labeling was located mainly in the rostral levels of LC, although in some cases the labeling was also distributed throughout the entire rostro-caudal extension of the nucleus (e.g., OM79, see below).

Figure 4A and B show how individual fiber segments were plotted and counted. The density of labeled fibers varied greatly according to the location of the injection site. The histogram in Figure 3C illustrate this variation using, for each area injected, an average of the ratio of the number of fiber segments labeled from one specific area relative to the total number of fibers labeled in the case with most labeling (OM66).

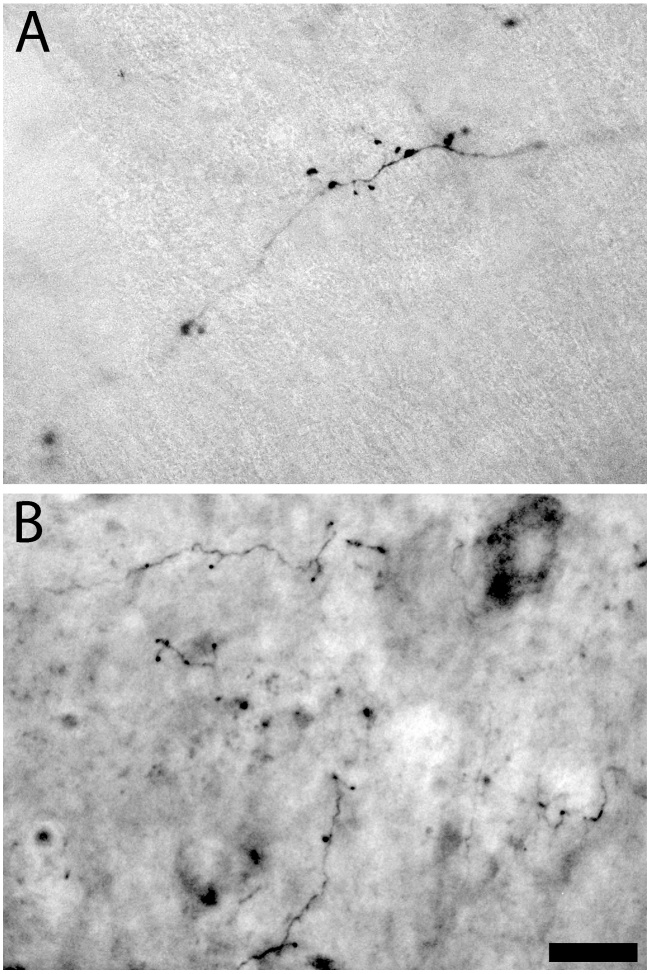

Figure 3. Photomicrographs of BDA-positive labeled fibers in the *Locus coeruleus*. Scale bar: 20 μm.

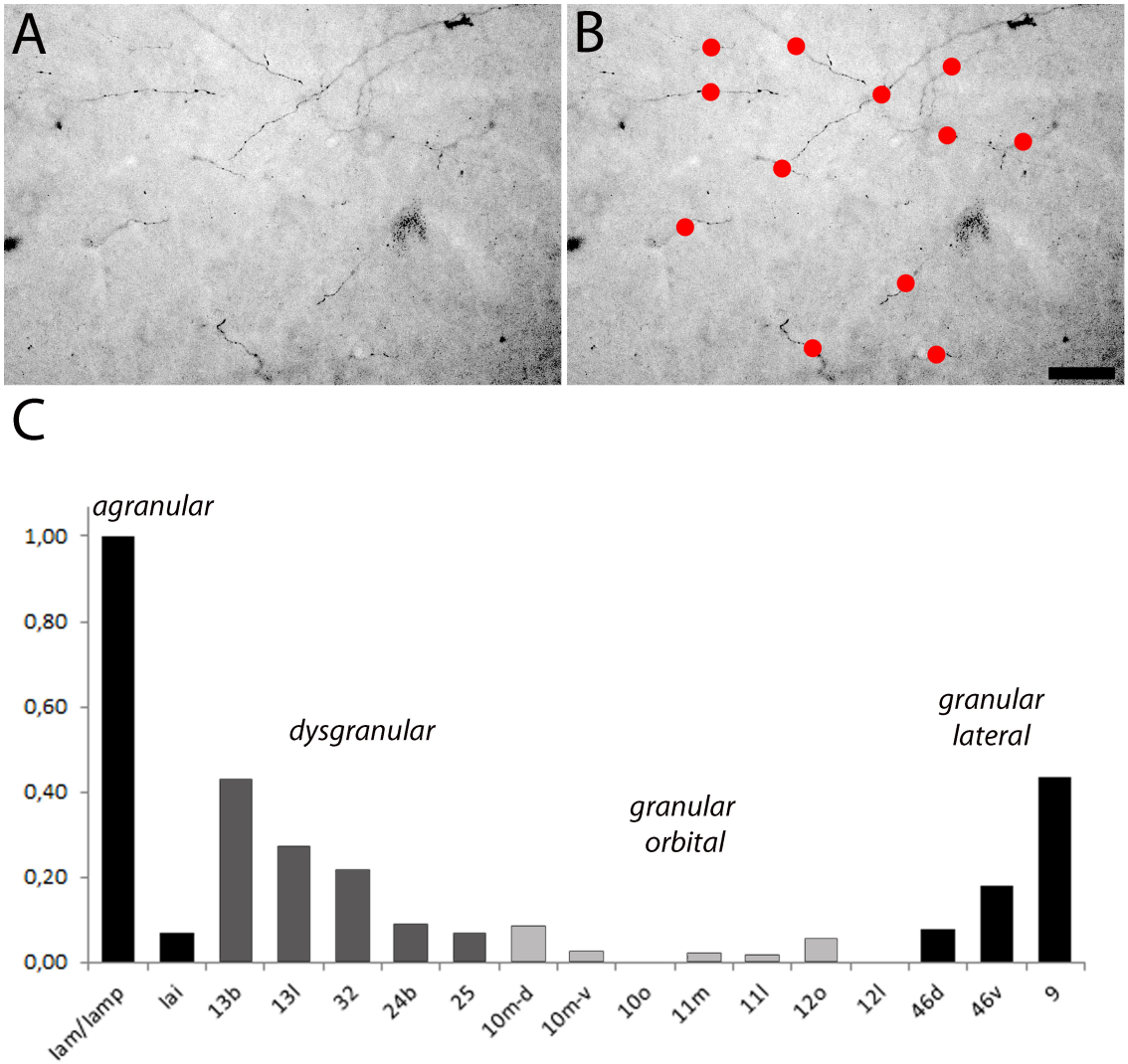

Figure 4. A and B, photomicrographs of the labeled axons in the *Locus coeruleus*. Each red dot represents one fiber. C, graph representation of the relative number of labeled fibers in LC after injections in different architectonic areas within the prefrontal cortex and anterior insular cortex. Scale bar: 20 μm.

Overall, injections placed in agranular or dysgranular areas produced a stronger labeling compared to those injections involving granular areas. Thereby, Injections in the agranular insular area (Iam) produced a very strong labeling in the core of LC, followed by injections placed in the medial part of the orbital prefrontal cortex (13b, 13l) and the medial prefrontal cortex (32, 24 and 25). In contrast, injections in granular areas of the orbital prefrontal cortex (11m and 11l) and the dorsolateral cortex (46d, 46v) produced sparse labeling. An exception was the granular area 9 that gave rise to a strong labeling compared to other granular areas. The next paragraphs describe the distribution and density of labeling in LC for all relevant

cases illustrated in Figures 5 and 6.

Orbital prefrontal cortex and anterior insula. Injections in the OPFC showed an overall rostro-caudal gradient in the density of the fibers sent to LC. Areas located rostral and medial in the OPFC (10o, 11m, 11l) projected very lightly compared to areas located more caudal and lateral (13b, 13l, Iam/Iamp).

Out of all of the areas examined here, the tracer injection located in Iamp/Iamp (case OM66) showed the highest density of anterograde labeling in LC (Fig. 5A). The labeled fibers distributed along the whole extension of the nucleus in both the core and the periphery. Injections in areas Iai and Ial that surround Iam and Iamp produced much less labeling. Notably, two small injections of BDA in cases OM28 and OM37 were placed in the rostral and caudal portions of Iai respectively, and the labeling obtained varied in density and distribution (Fig. 5B and C). The injection in the rostral part of Iai showed scarce labeling in the dorsal portion of the nucleus, whereas the caudal Iai showed a higher number of labeled fibers, but the distribution was located in the rostro-medial portion of LC.

High density of fibers was found after the injection of FR in area 13b (case OM79; Fig. 5D). The resulting labeling distributed all over the extension of LC in both the dense and sparse parts of the core, but it was more abundant in the rostral portion. Similar density of labeling was obtained after a small BDA injection into area 13l, although the spatial distribution of the labeling was slightly different showing preference for the lateral location within LC (Fig. 5E).

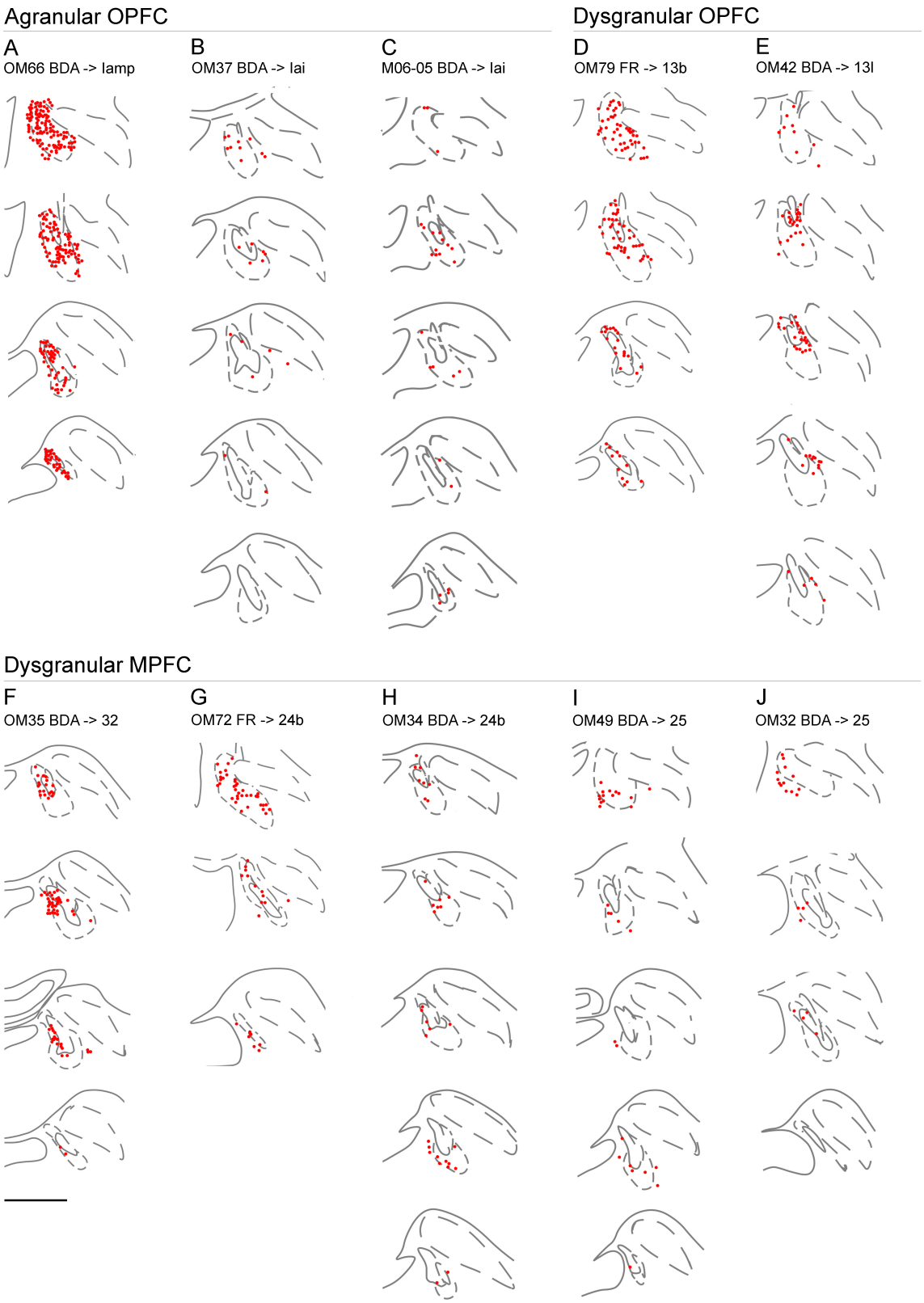

Figure 5. Drawings depicting the labeling obtained in the *Locus coeruleus* after injections of anterograde tracers in the prefrontal cortex and anterior insula. Each red dot represents 1 labeled fiber. Scale bar: 2mm.

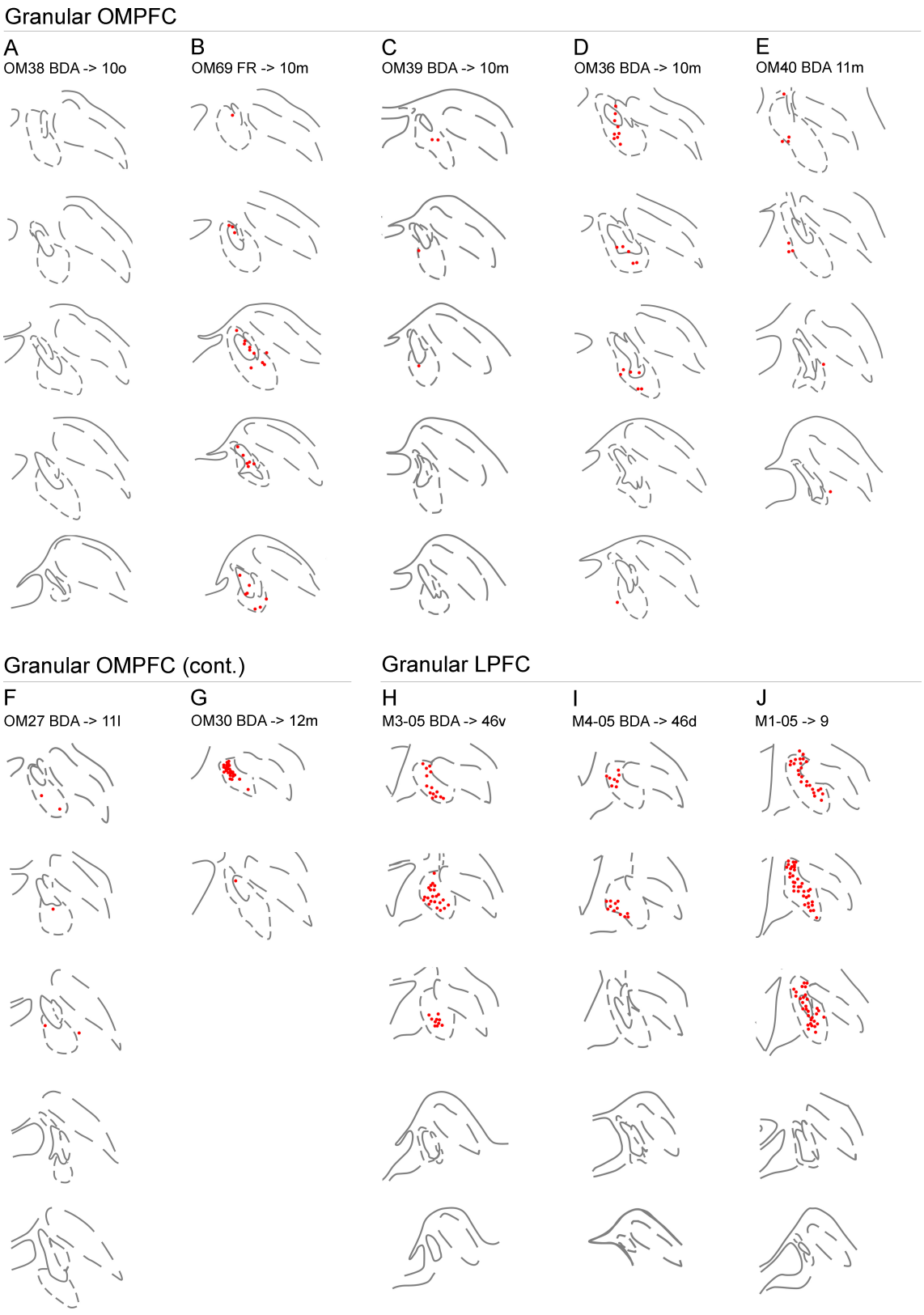

Figure 6. Continuation.

Finally, two BDA injections in area 11, one placed in 11m (case OM40; Fig. 6E) and the other in 11l (case OM27; Fig. 6F) showed few labeled fibers along the rostro-medial extension of the nucleus, specifically localized in the sparse part of the core. A small BDA injection in area 12m (OM30; Fig. 6G) produced sparse labeled fibers in the rostral LC.

Medial prefrontal cortex. Although all the injections produced a moderate to dense labeling, the distribution of fibers and boutons varied substantially across the different cases of these series.

The densest labeling resulted from deposits in area 32. One BDA injection involving area 10mc and area 32 (case OM35; Fig. 5F) resulted in moderate to dense labeling. The labeled terminals likely arose in area 32 since area 10mc projection is very light; therefore the bulk of the labeling in this case may originate substantially in area 32.

Injections in area 24b (cases OM34 and OM72; Fig. 5G and H) showed moderate density of labeling throughout the rostro-caudal extension of LC, and some fibers reached the dense part even though most of the fibers were distributed in the sparse part of the core.

Two injections in area 25 produced an anterograde labeling of moderate density and a similar spatial distribution of the fibers along the rostral to medial extension of the sparse portion of the core (Fig. 5I and J), mainly localized in the medial part close to the forth ventricle. Like in the previous cases, the caudal pole presented very few (1-2) labeled fibers while the bulk of the labeling was preferentially located in the rostromedial part of LC.

Finally, injections in different rostro-caudal portions within area 10m produced different labeling density. The BDA injection in the rostral part of 10m in case OM35 (Fig. 6D) produced a denser labeling, compared to the caudal part of 10m (case OM39; Fig. 6C), although the caudal deposit was smaller. The sparse labeled fibers obtained with the injection in 10mc were localized in the rostral periphery of the core of LC without entering the most compact part of the core. In contrast, the labeled fibers arising in 10mr were distributed throughout both the compact and the sparse portions, and covered all the extent of the LC, even though the caudal labeling was sparser than in rostral LC. The BDA deposit in area 10o (OM38) did not show any anterograde labeling in LC (Fig. 6A).

Lateral prefrontal cortex. Only area 9 deposits (case M01-05; Fig. 6J) produced a relatively high number of labeled fibers in the LC. These labeling was mainly distributed in the rostral LC, and some fibers entered the core in the most anterior portion of the nucleus. Two medium-size BDA injections in both 46d and 46v showed labeling in the most anterior rostral part of LC that is the rostral pole, and the density of which were higher in 46v compared to 46d (Fig. 6H and I, respectively).

DISCUSSION

The results in the present study show the existence of direct cortical projections from the insula, MPFC, OPFC and LPFC to LC. These projections are heterogeneous and show a crude topographical distribution in their terminal fields within LC. Interestingly, most of the studied areas innervate the core of LC, and most of them project directly to the densest part of the nucleus suggesting a modulatory influence of LC activity.

Methodological considerations

The BDA as anterograde tracer specifically labels axons and terminal arborizations that often show varicosities in the projected areas. We were able to detect and chart the projection at higher magnification despite that they were often scarce, very thin, and difficult to identify. Dark-field illumination also helped with the observation of these thin fibers.

In all tract-tracing experiment, the size of the injection site can markedly influence the density of the anterograde labeling. Yet, in the present study, large injections followed by sparse labeling were as large as injections where deposits resulted in much more dense labeling. This indicates that although injection size was an important factor in the density of cortical projections to LC, it did not confound the difference between dense projecting areas (agranular/dysgranular cortices) and those that did not. Retrograde labeling with injections of tracer in LC in our laboratory (unpublished results) and in prior studies (Aston-Jones et al., 2007) largely supports this heterogeneity.

The morphology of the LC and adjacent structures (represented in figures 6 and 7) varied slightly from animal to animal depending on the size of the animal and the angle of section, but this did not modify the overall results.

Comparison with prior studies in primates and rodents

Little is known about the cortical inputs in the primate LC. There are only few studies on the cortical afferents to LC in the monkey. Arnsten and Golman-Rakic (1984) showed the existence of direct cortical projections to LC in the nonhuman primate, although they suggested that the only cortical input to LC arises in the dorsomedial and dorsolateral PFC (areas 10 and 9), and they target the rostromedial part. Posterior studies suggested that only area 25 in the MPFC send moderate to scattered projections to the LC in the monkey (Freedman et al., 2000; Chiba et al., 2001). Aston-Jones and colleagues reported that OPFC and ACC also contribute to innervate LC (SfN 2000, 2002, 2004; Aston-Jones et al., 2007), and this clearly supports our data. Also, consistent with the present study, all these prior works showed that only about 5% of the total projections were contralateral.

A few previous anatomical studies in rodents described the existence of connections between the cerebral cortex and the LC, with a weak projection arising in the medial prefrontal, infralimbic and insular cortices, without reference to any specific topography (Cedarbaum and Aghajanian, 1978; Sesack et al., 1989; Luppi et al., 1995). A more recent tract-tracing study suggests that MPFC afferent terminals specifically innervate the rostromedial peripheral LC region in the rat (Lu et al., 2012). This rostral distribution of the terminals is consistent with our results in the nonhuman primate. Our experimental data show that most of the PFC areas target preferentially the rostral-to-medial part of the nucleus. The caudal pole is usually devoid of afferents, although some areas such as lamp, and 13 send projection homogeneously throughout the whole extension of LC. A major difference between rodents and our results in the nonhuman primate is that all the PFC areas (except 10o) directly target the core of LC, while in rodents the terminal fields are localized in the peripheral-LC, where the dendritic processes lie. Another important difference is that the monkey PFC sends overall qualitatively denser inputs to LC compared to the intensity of the projection described for rodents.

Functional interpretations

There is a wealth of functional evidence that indicates that PFC regulates the LC in the rodent. Jodo et al. (1997, 1998) suggested that the PFC has a potent excitatory influence on LC activity. Single pulse electrical stimulation (1 mA, 0.3-0.5

ms) of both the dorsomedial PFC and prelimbic cortex activate the 81% and 16% of the LC neurons respectively, and train stimulation (20 Hz for 0.5 s) activated a larger percentage of LC neurons (92% and 82%); however, electrical stimulation of the LPFC had no effect on LC activity (Jodo et al., 1998). Our anatomical results are in agreement with these data since the injections placed in rostrolateral PFC barely produced labeling in LC. Moreover, chemical inactivation of the MPFC suppressed LC firing. This indicates that MPFC also provides a resting tonic excitatory influence on LC activity (Jodo et al., 1998).

The cortical limbic system occupies the edges of the cortex as a ring above the corpus callosum and the base of the brain, where all cortical sensory, high-order association and motor systems abut (Barbas 2015). Our data show that the limbic prefrontal cortex (agranular and dysgranular areas) has a major input on LC compared to granular areas. The possibility arises that there might be a correlation between the laminar pattern existent across the different PFC areas and the intensity of the projections to LC. Overall, the agranular areas (Iam/Iamp) send the strongest input to LC, followed by the dysgranular areas in the MPFC and OPFC. The LPFC showed scarce labeling with the exception of DMPFC (area 9). This might be due to the fact that the injection site was precisely located in the most rostral portion of the dorsomedial area 9, which is very close and related to the dysgranular limbic cortex. Besides area 9, the areas 11, 12, 14 and 10 (granular) among others, produced scarce labeling in LC.

According to a recent structural model, feedforward connections project to less granular areas, and feedback projections originate from less granular areas (Barbas, 2015). Our data indicate that less granular areas do project to the LC at the same time that they present feedback projections to other cortical areas.

Despite its broad projection to the entire neuraxis, the LC is not homogeneous since there exists an inner specific organization of its cells with respect to the functions of its efferent targets (Chandler et al., 2013). Combining anatomical, molecular and electrophysiological methods, it was shown that different populations of cells in LC in the rat project specifically to different discrete prefrontal and primary motor cortex areas, with minimal overlapping and that LC cells innervating specific subregions of PFC are distinct from those terminating in M1 both in neurochemical content and electrophysiogically (Chandler et al., 2014).

In turn, LC receives direct inputs from numerous brain structures, with

substantial degree of topography, based on the rat model (Luppi et al., 1995; Valentino et al., 1996; Van Bockstaele et al., 1999, 2001). The central nucleus of the amygdala and the bed nucleus of the stria terminalis send afferent fibers mainly to the rostrolateral peripheral-LC (Ennis et al., 1991), the ventrolateral part of the periaqueductal grey area sends afferent fibers mainly to the rostromedial peripheral-LC (Ennis et al., 1991), the ventral tegmental area targets the rostral pole (Deutch et al., 1986), and the dorsal raphe nucleus to the caudal part of the peripheral-LC region (Lu et al., 2012), suggesting selective afferent patterns.

The present study demonstrates a direct top-down input to LC from agranular/dysgranular limbic areas in the prefrontal cortex and the anterior insula. These connections might underlie the areal-specific role of high cognitive, motivational and emotional processes in the control of LC activity and NA release in the brain.

REFERENCES

Arnsten AF, Goldman-Rakic PS (1984). Selective prefrontal cortical projections to the region of the locus coeruleus and raphe nuclei in the rhesus monkey. Brain Res 306(1-2):9-18.

Aston-Jones G, Iba M, Clayton E, Rajkowski J, Cohen J (2007). The locus coeruleus and regulation of behavioral flexibility and attention: clinical implications. In Brain Norepinephrine: Neurobiology and Therapeutics, ed. Ordway GA, Schwartz MA and Frazer A. Cambridge University Press. Pp 136-235.

Aston-Jones G, Rajkowski J, Cohen J (2000). Locus coeruleus and regulation of behavioral flexibility and attention. Prog Brain Res 126: 165–182.

Barbas H (2015). General cortical and special prefrontal connections: principles from structure to function. Annu Rev Neurosci 38: 269-289.

Berridge CW, Waterhouse BD (2003). The locus coeruleus-noradrenergic system: modulation of behavioral state and state-dependent cognitive processes. Brain Res Rev 42: 33-84.

Bush G, Luu P, Posner MI (2000). Cognitive and emotional influences in anterior cingulate cortex. Trends Cogn Sci 4:215-222.

Carmichael ST, Price JL (1994). Architectonic subdivision of the orbital and medial prefrontal cortex in the macaque monkey. J Comp Neurol 346(3):366-402.

Carmichael ST, Price JL (1995a). Limbic connections of the orbital and medial prefrontal cortex in macaque monkeys. J J Comp Neurol 363(4):615-641.

Carmichael ST, Price JL (1995b). Sensory and premotor connections of the orbital and medial prefrontal cortex of macaque monkeys. J Comp Neurol 363(4):642-664.

Carmichael ST, Price JL (1996). Connectional networks within the orbital and medial prefrontal cortex of macaque monkeys. J Comp Neurol 371(2):179-207.

Cedarbaum JM, Aghajanian GK (1978). Afferent projections to the rat locus coeruleus as determined by a retrograde tracing technique. J Comp Neur 178: 1-16.

Chandler DJ, Lamperski CS, Waterhouse BD (2013). Identification of projections from monoaminergic and cholinergic nuclei to functionally differentiated subregions of prefrontal cortex. Brain Res 1522: 38-58.

Chandler DJ, Gao WJ, Waterhouse BD (2014). Heterogeneous organization of the locus coeruleus projections to prefrontal and motor cortices. PNAS 111: 6817-6821.

Chiba T, Kayahara T, Nakano K (2001). Efferent projections of infralimbic and prelimbic areas of the medial prefrontal cortex in the Japanese monkey, *Macaca fuscata*. Brain Res 888: 83–101.

Deutch AY, Goldstein M, and Roth RH. (1986). Activation of the locus coeruleus induced by selective stimulation of the ventral tegmental area. Brain Res 363: 307-314.

Ennis M, Behbehani M, Shipley MT, Van Bockstaele EJ, Aston-Jones G (1991). Projections from the periaqueductal grey to the rostromedial pericoerulear region and nucleus locus coeruleus: new evidence of anatomical and physiological specifity. Physiol Rev 63: 844-914.

Evrard HC, Logothetis NK, Craig AD (2014). Modular architectonic organization of the insula in the macaque monkey. J Comp Neurol 522:64-97.

Freedman LJ, Insel TR, Smith Y (2000). Subcortical projections of area 25 (subgenual cortex) pf the macaque monkey. J Comp Neurol 421: 172-188.

Insausti R, Amaral DG (2008). Entorhinal cortex of the monkey: IV. Topographical and laminar organization of cortical afferents. J Comp Neurol 509(6):608-641.

Jodo E, Aston-Jones G (1997). Activation of locus coeruleus by prefrontal cortex is mediated by excitatory amino acid inputs. Brain Res 768(1-2): 327-32.

Jodo E, Chiang C, Aston-Jones G (1998). Potent excitatory influence of prefrontal cortex activity on noradrenergic locus coeruleus neurons. Neurosci 83(1): 63-79.

Kerns JG, Cohen JD, MacDonald III AW, Cho RY, Stenger VA, Carter CS (2004). Anterior cingulate conflict monitoring and adjustments in control. Science 303: 1023-1026.

Kondo H, Saleem KS, Price JL (2003). Differential connections of the temporal pole with the orbital and medial prefrontal networks in macaque monkeys. J Comp Neurol 465(4):499-523.

Lu Y, Simpson KL, Weaver KJ, Lin RCS (2012). Differential distribution patterns from medial prefrontal cortex and dorsal raphe to the locus coeruleus in rats. Anat Rec 295: 1192-1201.

Luppi PH, Aston-Jones G, Akaoka H, Chouvets G, Jouvet M (1995). Afferent projections to the rat locus coeruleus demonstrated by retrograde and anterograde tracing with cholera-toxin b subunit and *Phaseolus vulgaris leucoagglutinin*. Neurosci 65(1): 119-160.

Milstein JA, Lehmann O, Theobald DE, Dalley JW, Robbins TW (2007). Selective depletion of cortical noradrenaline by anti-dopamine beta- hydroxylase-saporin impairs attentional function and enhances the effects of guanfacine in the rat. Psychopharmacol (Berl) 190: 51-63.

Mohedano-Moriano A, Muñoz-López M, Sanz-Arigita E, Pró-Sistiaga P, Martínez-Marcos A, Legidos-Garcia ME, Insausti AM, Cebada-Sánchez S, Arroyo-Jiménez MM, Marcos P, Artacho-Pérula E, Insausti R (2015). Prefrontal cortex afferents to the anterior temporal lobe in the Macaca fascicularis monkey. J Comp Neurol 523: 2570–2598.

Radley JJ, Williams B, Sawchenko PE (2008). Noradrenergic innervation of the dorsal medial prefrontal cortex modulates hypothalamo-pituitary-adrenal responses to acute emotional stress. J Neurosci 28(22): 5806-5816.

Rajkowski J, Lu W, Zhu Y, Cohen J, Aston-Jones G (2000). Prominent projections from the anterior cingulate cortex to the locus coeruleus in the Rhesus monkey. Soc Neurosci Abstr 26: 838.15.

Ramos BP, Arnsten AF (2007). Adrenergic pharmacology and cognition: focus on the prefrontal cortex. Pharmacol Ther 113: 523–536.

Saleem KS, Kondo H, Price JL. 2008. Complementary circuits connecting the orbital and medial prefrontal networks with the temporal, insular, and opercular cortex in the macaque monkey. Journal of Comparative Neurology 506(4):659-693.

Sesack SR, Deutch AY, Roth RH, Bunney BS (1989). Topographical organization of the efferent projections of the medial prefrontal cortex in the rat: an anterograde tract-tracing study with Phaseolus vulgaris leucoagglutinin. J Comp Neurol 290(2):213-42.

Szabo J, Cowan WM (1984). A stereotaxic atlas of the brain of the cynomolgus monkey (*Macaca fascicularis*). J Comp Neurol 222: 265-300.

Valentino RJ, Chen S, Zhu Y, Aston-Jones G (1996). Evidence for divergent projections to the brain noradrenergic system and the spinal parasympathietic system from Barrington's nucleus. Brain Res 732: 1-15.

Van Bockstaele EJ, Bajic D, Proudfit H, Valentino RJ (2001). Topographic architecture ofstress-related pathways targeting the noradrenergic locus coeruleus. Physiol Behav 73: 273-283.

Van Bockstaele EJ, Peoples J, Telegan P (1999). Efferent projections of the nucleus of the solitary tract to peri-locus coeruleus dendrites in rat brain: evidence for a monosynaptic pathway. J Comp Neurol 412(3):410-28.

Zhu Y, Aston-Jones G (1996). The medial prefrontal cortex prominently innervates a peri-locus coeruleus dendritic zone in rat. Soc Neurosci Abstr 22, 601.

Zhu Y, Iba M, Rajkowski J, Aston-Jones G (2004). Projections from the orbitofrontal cortex to the locus coeruleus in monkeys revealed by anterograde tracing. Soc Neurosci Abstr 30: 211.3

CHAPTER 3. Heterogeneus prefrontal projections to the midbrain ventral tegmental area in the macaque monkey

ABSTRACT

The orbital and medial prefrontal cortex (OMPFC) is divided on the basis of its connectivity into orbital 'viscerosensory' (OPFC) and medial 'visceromotor' (MPFC) networks. Previous reports proposed that both networks exert a strong influence onto the ventral tegmental area (VTA) activity through interposed diencephalic nuclei, and influence VTA function through sparse direct connections. Here, we analysed the density and topographical organization of the projections of the OMPFC areas projections to VTA in the macaque monkey. Injections of biotin dextran amine or fluororuby in distinct OMPFC resulted in anterogradely labelled fibres with varicosities in VTA. The density of labelled fibres varied with the location of the injection site, so that each network had areas contributing more projections than others. Overall deposits in the medial network produced more labelling than injection in the orbital network. Specifically, deposits in areas 25 and medial 9, and the intermediate agranular insula (Iai) of the "medial" network produced relatively dense labelling. In contrast, injections in areas 10o, 11m and 12m produced sparse or no labelling. In the orbital network, only injections in area 13b and in the posterior median agranular insula (Iapm) produced relatively dense labelling with no major difference between areas. Injections in the remainder OMPFC areas including areas 10mr, 46d and 12r produced no labelling. A comparison of the spatial distribution of the labelled fibres in VTA revealed a considerable overlap of the projections from the different areas; only a trend for more lateral and rostral distribution in medial areas relative to orbital areas was noticed. Our results suggest for the first time a complex organization of prefrontal cortex afferents to VTA. This diversity of inputs to the VTA could provide new insight in the top-down control of dopamine release, and in the study of new possible targets for the treatment of neurological disorders.

INTRODUCTION

The connections between the prefrontal cortex (PFC) and the ventral tegmental area (VTA) are critical for memory, novelty detection and reward. At the cellular level, they play a key role in behaviorally relevant burst firing of DA within VTA (Gariano et al., 1988; Murase et al., 1993). Impairment of this control has been associated to the pathophysiology of schizophrenia (Sesack et al., 2002) and drug addiction (Lodge et al., 2011; Laurelle et al., 1996). Most of the experimental studies on the cortical control of DA release have been investigated in rodents. In this species excitatory (glutamatergic) projections or inhibitory (GABAergic) intermediary synapses has been described (with the ventral pallidum, nucleus

accumbens and pedunculo-pontine) into the different DA and non-DA subpopulations of the VTA (Lammel et al., 2012; Grace et al., 2007).

Still, little is known about the anatomical organization of the projections from the PFC to VTA in nonhuman primates, and in particular which PFC areas contribute most with projections to VTA, and whether these projections are topographically organized. The rodent PFC is not comparable to primates and is composed mostly by agranular cortices (Ongur et al., 2000). The rat PFC is subdivided into only a few "areas" (infralimbic, prelimbic and cingulate areas) that do not include a proper lateral prefrontal cortex and barely has an equivalent of monkey area 10 (Burgess et al., 2007). These cytoarchitectonic differences between rat and primate can account for a higher parcellation of the different PFC areas based on their different set of connections and functions found in primates (Price, 2007). This is a factor to be kept in mind when considering the density of projections, and the presence of superior cognitive processing functions in primates.

In addition, whereas some authors claim that rat PFC (prelimbic and infralimbic) projections contributes denser projections to VTA (Hurley et al., 1991 and Takagishi et al.,1991, Geiser et al., 2006) than PFC does in monkeys (Frankle et al., 2006), other authors suggest that the density of the connections is low in both species (Sesack and Pickel, 1992). Most of what is known about the organization of the PFC projections to VTA comes from the rodent literature and there is, to this date, no data suggesting that the vast expansion and diversification of the monkey PFC may be accompanied with a more complex and heterogeneous organization than in rodents. Along with the cortical expansion, subcortical nuclei and regions such as the VTA might have expanded and/or reorganized in order to relate with new areas in the cortex. So far it has been assumed that the rodent and primate VTA shares the same overall organization (Sesack and Grace, 2010). However, VTA in rats has been described as being made up to 8 small nuclei (Gasbarri et al., 1994b) while in monkeys, some authors refer only up to 2 nuclei (Ritchie et al., 1998; Wilhelmus et al., 2000; Cho et al., 2010).

In the present study we examined the organization of the projections of the different areas and subareas of the PFC to VTA in macaque monkeys. We observed that only a distinct set of cortical areas contribute major projections to VTA. Particularly, the areas of the PFC that are first affected by cocaine exposure (Beveridge et al., 2008; Porrino et al., 2000) and present strong interconnections with the Ventral striatum involved in motivation (further information, see Joel et al., 2000), send direct projections to the VTA (Ferry et al., 2000).

MATERIALS AND METHODS

The present data were obtained from 25 adult cynomolgus or rhesus macaques (Macaca fascicu-laris or mulatta, respectively; 5-10 kg) in three different laboratories (Price, Insausti, and Evrard). All cases from Price's laboratory and some cases from the Insausti's laboratory were prepared and used in the context of prior tract-tracing studies (Carmichael and Price, 1995b, a, 1996; Kondo et al., 2003; Insausti and Amaral, 2008; Saleem et al., 2008). The animals were treated according to the guidelines of the American Physiological Society, the NIH and the European Parliament and Council Directive 2010/63/EU on the protection of animals used for experimental and other scientific purposes. All animal protocols were reviewed and approved by the Animal Studies Committee of Washington University, St.-Louis, USA, and the Ethical Committee of Animal Research of the University of Castilla-La-Mancha (UCLM), Spain, or the German authorities (Regierungspräsidium).

Surgery and tracer injections

Anesthesia was induced by an intramuscular injection of ketamine (10mg/kg) and xylazine (0.67mg/kg) for of MRI, surgical procedures and also at the time of perfusion (see below). During surgery, the anesthesia level was maintained by intubation with isoflurane. Thereafter, the animal was placed in a Kopf stereotaxic frame for craniotomy. After surgery, a long lasting analgesic, buprenorphine (0.1mg/Kg, i.m) was given to the animal upon recovery.

Most of the PFC injections had the stereotaxic coordinates for the injection site were calculated from the MRI obtained in a Phillips Intera 1.5T (Insausti's laboratory). However, for tracer injections into deep cortical areas, a tungsten electrode was inserted along the expected track of the pipette for electrophysiological recordings of spontaneous activity which allowed to determine the vertical coordinates of the structural boundary between grey and white matter or the bottom of the brain to correct the vertical coordinates determined by the MRI.

Retrograde tracer (Fast Blue [FB; 3 %]) and anterograde tracers (biotinylated dextran amine [BDA; Molecular probes 10%]) and two bidirectional tracers (FluoroRuby [FR; Molecular Probes 5% or 10%], and Lucifer Yellow [LY; Molecular Probes 5% or 10%]) were injected. The injections were made through an air pressure system using 25 msec air pulses. The air pressure was adjusted so that very small volumes of tracer were injected in each pulse (for details, see Kondo et al., 2005). To avoid spread of the tracer into areas along the pipette track, the micropipette was left in place for 30 minutes after the injection was completed.

Perfusion and histological processing

After a survival period of two weeks, the animals were anesthetized with ketamine i.m, followed by sodium pentobarbital (25-30mg/kg i.v. or intraperitoneally). After the animals were deeply anesthe-tized, they were perfused transcardially with saline, followed of 4% paraformaldehyde solutions at pH 6.5 and pH 9.5 (Carmichael et Price, 1994) and 10% sucrose at pH 9.5. Then the brain was removed and placed in 30% sucrose in phosphate-buffered until it sank. Three days later, the brain was frozen in isopentane cooled with dry ice and cut into 10 collated coronal sections series of 50 µm (T.HSU et al 2007). FR and LY were processed immunohistochemically with avidin-biotin-horseradish peroxidase technique; BDA was processed with the avidin-biotin-peroxidase method (Carmichael and Price 1994).

Data analysis and presentation of illustrations

Sections were examined with light microscope. Injection sites and axonal varicosities were manually plotted by using a microscope-digitalized system (AccuStage, Shoreview, MN). For sparse labeling, each fiber was plotted as a single point. However for densely labeled areas, 4 points indicate moderately dense varicosities greater than 10 fibers / per surface unit; a rating of 6-8 points indicate strong labeling, greater than 25 fibers / per surface unit. We mapped in Sequential linear passes across the section. Midbrain boundaries were drawn onto printed plots by using camera lucida drawings on adjacent sections stained for Nissl.

We evaluated the relative strength of connections but not absolute values, as it is not possible to compare absolute values because of factors such as differences in transport levels between tracers, injection volumes and location of each injection. Midbrain areas were analyzed bilaterally. Coronal series of sections were prepared in order to visualize the distribution and density of the labeling. Because individual maps were prepared for each case, we could not compare the overlap labeling.

Nomenclature

The terminology used for the VTA nuclei was adapted from Paxinos and the borders of each nuclei were defined according to the morphology of the cells in the Nissl staining and the boundaries of the area along the rostro-caudal VTA level. Based on functional studies, two main cell clusters within the VTA were defined.

The most caudal and medial part was related to anticipation reward and novelty, while the ros-tral and medial part was exclusively modulated by novelty (Krebs et al., 2011) and our anatomical results and immunohistochemistry support this division (see Hernandez-

Mombiela et al., in preparation). According to our division, the VTA consists into: proper VTA, lateral VTA or PBP; ventral VTA or PN and tail of the VTA. However for consistency, we will show the labeling obtained in the entire nucleus of the VTA.

RESULTS

Injection sites in PFC

Figure 1. Illustrates a representative injection site from case M315 with an injection of BDA in the area 12o. In most cases, like in M315, the injection site was confined to the cortical grey matter and included layers III and/or V. They all had a dense central 'core' around the tip of the micropipette penetration track and a more diffuse 'halo' extending for approximately 100 to 300 µm around the core. Injection sites for BDA always appeared larger and denser than injection sites for comparable volumes of FR and LY (not shown).

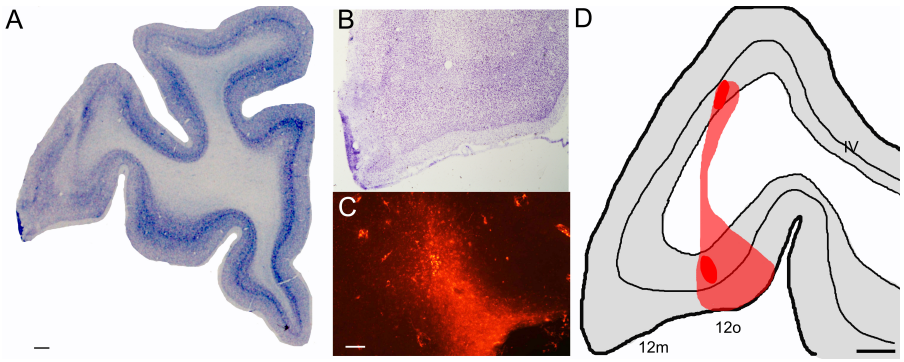

Figure 1. Representative example of an injection site (case M315). (A) Nissl-stained coronal section photomicrographa the level of the deposit (B-C) Higher magnification view of the injection site in Nissl and BDA. (D) Drawing of the maximal extent of the deposit. Scale bar 1mm

The anterograde labelling from a total of 27 anterograde tracer injections made in PFC or anterior insula was analysed in the present report. Figure 2 shows the location of each injection site in a standard map of the PFC.

Two injections were made in orbitofrontal cortex area 10o (OM38BDA and OM65FR). Three injections were made in medial prefrontal-cingulate areas 24b and 25 (cases OM34BDA, OM32FR/BDA and OM49BDA), and ten injections were made in orbital prefrontal cortex areas 11m, 11l, 12m,12r, 12, 13b, 13l (OM40BDA, OM27BDA, OM30BDA, OM29BDA, M2.15BDA, M3.15BDA, OM28BDA, OM79FR, OM65 LY, and OM42BDA). Two injections were made in anterior insula in areas Iai/Ial and Iam/Iamp (M615FR, OM68BDA). Five injections were made in lateral prefrontal cortex areas 9, 46v, 46d and multiple injection site in area 45,46v,12 (M105BDA, M305BDA, M205BDA, M405BDA and OM69LY).

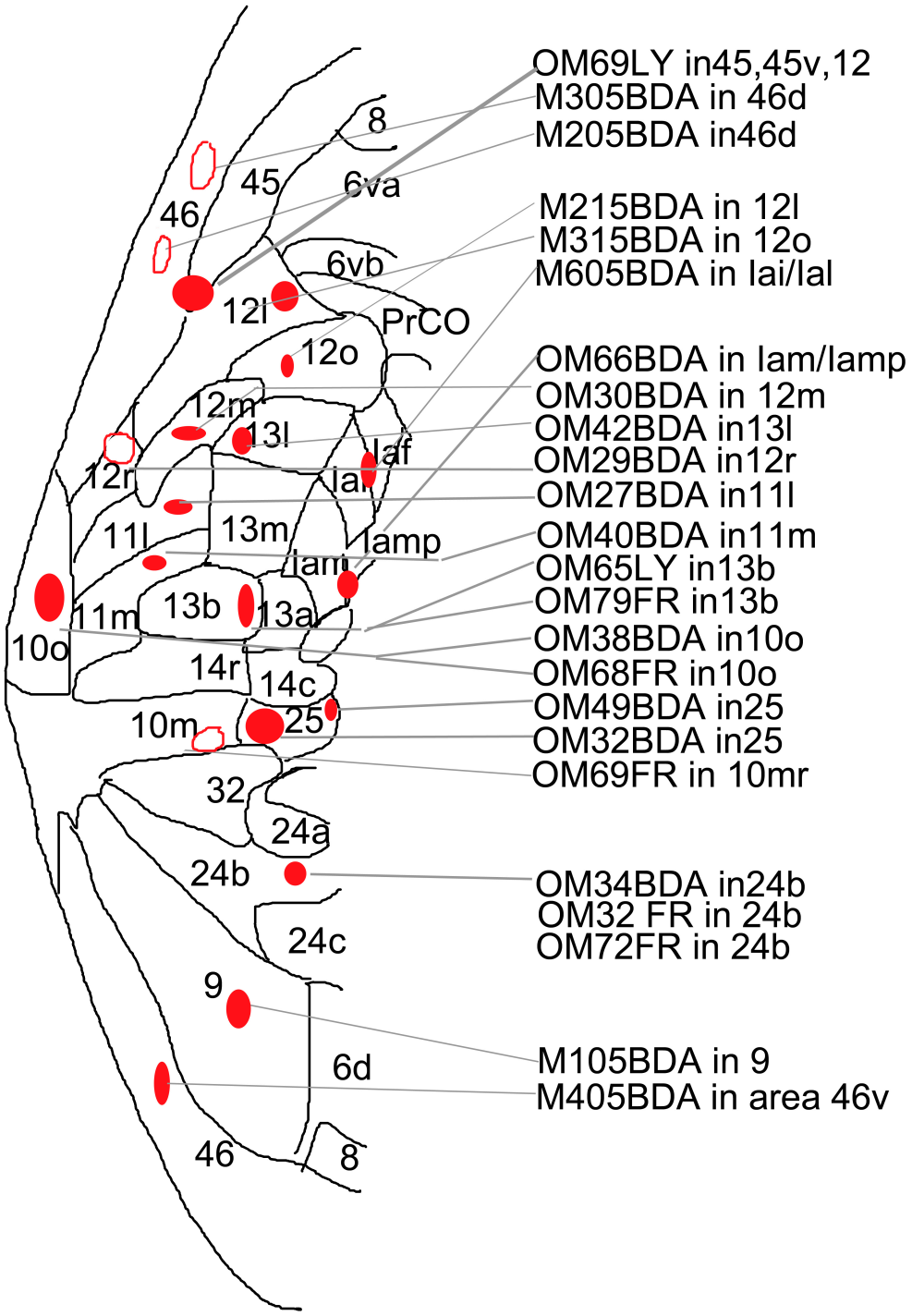

Figure 2: Topology of the injection sites in PFC using a relative collation of all injection sites onto a standard map of PFC. The ellipsoid shapes represent both the core and halo of the injection site. The ellipsoid shapes filled in red indicate the injection sites that produced anterograde labeling in VTA. The empty ellipsoid shapes indicate injection sites that did not produced labeling in VTA.

Some of the injections listed above spread to more than one architectonic area. In case OM66, the large BDA injection included both Iam and Iamp. In case M615, the injection included areas Iai/Ial. In case OM72FR, the injection spread to areas 24a' and b'. In case OM69, it included areas 45,46v and 12. Single injections of various small-middle sizes were also made in the same area; 46v (M3.05BDA and M4.05BDA) and area 13 and subareas 13b, 13l (M605BDA, OM65LY, OM42BDA, M315BDA).

As some of the tracers (FR, LY) are transported both retrogradely and anterogradely, we verified the injections by examining the location of anterogradely labelled fibres in the striatum (Haber et al., 1995) and neurons in the Amygdala (Carmichael et al., 1995).

Anterograde labelling in VTA

Architectonic organization of VTA.

A pre-requisite to the description of the distribution of anterograde labelling in VTA is a mapping of VTA to use as a reference. Figure 3 shows an architectonic map of VTA and various neighbouring nuclei or regions of the midbrain across 4 representative anteroposterior levels of the left VTA. The absence of the mammillary nuclei at the most rostral level indicated somewhat the rostral end of VTA at approximately -10.80 mm from the antero-posterior Bregma (AP) which correspond to our level 0 in Figure 3. VTA was co-existent with and ventral to the obvious red nucleus (RN and then its magnocellular part, RMC) throughout its almost entire rostro-caudal extent (level 1350 to 3150), and it was intermingled within the fibres of the third (oculomotor) nerve at the level of 2500. At its middle level, VTA was located dorsal to the interpeduncular fossa (IF), which, with the middle line nucleus, splitted VTA into two distinct sides. At more caudal levels, IF was replaced by the interpeduncular nucleus (IP) at (AP -14.40 mm; level 2500). The level where RM led to RMC also indicated the beginning of the tail of the VTA. The level of decussation (xscp) delimits the caudal level of the VTA that will continue further caudally until reaching AP 16.40mm (not shown).

General observation on the anterograde labelling.

All of the injections reported here produced anterograde labelling and in some cases retrograde labelling in VTA. Figure 4 shows examples of labelled fibres (4A) and neurons (4B) in VTA. The size of the segment of labelled fibres varied depending on the injection site; however the general overview showed short-medium fibres. Anterograde labeled fibers were counted on the contra- and ipsilateral sides. The labeling was bilateral, although the number of anterogradely labeled fibers in the ipsilateral side represented barely 5 % of the number of

labeled fibers in the contralateral side; this observation is consistent with prior anterograde studies (Frankle and Haber, 2006).

The intensity of labeling varied, with most labeled fibers being moderately to intensely labeled, regardless of the tracer used, with the exception that immunohistochemically series showed greater density than the fluorescence series. The amount of labeling also varied with the size of the injection site. For example two different deposit sizes placed in area 25 (case OM32BDA and OM49BDA) showed more labeling in the larger deposit. In the following text the labeling in the OMPFC is described and analyzed arranged in networks.

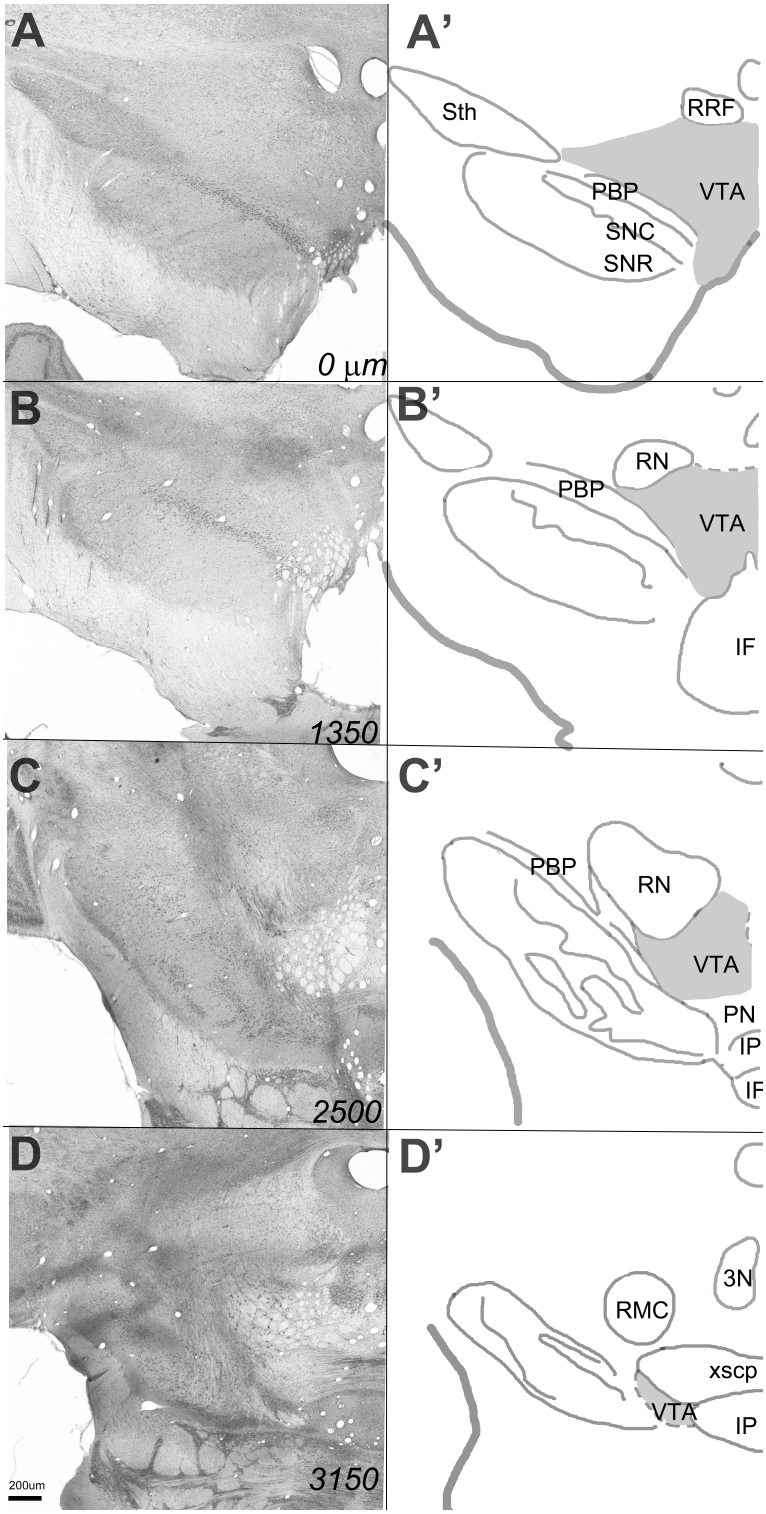

Figure 3. Architectonic mapping on a series of (A-D) coronal photography's of Nissl and the corresponding drawing (A'-D') through the rostro-caudal axis of the VTA. STh: Hypothalamic nucleus; RRF: Retrorubral Field; PBP: Parabrachial Pigmentosus nucleus; SNC: Sustancia Nigra Compacta; SNR: Sustancia Nigra Reticulata; RN: Red nucleus; IF: Interpeduncular Fossa; IP: Interpeduncular nucleus; RMC: Red magnocellular nucleus; xscp: decussation. Scale bar 200um

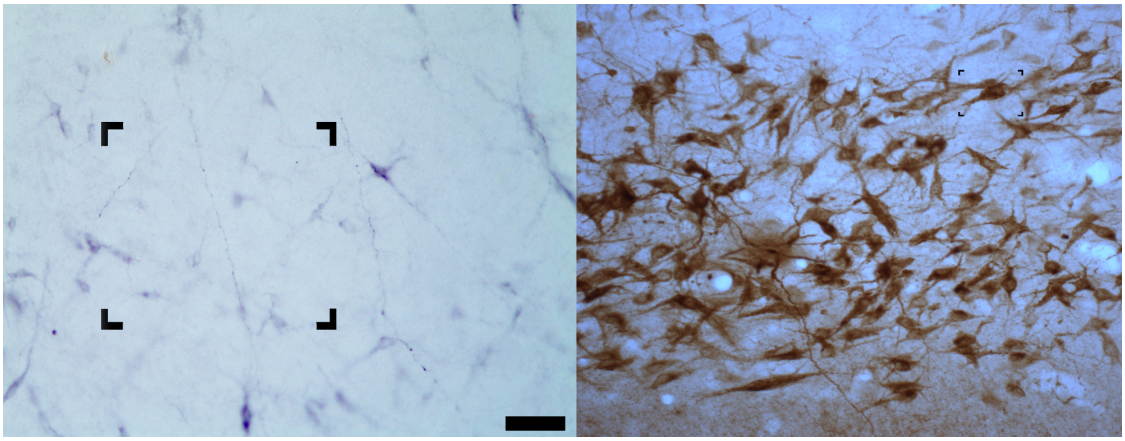

Figure 4. Photomicrographs of examples of labelled fibers bearing varicosities in VTA (A) and neurons (B) labeled with injections of FluoroRubi. Scale bar 1mm

Largely, the MPFC deposits resulted in the densest labeling of all PFC areas. The MPFC projections are representative of the labeling observed. The distribution of the projections within the VTA nuclei was characterized by broadly dispersed fibers, with clusters of denser labeling and patches of sparse labeling, generally within the anterior VTA that varied according to the PFC area explored. The property of bidirectionality in the used tracers allowed the observation of some neurons. The rostrocaudal location of the labelling was approximately similar regardless of the location of the injection site in the PFC. However the medio-lateral distribution within the different subnuclei showed a small tendency for more lateral and rostral distribution sites in MPFC relative to OPFC.

The following paragraphs describe the general density and location of the anterograde labelling in VTA. Figure 5 shows the plot of anterograde labelling in sets of coronal sections through the ventral midbrain for selected cases. The outline of the nuclei in these plots is a direct mirroring of the map shown in Figure 3. The different cases are arranged in 6 groups, from “dysgranular MPFC” to “eulaminar LPFC”.

Dysgranular MPFC.

The projections from the area 24b, case OM32 FR (Fig. 5A) and case OM32BDA (not shown) (Kondo et al., 2005) showed scarce projections into the rostral and middle levels of the VTA, mostly to the lateral VTA and to a subgroup of cells in the ventral part but not into the SN (Freedman 2000; Mar et al., 2013; Frankle et al., 2006). However, in area 25, case OM32BDA (Fig. 5B) the density of the projections was greater, despite that the pattern of distribution was similar to area 24b (Price 1998; An X et al., 1998 case 36; Frankle et al., 2006; Mar et al.,2013).

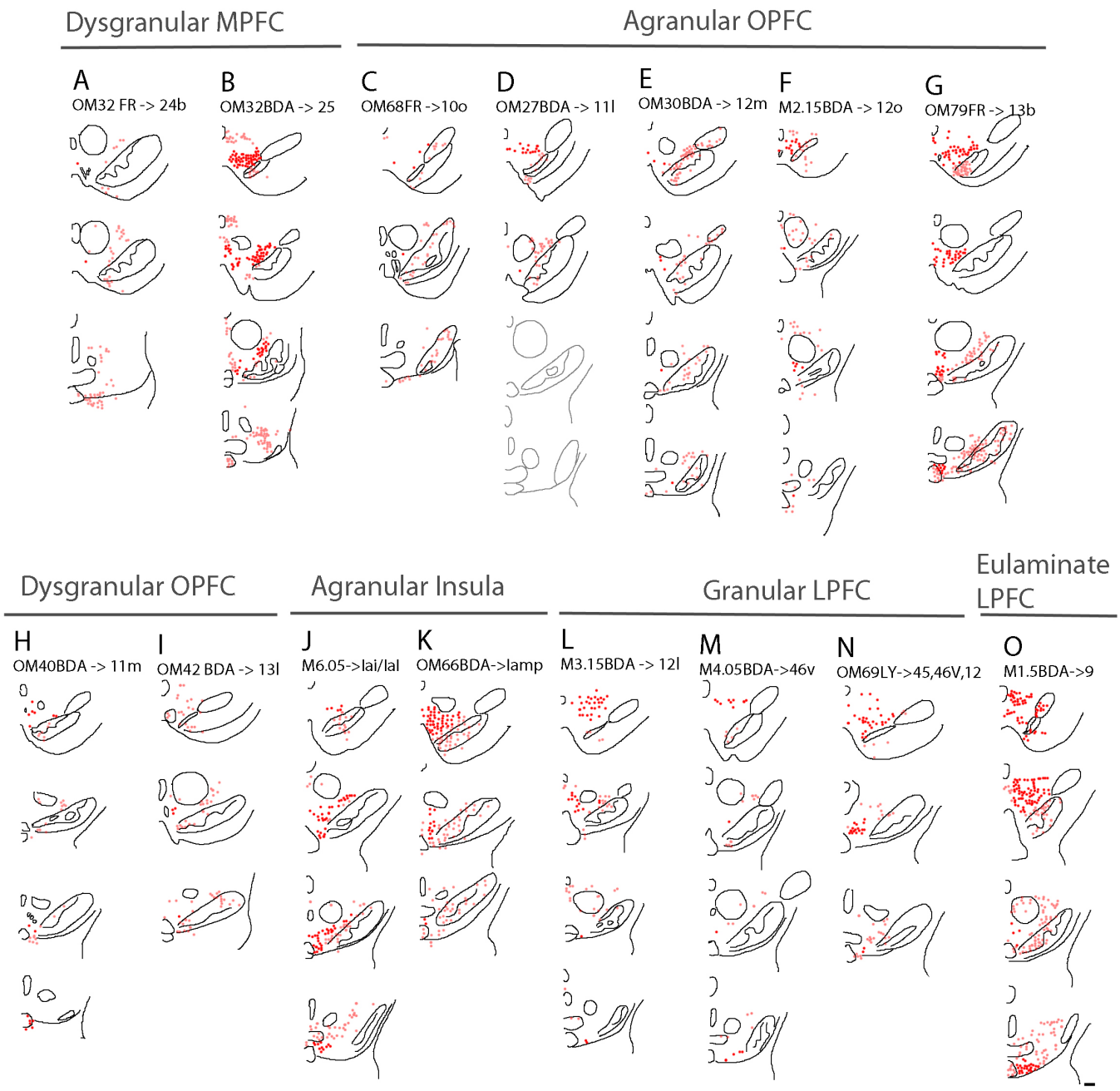

Figure 5: (A-O) Plot of anterograde labeling in the midbrain, produced with injections of tracers in the PFC. The dark red labeling corresponds to labeling in VTA. The pink labeling corresponds to labeling outside VTA. Scale bar= 1mm

Agranular OPFC

In the frontopolar cortex, two cases (Fig. 5C) OM68FR (Hsu et al., 2007) and OM38BDA (Shown in Saleem et al., 2008) received small tracer injections orbitofrontal cortex subarea 10o. No major difference in the VTA/SN projection was observed, although it was present in the hypothalamus. Labelled fibres were distributed in the rostral and middle parts of the lateral VTA and SNC (Results confirmed in AN X. et al., 1998 case OM36BDA).

Further modest projections arose from area 11l, case OM27BDA (Fig5.D) (shown in Hsu et al., 2007) with small-medium size injections of BDA resulted in a similar density and pattern distribution as the projections from the dysgranular area 11m. It contributed with some fibbers to the rostral, ipsilateral VTA, lateral (PBP), ventral (PN) and a few along SNC. Major differences were found within area 12. Four cases OM30BDA (Saleem et al., 2008) (Fig. 5E) OM29BDA (D.T. Hsu et al., 2007) (not shown), M3.15FR (Fig. 5E) and M2.15FR (Fig. 5F) of small-medium size injections placed in the caudal area 12r, rostral 12m and 12 show two distinct patterns. Area 12r yielded negative results, while areas 12 and 12m resulted in a decreasing rostro-caudal gradient projection to VTA and lateral VTA, but also from 12m to the SNC (Ongur et al., 2008). Moreover, three more cases OM79FR (Fig. 5G) OM65LY (Not shown) (Kondo et al., 2005), and OM72 (not shown) with medium size injections of FR, LY and BDA showed heavy projections from area 13b. No major differences dependent on the tracer were noticed (Frankle et al., 2006, case 133). The labelling was mostly ipsilateral and all over the VTA and SN.

Dysgranular OPFC

In the frontopolar cortex, one medium size injection OM69FR (not shown) in the 10mr produced no labelling un the VTA (Saleem et al., 2014).However, two cases, one case OM40BDA (shown in Hsu et al., 2007) (Fig. 5H) with small-medium size injections of BDA in area 11l resulted in positive fibbers projection to the rostral, ipsilateral VTA, lateral (PBP), ventral (PN) and a few along SNC. Another case OM42BDA (Fig. 5I) (Saleem et al.,2008) in area 13l resulted in la week labelling along the rostral and middle parts of the VTA but almost not in the SN.

Agranular Insula

Two cases (Fig. 5K and J) were injected in different parts of the insula, one in the agranular insula (Iam/Iamp, OM66BDA) and another case in area Ial/IaL (M6.05BDA). Projections from the Iam/Iamp showed strong projections along the VTA and SN (An et al., 1998; Price 1998; Ongür et al., 1998). Area Ial/IaL showed projections to VTA, although less dense and no labelling in the SN.

Granular LPFC

Three cases M205 and M305 (not shown) of medium size injections of BDA in area 46d gave few labelled fibres in the rostral-most part of the VTA, but not in the SN; although in case M405 (Fig. 5M) with a mid-injection size of BDA in area 46v presented scarce labelling in the VTA. One extra case with a big injection size of LY in area 45,46v and 12 (Fig. 5N) showed ipsilateral projections along the VTA particularly in the PBP nucleus and non in the SN.

Eulaminate or pseudolaminate LPFC

In the lateral prefrontal cortex, only injections in area 9 produced dense labelling. One case M105 (Fig. 5O) with a mid-size BDA deposit in area 9 showed strong ipsilateral labelling distributed all along VTA and SN.

Topographic distribution and overlap of anterograde labelling in VTA

The anterograde labelling in VTA occurred throughout the entire rostro-caudal extent of VTA, with however a preferential labelling in the rostral half, and no cases with only caudal portions of the VTA labelled. We found subtle differences in the medio-lateral distribution within the VTA region, depending on the network. For instance orbital PFC projections distributed more medial with the exception of area 11m (Fig. 5). Injections in the medial prefrontal cortex produced a similar pattern projection from the area 25 and insula that in turn are the areas that project most to VTA. Finally in the lateral PFC, despite that the projections are scarce we found that area 46 labelling distributes more along the lateral parts of the midbrain while area 9 projects strongly all along VTA. This could be due to the fact that part of area 9 belongs to the medial prefrontal network

To study the possible overlap or the spreading of the projection labeling within the VTA coming from different PFC areas, we paid attention to cases that had more than one injection in the PFC. Two cases were valid for this study. OM32 received injections of FR in area 24b and of BDA in area 25. OM72 received injections of FR in areas 24a'/24b' and LY in area 23b. OM69 received injections of FR in 10mr and LY in area 45, 46, 12 (not shown). The results from the first case (Fig 5.A-B) showed that the projections that arise in area 25 target the most medial and lateral parts of the VTA while projections from area 24b only reach a subgroup of ventral cells lying at the base of VTA. In the second case (data not shown), the injection in area 23b produced sparse labelling in the rostral midlevel of VTA and the injection in area 24a'/24b' produced no labelling. In the third case, no labelling was found from area 10mr and from the forth injection, rostro-medial levels of the VTA showed positive

fibbers.All together, this simple comparative examination suggests that the PFC projections to VTA may have some subtle degree of internal topographic organization.

Injection sites in VTA

To confirm the projections inferred from the analysis of the anterograde labelling in VTA, retrograde tracers injections were made in or around VTA. Injections within VTA involved different adjacent nuclei and were placed at different rostro-caudal levels or more lateral. Out of the seven cases injected (see Methods), only three produced technically reliable retrograde labelling (M2-15FB, M3-15FB and M9-9FB). Figure 6 depicts the injections sites in the VTA drawn coronal drawings. The injections were relative small and showed a core and a hallo of deposit. Injections within VTA involved different nuclei and were placed at different rostro-caudal levels or more lateral.

One injection of FB was made in rostral VTA (M3-15; Fig. 6D). One injection of FB was made in the lateral aspect of the middle AP extent of VTA (M2-15; Fig. 6E).

One injection of FB was made in the caudal end of VTA (M9.09 Fig. 6I). All sites were relatively small and did not extensively spread to adjacent regions.

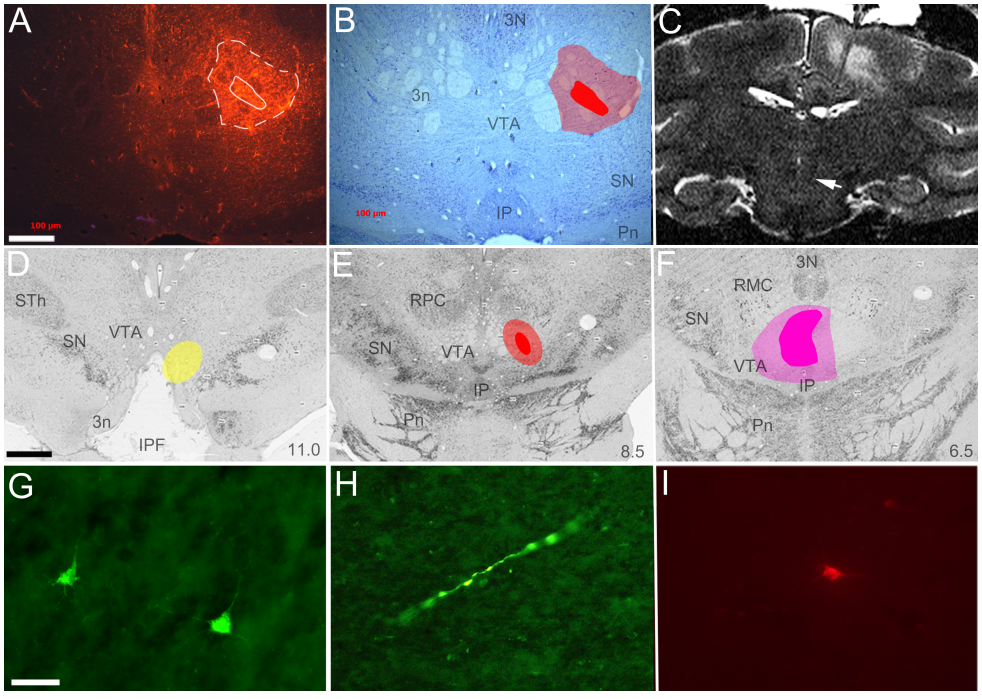

Figure 6: Photomicrographs of adjacent coronal fluorescent (A) and Nissl-stained (B) sections showing Pdex injection site in case cm28; the core and halo (circled by continuous and dashed lines, respectively) and their plots onto Nissl-stained photomicrographs of VTA, respectively. C. MRI section showing the location of the fused silica micropipette used to inject Pdex in VTA. D-F. Injection sites from cases cm018Rdex ('yellow'), cm017Rdex ('green'), cm020Rdex ('purple') and cm024Pdex ('red') depicted on a set of 3 photomicrographs through four representatives AP levels

of VTA. G-I. Photomicrographs of representative retrograde (G) and anterograde (H, I) labelling produced with an injection of Rdex (G, H) or BDA (I) in VTA. Left is medial and top is dorsal. Scale bar = 150 µm (A, B), 1 mm (D-F), and 20 µm (G-I).

Retrograde labelling in PFC

Figures 7-9 show plots of the retrograde labelling into individual coronal maps of PFC and at a more posterior level passing through the ventral striatum in all three cases: M3.15 BDA (Fig. 7), M2.15 (Fig. 8), and M9.09 (Fig. 9). All three injections in VTA produced retrograde labelling in the ventral striatum and in PFC; however the density of the labelling greatly varied with the location of the injection site in VTA, in a manner that fitted the results obtained with the anterograde labelling.

Rostral VTA.

The FB injection in rostral VTA in M3.15 produced a relatively dense to moderate labelling in several distinct architectonic areas in PFC, the insula and the cingulate cortex (Fig. 7). The pattern of labelling confirmed the anterograde labelling obtained in VTA with injections in PFC. Namely, MPFC and insular areas showed in general more labelling than OPFC and LPFC areas. The labelling seemed to decrease in a top down density from the most medial to lateral areas starting from the Prefrontal Cortex. The strongest labelling was produced in area 25, the anterior insula and some subdivisions of area 13, in complete accordance with the anterograde labelling. Moderate labelling was produced in areas 24b and 9; and the lowest labelling occurred in areas 10, 11 and 46. In detail, we can see that in some areas the projections arise from a particular group of cells within that area, for example in area 9.

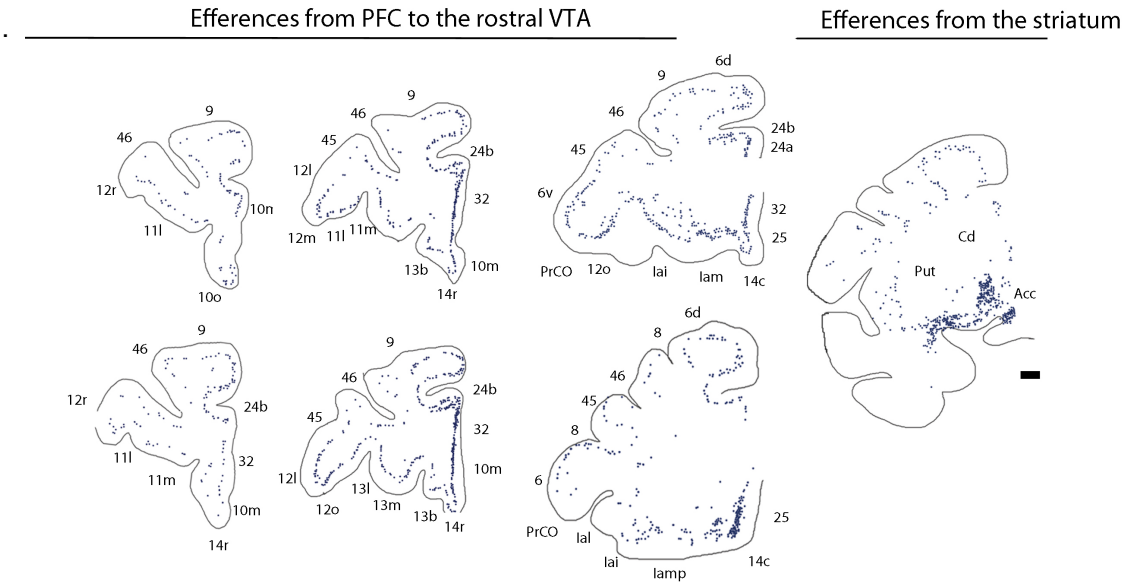

Figure 7: Plots of retrograde labelled cells in the cortex and ventral striatum from an injection placed in the rostral VTA, case M3.15FB. The labeling is represented by individual dots, and corresponds to retrograde labeling within the PFC. Scale bar = 1 mm.

These results confirm the observations found in the anterograde labelling and confirm the idea of subparcellation of the PFC in primates. For example, the dorsal and ventral parts of area 46 have clearly different patterns of labelling, from non-existing projections in the dorsal part, to some labelling in the ventral part. On the other hand, unlike the rest of the injections described below (Fig8 and Fig. 9), the rostral VTA also receive strong projections from the VS suggesting a possibly rely in this structure through the indirect pathway projection to the VTA.

Lateral VTA.

One injection placed in the most lateral part of the VTA, M2.15 of a retrograde FB in the Parabrachial Pigmentosus nucleus (pbp) and the deep mesencephalic tegmentum, showed a similar pattern of labeling as in M3.15, except the most caudal levels of area 24 and along the insula

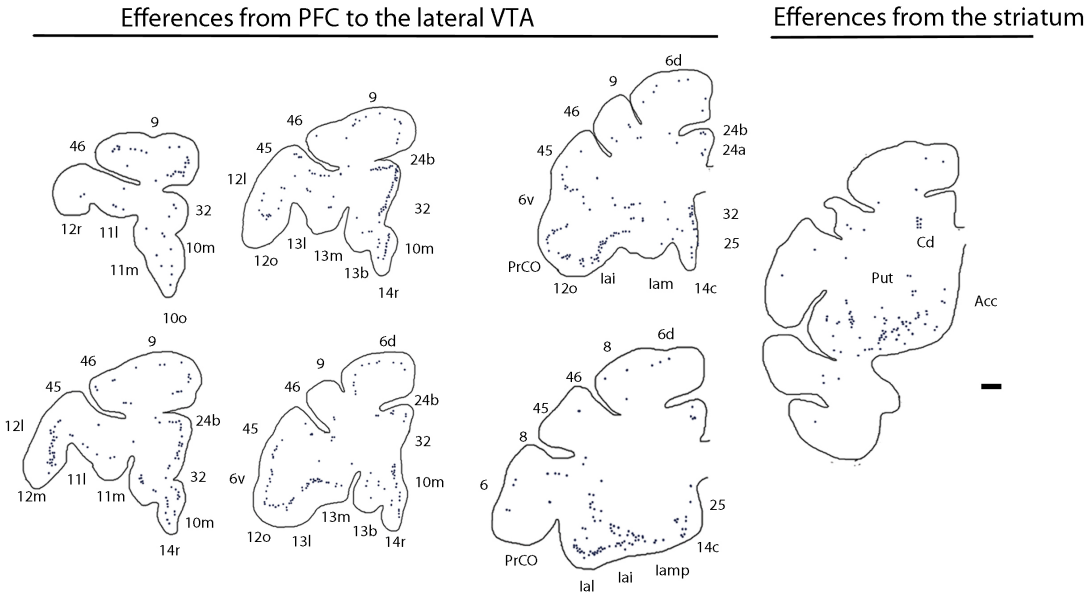

Figure 8: Plots of retrograde labelled cells in the cortex and ventral striatum from one injection placed in the lateral VTA, case M2.15FB. The labeling is represented by individual dots to represent retrograde labeling within the PFC. Scale bar = 1 mm.

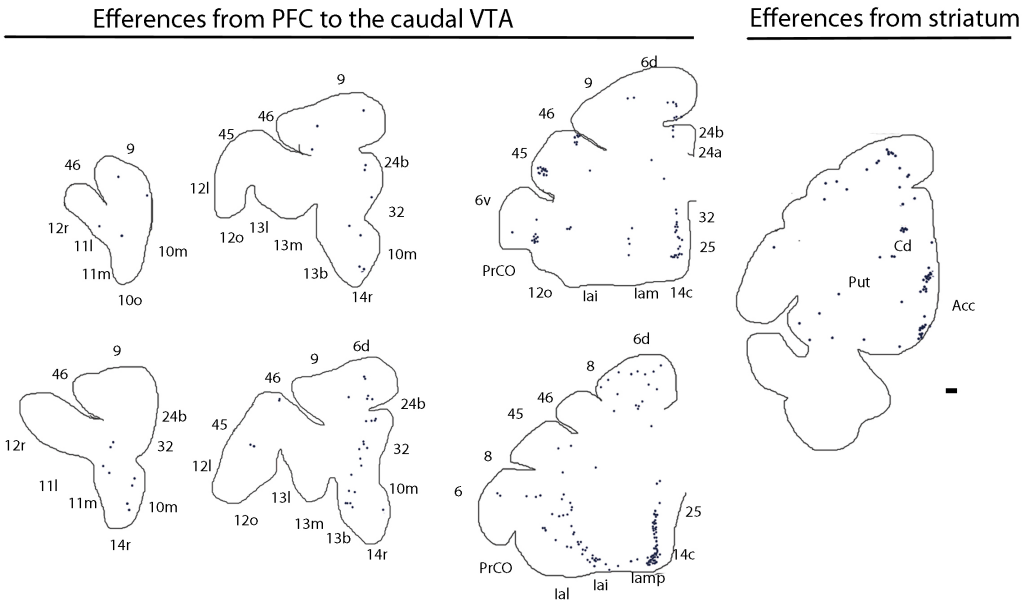

Figure 9: Plots of retrograde labelled cells in the cortex and ventral striatum from one injection placed in the caudal VTA, case M9.09FB. The labelling is represented by individual dots to represent retrograde labelling within the PFC. Scale bar = 1 mm

Caudal VTA.

The injection of FB in caudal VTA in case M2.15 produced a somewhat different density of labelling in PFC, although the overall pattern of areal labelling was similar. The results fits with the pattern projections shown from the different PFC areas along the VTA, although there were some differences. The projections to the caudal VTA, mainly arised from the MPFC and very few projections from the lateral cortex, areas 10, 11 and 46, and almost no projections from area 9.

However, this internal variability could be due to the possibility that the injection did not reach particular parts of VTA that may harbour the terminals from this area, an idea that is in conflict with the quasi-absence of topography in our anterograde labelling experiments.

DISCUSSION

The present study confirms the existence of projections from PFC to VTA in the macaque monkey. In addition to prior studies (Frankle et al., 2006), the present study reveals that not all PFC areas project to VTA and that some areas (in particular the cortical limbic areas 25, lam/p and 13b) send relatively heavy projections to VTA, contrary to prior assumptions that PFC projections to VTA are only mild compared to the projections from the

ventral striatum. The patterns of labelling in VTA suggest the existence of a subtle topography in the organization of the cortical projections to VTA. The next paragraphs will first compare our results to prior studies in primates and rodents, and then discuss the possible functional meaning of the PFC projections to VTA.

Comparison with prior tracing studies in primates and rodents

Consistent with our findings, previous studies observed that overall, the projections in primates are not strong, and it has been suggested that the projections in primates are weaker compared to rodents. (Frankle et al., 2006). In contrast, one recent study conducted in rats suggested that projections from the PFC are also weaker in rodents relative to projections from the striatum, subthalamic nuclei and dorsal raphe (Watabe et al., 2013). This discrepancy in the density of projections between both species might be because only some areas of the PFC of the rodents are compared to the whole PFC cortex in primates. Particularly they compared the infralimbic (homologous with area 25 in monkeys) and prelimbic cortex (comparable with area 32) and dorsolateral anterior cingulate cortex (homologous with area 24b) that in primates also send heavier projections compared to the rest of the prefrontal cortical areas.

Further anatomical evidence in primates has reported projections to the midbrain, although the objective of the study was different, to adjacent areas. Ongür and Price (1998) found labeling arising from area 25, 12o and Iai, but (not from area Iam and 12m) in the VTA on their study of connections with the hypothalamus. Other studies are more specific looking for projections from areas of the PFC such as area 25 (Freedman et al., 2000) without too much detail on the projections to the VTA, showing medium density labeled fibers in the rostral VTA. Chiba et al., (2001) reported projections also from area 25, 24 and 10. Although those projections are confined, it has been postulated that they could have a profound top down effect on the regulation of the DA neuron activity. One possibility could be through the release of modulator peptides that are known to promote burst firing within VTA (Skriboll et al., 1981). Other possibility is that the increase of the neuron activity wouldn't be only synaptic (Rosseti et al.,1998), as the extracellular glutamate released could also affect the DA cells not directly target inducing burst firing (Lodge et al.,2006) and activation to silent neurons (Grace and Bunney et al.,1984b).

It should be noted also, that the projections from the PFC networks are segregated. Previous anatomical studies in rodents show different density of projections from the medial and orbital PFC to the brainstem (Sesak et al., 1989), comparable to our study in primates. Thus, despite the fact that the architectonic parcellation of the rat PFC is not as diversified and expanded as in primates (Burman et al., 2009 and Cavada et al., 2003), and despite the

fact that rat PFC areas do not seem to harbor the vast functional diversity of the abundant monkey PFC areas (Price, 2007), the PFC regions that show heaviest projections to the midbrain appear to be comparably similar in rodents and primates. However, some of the monkey PFC areas are not comparable to any rat PFC areas, in particular in lateral PFC.

Those common area, named as “limbic cortex” share a cytoarchitectonic organization. They are composed by agranular and dysgranular areas that lack layer IV or have a rudimentary layer IV, that are not present in rodent PFC (Berger et al., 1991). In most cases, they occupy the ‘edges’ of the cortex as a ring above and below the corpus callosum (Barbas 2015). These converging observations perfectly fit with our results except for the projections from area 9. However the part from the area 9 that projects to VTA is the middle part of area 9, a part that has a pseudolaminar grade of complexity, not a canonical 6-layered isocortical organization.

Organization of the PFC projections

In the study of the organization of the PFC projections, we observed that projections from the MPFC distributed in the most dorso-lateral part of the midbrain, the VTA nucleus, than the projections arising from the OPFC, distributed more in the ventral (PN) and medial VTA, except in some cases that also distributes in the lateral (PBP). These results are supported by studies in rodents that demonstrated an inner organization of the projections within the VTA dependent on the medio-lateral axis, so that more medial cell groups innervate more medial and rostral structures while lateral cells innervate more lateral and caudal structures (Loughing and Fallon 1984).

Interestingly, one hypothetical schema shown by Williams et al., in 1998 demonstrated by rotating 45 degrees the prefrontal cortex sections that the topographical organization of the connections with the midbrain perfectly matched not only in the medio-lateral axis but in the dorsoventral axis as well.

On the other hand, functional studies proposed a feedback loop from VTA neurons to the mPFC after observing burst firing in pyramidal cells of the layer V of the mPFC induced by DA, via D2 receptors (Wang et al., 2004). In detail, only those DA cells that project back to the MPFC area innervated (Carr and Sesack, 2000a,b) but also, the GABAergic cells of the VTA that project to the nucleus accumbens (Sesack and Carr, 2002). Those findings agreed with our observations of retrograde labeling produced after deposits of bidirectional traces such as LY and FR that showed that some of the connections are reciprocal (data not shown) (Further information see Williams et al., 1998; Saleem et al., 2014 Gaspar et al., 1992; Porrino et al., 1982).

To explain these possible results, we looked carefully at studies of the indirect pathway projections from the PFC trought the striatum to the midbrain (Ferry et al, 2000) and we found out that the areas projecting the most to VTA are the same areas that do project the most to the ventral striatum that in turn projects the most to the VTA, through the indirect pathway (Haber et al., 2010). Those areas have in common a particular feature; they are dysgranular and are distributed all along the corpus callosum (Barbas 2015). The density of the projections shows a decreasing gradient in the midbrain, as far as the cortex is from the limbic structures. The results suggest that the limbic system is a robust system shared by rodent and primates with the only exception of the subparcellation of the PFC projections to the midbrain.

Functional interpretation

In 2012, Logde et al, demonstrated the importance of the segregated direct control of the DA from the MPFC and OPFC network. He showed that each network carries independent but complementary information that can regulate differentially the DA system (Asher et al., 2011).

In response to cognitive tasks, it has shown that the mPFC fires with high frequency bursts enhancing a dramatically increase of DA activity (Chagnac-Amitai et al., 1990; Chang et al., 2010). However, a single pulse of tonic activation of the mPFC can also induce inhibition in less than the half of the DA cells population (Lodge et al., 2011; Tong et al., 1998). This is because; only previously excited cells receive monosynaptic (glutamatergic) inputs from the mPFC. In contrast, the phasic activation of the OPFC regulates negatively the DA activity (Lodge in 2011) by stopping the positive feedback loop with the mPFC. Clinical studies have reported the importance of this negative control that occurs for example, during over expectation (Schoenbaum et al., 2009). During reward expectation DA activity is enhanced while the activity of the OPFC is decreased; although, the opposite happens when unexpected reward (Takahashi et al., 2009). The mechanism of this activity has been anatomically demonstrated by Carr (2000), and it is more likely through the activation of secondary GABAergic cells from the NA or within the VTA.

However, if this would be true, we would expect projections from the OPFC only restricted to the tail of the VTA, which is the part of the nuclei that contains the most of the GABAergic cells (Bourdy et al., 2012). Our results although, do not support this idea. In fact, the projections from the OPFC are localized mostly in other nuclei than the proper VTA (PB and PN), suggesting that these nuclei might contain GABAergic cells. Taken together, it can be hypothesized that direct projections from the different subareas of the PFC might be implicated in different aspects of cognition by means of controlling VTA activity.

Technical limitations

Technical limitations such as different sizes and layers involved in the injection, the different characteristics of the tracers in terms of sensitivity and efficacy of transport may be responsible for some variability in the results. One important feature to take into account is the involvement of the deep layers of the PFC, particularly layer 5 by the injection site (Gabbot et al., 2005). Functional studies have supported this idea by showing that the layer five pyramidal cells of the cortex are responsible for the increase of VTA activity (De Felipe J. et al., 1992; Gabbot et al., 2005). In our study, most of the injections target almost all the layers, although in some cases, the spread of the tracer in the halo might not have been enough to transport the tracer effectively. This fact could, for example, explain the differences in density of the projections observed in the study. Moreover, the retrograde labeling produced by injections in the VTA, we found that in some areas of the PFC, only subgroup of cells projected downstream. For example area 9, labeled only a few cells, thus indicating that the projections depend on the size and the location of the injection. Therefore some negative cases in which we did not observe labeling could be due to size and injection site that didn't reach that particular group of cells that project to the VTA.

REFERENCES

An. X, Bandler R, Ongür D, Price JL (1998). Prefrontal cortical projections to longitudinal columns in the midbrain periaqueductal gray in macaque monkeys. J Comp Neurol. 401:455-79.

Asher A, Lodge DJ (2012). Distinct prefrontal cortical regions negatively regulate evoked activity in nucleus accumbens subregions. Int J Neuropsychopharmacol. 1287-94.

Barbas H.(2015) General cortical and special prefrontal connections: principles from structure to function. Annu Rev Neurosci. 38:269-89

Barbas, H. & G.R. Blatt. (1995). Topographically specific hippocampal projections target functionally distinct prefrontal areas in the rhesus monkey. Hippocampus 5: 511–533.

Baxter MG, Murray EA (2002). The amygdala and reward. Nat Rev Neurosci. 563-73. Review.

Berger, B., Gaspar, P., & Verney, C. (1991). Dopaminergic innervation of the cerebral cortex: unexpected differences between rodents and primates. Trends in neurosciences, 14, 21-27.

Beveridge, T. J., Gill, K. E., Hanlon, C. A., & Porrino, L. J. (2008). Parallel studies of cocaine-related neural and cognitive impairment in humans and monkeys. Philosophical Transactions of the Royal Society B: Biological Sciences, 363, 3257-3266.

Björklund A, Dunnett SB (2007). Dopamine neuron systems in the brain: an update. Trends Neurosci. 30194-202. Review.

Borra, E., Gerbella, M., Rozzi, S., & Luppino, G. (2013). Projections from caudal ventrolateral prefrontal areas to brainstem preoculomotor structures and to basal ganglia and cerebellar oculomotor loops in the macaque. Cerebral Cortex, bht 265.

Bourdy R, Barrot M. (2012) A new control center for dopaminergic systems: pulling the VTA by the tail. Trends Neurosci. 35:681-90.

Burgess, P. W., Dumontheil, I., & Gilbert, S. J. (2007).The gateway hypothesis of rostral prefrontal cortex (area 10) function. Trends in cognitive sciences, 11, 290-298.

Burman KJ, Rosa MG (2009). Architectural subdivisions of medial and orbital frontal cortices in the marmoset monkey (Callithrix jacchus). J Comp Neurol. 514:11-29.

Bush, G., Luu, P., & Posner, M. I. (2000). Cognitive and emotional influences in anterior cingulate cortex. Trends in cognitive sciences, 4, 215-222.

Carmichael ST, Price JL (1995). Limbic connections of the orbital and medial prefrontal cortex in macaque monkeys. J Comp Neurol. 363(4):615-641.

Carmichael ST, Price JL (1995). Sensory and premotor connections of the orbital and medial prefrontal cortex of macaque monkeys. J Comp Neurol. 363:642-664

Carmichael, S. T., Clugnet, M. C., & Price, J. L. (1994). Central olfactory connections in the macaque monkey. Journal of Comparative Neurology, 346 403-434.

Carr DB, Sesack SR (2000). GABA-containing neurons in the rat ventral tegmental area project to the prefrontal cortex. Synapse. 38:114-23.

Carr DB, Sesack SR (2000). Projections from the rat prefrontal cortex to the ventral tegmental area: target specificity in the synaptic associations with mesoaccumbens and mesocortical neurons. J Neurosci. 20:3864-73.

Cavada C, Compañy T, Tejedor J, Cruz-Rizzolo RJ, Reinoso-Suárez F(2000). The anatomical connections of the macaque monkey orbitofrontal cortex. A review. Cereb Cortex. 10:220-42. Review

Chagnac-Amitai Y, Luhmann HJ, Prince DA (1990). Burst generating and regular spiking layer 5 pyramidal neurons of rat neocortex have different morphological features. J Comp Neurol. 296:598-613.

Chandler DJ, Lamperski CS, Waterhouse BD (2013). Identification and distribution of projections from monoaminergic and cholinergic nuclei to functionally differentiated subregions of prefrontal cortex. Brain Res. 1522:38-58

Chandler DJ, Waterhouse BD, Gao WJ (2014). New perspectives on catecholaminergic regulation of executive circuits: evidence for independent modulation of prefrontal functions by midbrain dopaminergic and noradrenergic neurons. Front Neural Circuits. 8:53. eCollection . Review

Chang CH, Berke JD, Maren S (2010). Single-unit activity in the medial prefrontal cortex during immediate and delayed extinction of fear in rats. PLoS One. 5:e11971.

Chiba T, Kayahara T, Nakano K, (2001). Efferent projections of infralimbic and prelimbic areas of the medial prefrontal cortex in the Japanese monkey, Macaca fuscata. Brain Res. 888:83-101.

DeFelipe J, Fariñas I (1992). The pyramidal neuron of the cerebral cortex: morphological and chemical characteristics of the synaptic inputs. Prog Neurobiol. 39: 563-607. Review.

Ferry AT, Ongür D, An X, Price JL (2000). Prefrontal cortical projections to the striatum in macaque monkeys: evidence for an organization related to prefrontal networks. J Comp Neurol. 425:447-70.

Frankle WG, Laruelle M, Haber SN (2006). Prefrontal cortical projections to the midbrain in primates: evidence for a sparse connection. Neuropsychopharmacology. 31:1627-36.

Freedman LJ, Insel TR, Smith Y (2000). Subcortical projections of area 25 (subgenual cortex) of the macaque monkey. J Comp Neurol. 421:172-88.

Frey S, Petrides M (2000). Orbitofrontal cortex: A key prefrontal region for encoding information. Proc Natl Acad Sci U S A. 97:8723-7.

Gabbott PL, Warner TA, Jays PR, Salway P, Busby SJ (2005). Prefrontal cortex in the rat: projections to subcortical autonomic, motor, and limbic centers. J Comp Neurol. 2005 492:145-77.

Gaspar, P., Stepniewska, I., Kaas, J. H. (1992). Topography and collateralization of the dopaminergic projections to motor and lateral prefrontal cortex in owl monkeys. Journal of Comparative Neurology, 325 1-21.

Geisler S, Derst C, Veh RW, Zahm DS (2007). Glutamatergic afferents of the ventral tegmental area in the rat. J Neurosci. 27:5730-43

Grace AA, Bunney BS (1984). The control of firing pattern in nigral dopamine neurons: burst firing. J Neurosci. 4: 2877-90.

Grace AA, Floresco SB, Goto Y, Lodge DJ (2007). Regulation of firing of dopaminergic neurons and control of goal-directed behaviors.Trends Neurosci. 30:220-7

Haber SN (2003). The primate basal ganglia: parallel and integrative networks. J Chem Neuroanat. 26:317-30. Review.

Haber SN, Knutson B (2010). The reward circuit: linking primate anatomy and human imaging. Neuropsychopharmacology. 35:4-26. Review.

Haber SN, Kunishio K, Mizobuchi M, Lynd-Balta E (1995). The orbital and medial prefrontal circuit through the primate basal ganglia. J Neurosci. 15:4851-67.

Hsu DT, Price JL (2007). Midline and intralaminar thalamic connections with the orbital and medial prefrontal networks in macaque monkeys. J Comp Neurol. 504:89-111.

Hurley KM, Herbert H, Moga MM, Saper CB (1991). Efferent projections of the infralimbic cortex of the rat. J Comp Neurol. 308:249-76.

Insausti R, Amaral DG, Cowan WM (1987). The entorhinal cortex of the monkey: III.Subcortical afferents. J Comp Neurol. 264:396-408.

Joel, D., Weiner, I. (2000). The connections of the dopaminergic system with the striatum in rats and primates: an analysis with respect to the functional and compartmental organization of the striatum. Neuroscience, 96, 451-474.

Jonides, J., Smith, E. E., Koeppe, R. A., Awh, E., Minoshima, S., Mintun, M. A. (1993). Spatial working-memory in humans as revealed by PET. Nature 363.

Kahn I, Shohamy D (2013). Intrinsic connectivity between the hippocampus, nucleus accumbens, and ventral tegmental area in humans. Hippocampus. 23:187-92.

Kondo H, Saleem KS, Price JL (2005). Differential connections of the perirhinal andparahippocampal cortex with the orbital and medial prefrontal networks in macaque monkeys. J Comp Neurol. 493:479-509

Lewis DA, Foote SL, Goldstein M, Morrison JH (1988).The dopaminergic innervation of monkey prefrontal cortex: a tyrosine hydroxylase immunohistochemical study. Brain Res. 449 :225-43.

Lodge DJ (2011). The medial prefrontal and orbitofrontal cortices differentially regulate dopamine system function. Neuropsychopharmacology. 36:1227-36.

Lodge DJ, Grace AA (2006). The laterodorsal tegmentum is essential for burst firing of ventral tegmental area dopamine neurons. Proc Natl Acad Sci U S A. 103:5167-72.

Loughlin SE, Fallon JH (1984). Substantia nigra and ventral tegmental area projections to cortex: topography and collateralization. Neuroscience. 11:425-35.

Miller, E. K., & Cohen, J. D. (2001). An integrative theory of prefrontal cortex function. Annual review of neuroscience, 24, 167-202.

Ongür D, An X, Price JL (1998). Prefrontal cortical projections to the hypothalamus in macaque monkeys. J Comp Neurol. 401:480-505.

Ongür D, Price JL (2000). The organization of networks within the orbital and medial prefrontal cortex of rats, monkeys and humans. Cereb Cortex. 10:206-19. Review.

Petrides, M., Alivisatos, B., Meyer, E., & Evans, A. C. (1993). Functional activation of the human frontal cortex during the performance of verbal working memory tasks. Proceedings of the National Academy of Sciences, 90, 878-882.

Porrino, L. J., & Goldman‐Rakic, P. S. (1982). Brainstem innervation of prefrontal and anterior cingulate cortex in the rhesus monkey revealed by retrograde transport of HRP. Journal of Comparative Neurology, 205, 63-76.

Porrino, L. J., & Lyons, D. (2000). Orbital and medial prefrontal cortex and psychostimulant abuse: studies in animal models. Cerebral Cortex, 10, 326-333.

Preuss TM (1995). Do rats have prefrontal cortex? The rose-woolsey-akert program reconsidered. J Cogn Neurosci. 7:1-24.

Price JL, Amaral DG (1981). An autoradiographic study of the projections of the central nucleus of the monkey amygdala. J Neurosci. 1:1242-59.

Price, J. L. (1999). Prefrontal cortical networks related to visceral function and mood. Annals of the New York Academy of Sciences, 877, 383-396.

Price, J.L., F.T. Russchen & D.G. Amaral. (1987). The limbic region. II: The amygdaloid complex. *In* Handbook of Chemical Neuroanatomy, Vol. 5: Integrated Systems of the CNS, Part I. A. Bjorklund, T. Hokfelt & L.W. Swanson, Eds: 279– 388. Elsevier Science Publishers. Amsterdam.

Rolls ET (2000) The orbitofrontal cortex and reward. Cereb Cortex. 10:284-94. Review.

Romanski LM (2007). Representation and integration of auditory and visual stimuli in the primate ventral lateral prefrontal cortex. Cereb Cortex. 17.

Rossetti ZL, Marcangione C, Wise RA (1998). Increase of extracellular glutamate and expression of Fos-like immunoreactivity in the ventral tegmental area in response to electrical stimulation of the prefrontal cortex. J Neurochem. 70:1503-12.

Rudebeck PH, Buckley MJ, Walton ME, Rushworth MF(2006). A role for the macaque anterior cingulate gyrus in social valuation. Science. 313:1310-2.

Saleem KS, Kondo H, Price JL (2008). Complementary circuits connecting the orbital and medial prefrontal networks with the temporal, insular, and opercular cortex in the macaque monkey. J Comp Neurol. 506:659-93.

Saleem KS, Miller B, Price JL, (2014). Subdivisions and connectional networks of the lateral prefrontal cortex in the macaque monkey. J Comp Neurol. 522:1641-90.

Saunders R.C., D.L. Rosene & G.W. Van Hosen (1988). Comparison of the efferents of the amygdala and the hippocampal formation in the rhesus monkey: II.Reciprocal and non-reciprocal connections. J. Comp. Neurol. 271: 185–207.

Sesack SR, Carr DB (2002). Selective prefrontal cortex inputs to dopamine cells:implications for schizophrenia. Physiol Behav. 77:513-7. Review

Sesack, S. R., & Pickel, V. M. (1992). Prefrontal cortical efferents in the rat synapse on unlabeled neuronal targets of catecholamine terminals in the nucleus accumbens septi and on dopamine neurons in the ventral tegmental area. Journal of Comparative Neurology, 320, 145-160.

Skirboll LR, Grace AA, Hommer DW, Rehfeld J, Goldstein M, Hökfelt T, Bunney BS (1981). Peptide-monoamine coexistence: studies of the actions of cholecystokinin-like peptide on the electrical activity of midbrain dopamine neurons. Neuroscience. 6:2111-24.

Sugihara, T., Diltz, M. D., Averbeck, B. B., & Romanski, L. M. (2006). Integration of auditory and visual communication information in the primate ventrolateral prefrontal cortex. The Journal of Neuroscience, 26, 11138-11147.

Takagishi M, Chiba T (1991). Efferent projections of the infralimbic (area 25) region of the medial prefrontal cortex in the rat: an anterograde tracer PHA-L study.Brain Res. 566:26-39.

Takahashi YK, Roesch MR, Stalnaker TA, Haney RZ, Calu DJ, Taylor AR, Burke KA, Schoenbaum G (2009). The orbitofrontal cortex and ventral tegmental area are necessary for learning from unexpected outcomes. Neuron. 62:269-80.

Thiebaut de Schotten M, Dell'Acqua F, Valabregue R, Catani M (2012). Monkey to human comparative anatomy of the frontal lobe association tracts. Cortex. 48:82-96

Uylings HB, Groenewegen HJ, Kolb B (2003). Do rats have a prefrontal cortex? Behav Brain Res. 146:3-17. Review.

Wallis JD (2011). Cross-species studies of orbitofrontal cortex and value-based decision-making. Nat Neurosci. 15:13-9.Review

Williams SM, Goldman-Rakic PS (1998). Widespread origin of the primate mesofrontal dopamine system. Cereb Cortex. 8:321-45.

CHAPTER 4. Hippocampal formation and Amygdala projections to the ventral tegmental area in the macaque monkey

ABSTRACT

The primate limbic system is composed of mesencephalic and diencephalic structures including the ventral tegmental area (VTA), the hippocampal formation (HF) and the amygdala (Amy). Amy is composed of different nuclei including the basal (B), basal accessory (BA), lateral (L), central (CeA), peryamigdaloid (PAC), paralaminar (PL) and medial (M) nuclei. The HF it is made up of the dentate gyrus (DG), Ammon Horn's fields (CA fields), Subiculum (S), Presubiculum (PrS), Parasubiculum (Pas) and entorhinal cortex (EC). In the present study, we examined the distribution of anterograde labelling produced in VTA with injections of biotin dextran amine or phaselous vulgaris lectin in distinct architectonic regions within Amy and HF. This examination confirmed prior evidence that CeA sends strong projections to VTA but it also revealed for the first time that other Amy nuclei do indeed projects to VTA as well. The lateral of B and dorsal part of BA provided the heaviest projections, and PAC and some specific parts of PL provided moderate projections. Injections in L, the medial part of B, the ventral part of BA and other parts of PL did not produce any labelling in VTA. Injections in HF produced in general sparse or no labelling with the exception of the Subiculum. Injections in EC produced labelling in VTA only if they spread to adjacent Amy nuclei, suggesting that EC does not project to VTA. The sources of these limbic afferent to VTA were all confirmed by the examination of the distribution of perikaryal labelling produced in Amy and HF with injections of retrograde tracers in VTA. A comparison of the spatial distribution of the anterogradely-labelled fibres in VTA revealed a considerable overlap of the projections from the different regions of Amy and HF with only a subtle trend to the rostral half of VTA, or distributed throughout the entire rostrocaudal extent of VTA, suggesting a coarse internal topography within the organization of the limbic projections to the midbrain. The present study reveals the existence of new direct monosynaptic projections to the VTA that may have a crucial role in the descending limbic control of dopamine release, in addition to classically known indirect polysynaptic projections. These direct projections could play a crucial role in optimizing the descending control of dopamine release in key limbic regions involved in the emotional valuation during reward and learning processing.

INTRODUCTION

Mesencephalic nuclei such as the ventral tegmental area (VTA) exert a broad and powerful modulation of hippocampal and amygdalar functions through the release of dopamine (DA). DA regulates the hippocampal formation (HF) during reward (Marting et al., 2011) and novelty detection (Ljunberg et al., 1992), and the amygdala (Amy) during fear conditioning (Blair et al., 2001; Fudge et al., 2010) and reward memory (Murray 2007, Gaffan et al., 1993). In turn, both HF and Amy has a potent excitatory (glutamatergic) effect on VTA (Harris et al., 2004; Jin et al., 2014; Floresco et al., 2001) that, along with inhibitory projections from the ventral pallidum (VP), peduncle pontine (PPT), and lateral dorsal tegmentum (LDT) (Floresco et al., 2001), controls the tonic and phasic release of DA during enhanced motor activity, cognition, and reward (Chergui et al, 1993; Johnson et al 1992b; Floresco et al., 2003). In the pathological side of the system, the desregulation of the DA neuromodulation has been associated with various serious psychiatric disorders such as autism, attention deficit, hyperactivity epilepsies (Janak et al., 2015), anxiety (Rauch et al., 2003) and Alzheimer (Gib et al., 1989). While there is a wealth of evidence for multiple indirect polysynaptic pathways substantiating the descending control of VTA by the limbic system in both rodents and primates (see below), the existence and organization of direct monosynaptic projections from HF and Amy to VTA has not yet been completely elucidated, in particular in non-human primates for which there are to date much less tract-tracing studies than in rodents.

Prior tracing studies, mostly in rodents, emphasized that the excitatory influence of HF on the activity of the DA cells of VTA occurs through two distinct polysynaptic pathways, one arising from the ventral hippocampus via the shell of the nucleus accumbens (NA) (Floresco et al., 2001) and another one from the dorsal hippocampus via the lateral septum (LS) and/or the rostro-lateral part of the NA (Rossato et al., 2009; Luo et al., 2011). In addition to these indirect projections, a recent functional imaging study in humans suggested a direct pathway from the ventral hippocampus (S and VCA1) to VTA during emotion and reward (Khan et al., 2013). Despite the lack of anatomical evidence for direct monosynaptic projection from the HF to the midbrain, retrograde tracer studies evidence direct projections from the VTA to the DG/CA1 (Amaral et al., 1980) and EC (specifically to midportions of the EC, Insausti et al., 1987).

In the case of the Amy, excitatory influence has been suggested to occur through a direct monosynaptic projection from the central (CeA) in monkeys (Price et al., 1981; Fudge et al., 2001; Fudge et al., 2000), in rats (Pardo-Bellver et al., 2012) and in cats (Holstege et al., 1985), and through indirect polysynaptic pathways from the basolateral (BLA) and

paralaminar (PL) nuclei and the intercalated cells loosely situated between the Amy nuclei (Millhouse et al., 1986) via LS, the reuniens nucleus of the medial thalamus and the Nucleus Accumbens (NA) (Price et al., 1981; Fudge et al., 2012). A recent study in rodents however indicated that most projections from CeA end in the neighboring substantia nigra with only limited direct projections to VTA (Lee et al., 2010). Furthermore, dopamine fibers occur not only in CeA but also in the parts of the basal and basolateral nuclei (Sadikot and Parent, 1990), both of which could also potentially send direct projections to VTA.

While most knowledge on the efferent projections to VTA come from rodent work, the existence and organization of projections from HF and Amy to VTA in primates cannot be simply derived from tract-tracing studies in rodents. For example, it is often assumed that the rodent and primate VTA share the same overall organization (Sesack and Grace, 2010); however, up to 8 nuclei have been defined for the rat VTA (Gasbarri et al., 1994b) whereas only 2 nuclei are usually mentioned for the monkey VTA (Wilhelmus et al., 2000; Cho et al., 2010; Mc Ritchie et al., 1998). Similarly, while the hippocampus *per se* remains fairly similar across species, the entorhinal cortex (EC) which is a major part of HF has two general areas in rats, the lateral and the medial, although a further number of subdivisions closer to the primate EC has also been described (Insausti et al., 1998), in primates we recognized 7 different areas (Amaral and Insausti 1987; Amaral and Insausti 1990). Specific nucleus of Amy in primates are relative enlarged (Pitkänen et al., 1988; Turner et al., 1980; Andy et al., 1968; Stephan et al.,1977) and shows particular cytoarchitecture features (Chareyon et al.,2011) responsible for the different processing of the incoming information that are not necessarily present in rodents. Specifically, the basal nucleus of Amy (B) which shows strong connections with HF, the prefrontal cortex (PFC), VS and other Amy nuclei (except for the lateral nucleus; L), heavily projects, all along with L, to the central Amy nucleus (CeA) inducing the enlargement of this structure in primates. Thus, in order to better appreciate the organization of the efferent to VTA in primates, a proper examination in the laboratory species closer to humans is needed.

In order to know how the information related to one hypothetical value, evaluated by the Amy and HF, could possibly modulate the DA cells of the VTA, one major source of the DA to the cortex and striatum (Haber et al., 2003), we examine the distribution of anterograde labelling produced in VTA with injections of tracers in various parts of HF and Amy, and the distribution of retrograde labelling in HF and Amy produced with injections of tracers in VTA in macaque monkey.

MATERIALS AND METHODS

The present data were obtained from a total of 71 adult male cynomolgus or long tailed macaque monkeys (*Macaca fascicularis*) that received microinjections of anterograde tracers in the HF or amygdala; seven monkeys received microinjections of retrograde tracers in or around the VTA. The experiments (tracer injections) were conducted, chronologically, at the MIND institute of the University of California in Davis, CA, USA, at the Max Planck Institute for Biological Cybernetics in Tuebingen, Germany, and at the University of Albacete in Spain. All procedures were approved by the corresponding local authorities and followed the directives of the National Institute for Health (USA) or the European Union directives 86/609/CEE. The tracer injections at the MIND institutes were made in the context of separate studies that have for the most part been published in prior reports (Amaral et al., 1981). The tracer injections in Spain and Germany were made mainly in the context of the present study and have not been reported elsewhere yet.

Tracer injection

The procedure of the tracer injection varied with the institution in which it was made. The anatomical guidance alternatively used basic stereotaxic, MRI guidance or a mix of both. The injections were made using Hamilton syringes or glass micropipettes, pressure injections or iontophoresis. Nevertheless, all tracers and the criteria to define the quality of an injection site were the same.

For the MRI, each monkey was placed in an MRI-compatible stereotaxic frame under anaesthesia. MRI scan images were obtained with a 1.5T Philips scanner using a coil placed over the top of the head of the animal (Spain) or with a 7T Bruker scanner using a 3-part head coil (Germany). For each individual animal, stereotaxic coordinates were calculated for every single desired injection in Amy, HF or VTA and compared with the atlas of Szabo and Cowan (1984) or of Saleem and Logothetis (2008). In some cases, additionally, electrophysiological recordings were made to refine the coordinates for deep injections (Amaral et al., 1981).

For the surgery, the animal was sedated by an intramuscular injection of ketamine (8 mg/kg) followed by sodium pentobarbital (25 mg/kg, i.v.); the anaesthesia was then induced and maintained either by intubation with isofluorane or remifentanil. The animal was placed in the Kopf stereotaxic frame. The skin was incised and the cranium trepanned above the region of interest. For most of the HF injections, the injection sites were determined using stereotaxic coordinates derived from the MRI. However, for some of the tracer injections into deep cortical areas, an insulated tungsten electrode was inserted along the expected track of

the pipette for electrophysiological recordings of spontaneous activity of the structural boundaries between grey and white matter or the bottom of the brain which allowed determining the exact vertical coordinates determined firstly by the MRI. Once the target identified, retrograde tracer (Fast Blue [FB; 3 %]; Cholera Toxin B [CTb 1%]; fluorescent dextrans [FD; 10%]) or anterograde tracers (biotinylated dextran amine [BDA; Molecular probes 10%] and Phaseolus Vulgaris [PHAL; 2.5 %]) were injected in the brain. The injections were made through a micropipette using 25-msec air or hydraulic pressure pulse (BDA, FB, CTb, and FD) or using iontophoresis (PHAL) with 7 second-ON and 7 second-OFF pulses during 45 min. The air pressure was adjusted so that very small volumes of tracer were injected in each pulse (Kondo et al., 2005). To avoid spread of the tracer into areas along the pipette track, the micropipette was left in place for 15-30 minutes after the injection was finished. After surgery, the skull and skin were closed, and a long lasting analgesic and antibiotics were given to the animal after anaesthesia.

Fixation and histological processing

After a survival period of approximately two weeks, the animals were sedated with ketamine followed by sodium pentobarbital (25-30mg/kg i.v. or i.m.). Then, the animals were euthanized with a lethal dose of pentobarbital and perfused transcardially with saline, followed of 4% paraformaldehyde solutions at pH 6.5 and pH 9.5 (Pitkanen et al., 1998) and 10% sucrose at pH 9.5. Then the brain was removed and placed in 30% sucrose in phosphate-buffered saline (PBS) until it sank. Three days later, the brain was frozen with dry ice and cut into 5 to 10 collated series of 50 microns coronal sections (Cowan et al., 1972). BDA was processed histochemically with biotin-horseradish peroxidase technique, and PHAL was visualized immunohistochemically, and counterstained with Giemsa, that allowed the visualization of the diaminobenzidine reaction product. FB and FD are readily visible via epifluorescence. CTb was visualized using standard CTb immunohistochemistry (Evrard and Craig, 2008).

Data analysis and presentation of illustrations

Mounted sections were examined under bright field and epifluorescence microscope. Injection sites, anterogradely-labelled axonal varicosities (in VTA), and retrogradely-labelled perikarya (in HF and Amy) were manually plotted using a microscope-digitalized system (Minnesota Datametrics, St. Paul NM). For sparse labelling, each fibre segment was plotted as a single point. However for dense labelled areas, 4 points indicated medium dense varicosities greater than 10 fibres/ per surface unit and a rating of 6-8 points indicated strong labelling with a density range greater than 25 fibres/ per surface unit . In some cases, strong

background staining had to be subtracted out. We mapped the injection sites and the labelling in successive linear traverses across the section. Finally, architectonic boundaries were drawn onto printed plots by using camera lucida with adjacent sections stained for Nissl. The labelling was analysed bilaterally. Coronal maps were prepared to visualize the distribution and the density of labelled varicosities or cell bodies. Because each map was prepared for each case, we could not directly compare the overlap of the labelling (see Results). Also, the relative strength of connections was qualitatively estimated but absolute values could not be determined. The reason why we could not compare absolute values are inherent to the tracing methods used; it was because of different factors such as differences in the efficiency of the transport between the different tracers, the variability in the volumes of the injection site and difficulty of the reproducibility of injection sites in the same location.

Nomenclature

The terminology used for VTA nuclei was adapted from Paxinos (2007) and the borders of each midbrain nucleus composing and surround VTA were defined according to the morphology of the cells in the Nissl staining along the rostro-caudal axis of VTA. A detailed description is provided in the Results section.

According to Amaral and Insausti, we considered 7 different Amy regions: the basal nucleus (B) that included a magnocellular (Bmc), intermediate (Bi) and parvicellular (Bpc) division; the basal accessory nucleus (BA) that included a magnocellular (ABmc), parvicellular (ABpc) and ventromedial (ABvm) division; the lateral nuclei (L) that contained a dorsal (Ld), dorsal intermediate (Ldi), ventral intermediate (Lvi) and ventral (Lv) division; the central nucleus (CE); the medial nucleus (M); the cortical nucleus (CO); the paralaminar nucleus (PL); the periamygdaloid cortex (PAC); and the amygdalo-hipocampal area (AHA) (Chareyron et al., 2011).

For the hippocampal formation we distinguished: the Dentate Gyrus (DG), the Ammon's fields (CA1, CA2, and CA3), the subicular complex (Subiculum, Presubiculum, Parasubiculum) and entorhinal cortex (EC). EC is the region that receives the information from the polysensory association regions of the neocortex and it is one of the major sources of HF inputs to Subiculum and the gateway of the information from the HF (Van Hoesen and Pandya 1975). EC was differentiated into seven different levels: two rostral levels (E_O and E_R), two lateral levels (E_{LR}, E_{Lc}), one intermediate (E_I) and two caudal (E_C, E_{CL}).

RESULTS

Injection sites in the HF and amygdala

A total 87 anterograde tracer injections were placed in different parts of the amygdala and HF, including 17 injections in the hippocampus and DG, 15 injections in EC (with 8 injections that included also some parts of the amygdala), and 27 injections in the amygdala. The photomicrographs and drawings in Figure 1 shows example of injection sites in HF and Amy. All injection sites consisted in a dense core surrounded by a distinct paler halo. Injection sites for BDA mostly appeared larger and denser than injection sites for comparable volumes of PHAL, which is largely due to the better control of the injections with iontophoresis (but lower tracing gain). Injection spread was generally greater in vertical penetration than medio-lateral. In most cases, the halo of the injection sites was small and confined to one architectonic region with no spread or with spread of varying size to adjacent regions, as described below. The following paragraphs describe all of the injections of anterograde tracers. Figures 2, 3 and 4 show a schematic composite collating all of representative injection site onto simplified maps of the amygdala, hippocampus, and EC, respectively. The ellipsoid shapes represent both the core and halo of the injection site. The ellipsoid shapes filled in red indicate the injection sites that produced anterograde labelling in VTA. The empty ellipsoid shapes indicate injection sites that did not produced labelling in VTA. Injections were made in the left or right hemisphere but were all illustrated on the right side for consistency.

Amygdala.

Twenty seven injections were placed in different regions of Amy (Fig. 2). Two injections were made in PAC; one spread to AHA (M2-15BDA) and the other one to the piriform cortex (M5-05 BDA). (Both AHA and the piriform cortex were located at a level posterior to the level shown in the standard map.) Eight injections were centred in Bmc; six injections were confined within Bmc (M2L-03BDA; M1-03RBDA, M6-97BDA, M4-09BDA, M6-94PHAL; M2-03PHAL); one spread to Bi (M3-95BDA) and another one to Bi and L (M5-97PHAL). Seven injections were centred in Bi (M1-95PHAL; M6-98BDA; M7-98BDA; M12-98PHAL; M6-94PHAL), including two that spread to Bpc (M11-98BDA, M2-98BDA). One injection was confined to Bpc (M4-97BDA). Four injections were made in PL (M12-91PHAL; M2-95LPHAL; M3-98PHAL; M3-10BDA) with a minimal spread to Bpc. Three injections were made in L, two in Lv (M11-88PHAL, M6-91PHAL) and one in Ld (M8-89PHAL). Two injections were made in ABpc (M15-98BDA; M14-97BDA).

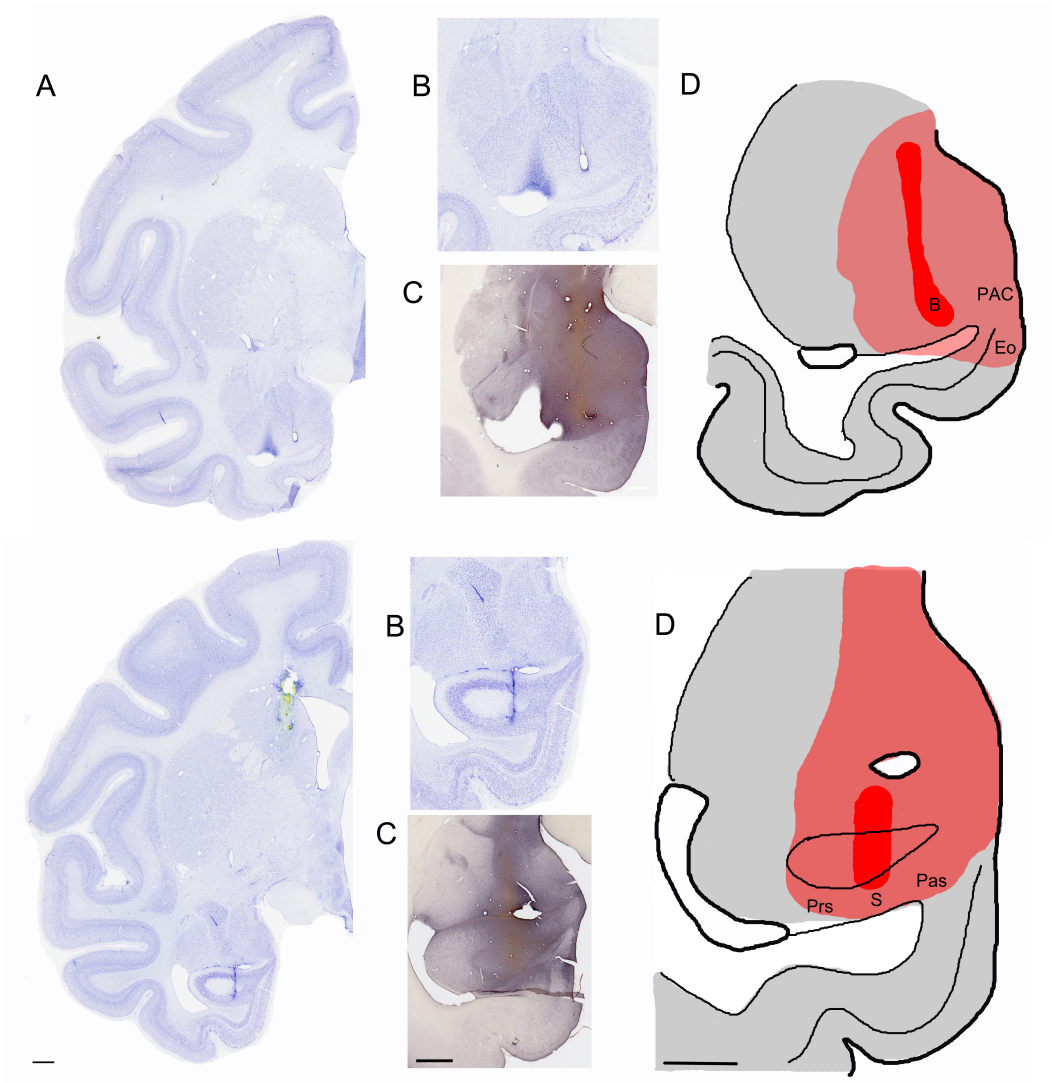

Figure 1. From the top to the bottom: examples of injections sites in Amygdala (M1-09BDA) and Hippocampal Formation (M4-08BDA). (A) Photograph of coronal section of half of the hemisphere of the monkey brain (B) Detail of the Injection site in Nissl (C) Detail of the injection site BDA (D) Drawing of the injection site in red the core and in pink the hallux. Scale bar =1mm

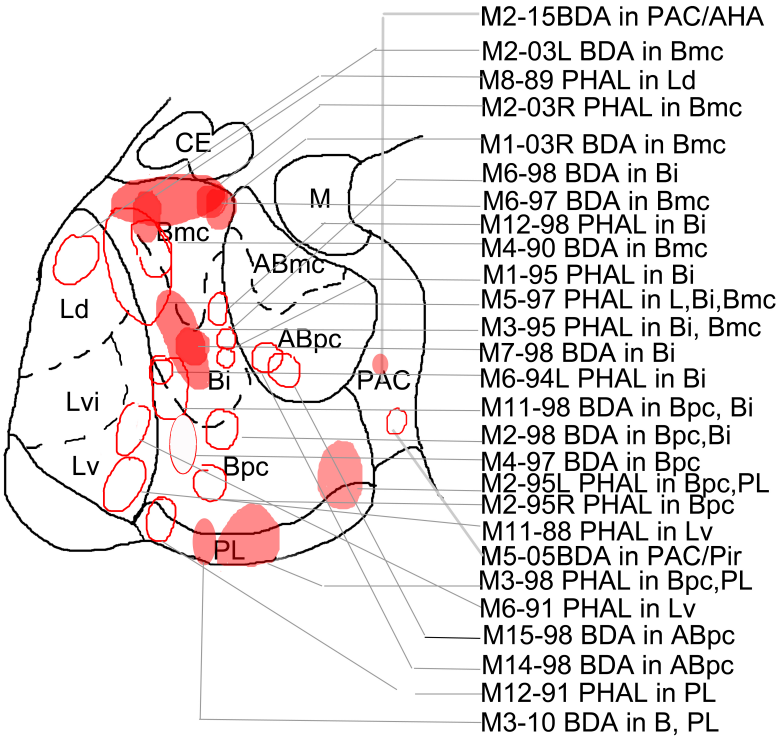

Figure 2. Topology of the injection sites in Amy using a relative collation of all injection sites onto a standard map of Amy. The ellipsoid shapes represent both the core and halo of the injection site. The ellipsoid shapes filled in red indicate the injection sites that produced anterograde labeling in VTA. The empty ellipsoid shapes indicate injection sites that did not produced labeling in VTA.

Entorhinal cortex.

Twenty three injections aimed EC (Fig. 3). Four injections were made in the rostral E_R (M06-98BDA; M12-98BDA, M3-98BDA and M10-97PHAL), one in E_C (M10-98BDA), one in E_I (M3-15BDA) and two in E_{CL} (M6-11BDA and M5-08BDA). Other injections included different parts of EC; one included E_I and E_O (M7-09BDA), one included E_I, E_C and E_{CL} (M3-98FR), three injections included E_C and E_{CL} (M2-97PHAL, M10-96PHAL and M13-98FR), one included E_{LC} and E_{CL} (M1-97PHAL), and one included E_{LC} and E_{LR} (M11-97BDA).

Eight injections centred in EC spread to some parts of Amy or HF. One injections made in E_{lr} included AB (M8-09BDA); another that included E_O and E_R also spread to AB (M1-07BDA). Injections in E_o included also PAC and B (M1-09BDA) or PAC (M7-09BDA), and one injection that included E_O, E_R and E_{LR} also spread to Bpc (M11-09BDA). Finally, two injections included PAC, Prs and EC (M4-10BDA), or Prs and E_I (M6-09BDA).

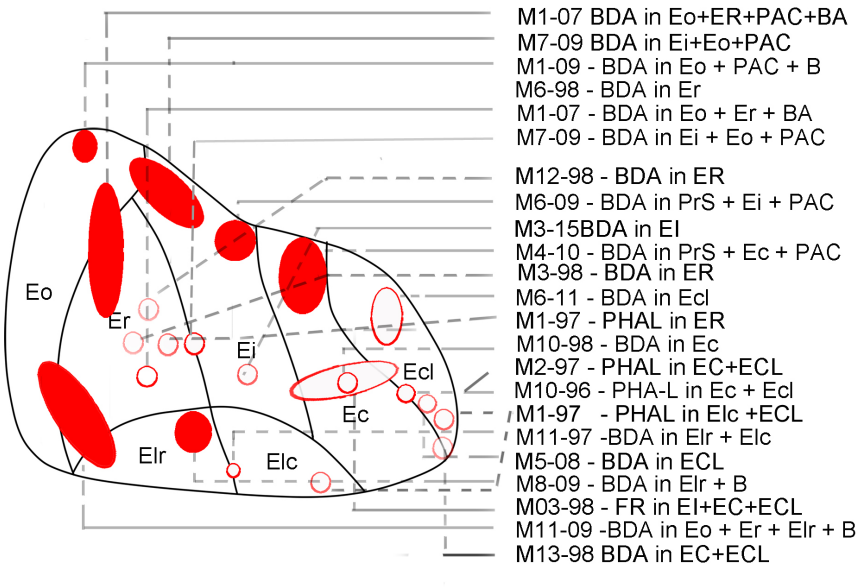

Figure 3. Topology of the injection sites in EC using a relative collation of all injection sites onto a standard map of EC. The ellipsoid shapes represent both the core and halo of the injection site. The ellipsoid shapes filled in red indicate the injection sites that produced anterograde labeling in VTA. The empty ellipsoid shapes indicate injection sites that did not produced labeling in VTA.

Hippocampus and Subiculum.

A total of 30 injections were placed in the hippocampus and Subiculum. Because most of these injections did not produce labelling in VTA (see below) and because many injections sites overlapped, only subsets of resentative injections were mapped onto the standard composite map (Fig. 4). Seven injections were placed in DG (M2-01PHAL; M2-01BDA; M4-01PHAL; M4-01BDA; M1-02PHAL; M2-02BDA; M10-02PHAL) among which two are shown in Figure 4 (M02-02BDA; M04-01PHAL). Five injections were made in CA3 (M4-02PHAL; M3-02PHAL; M4-02BDA; M10-02BDA; M9-03BDA) among which one is represented (M10-02BDA). One injection was made in CA1 (M2-04PHAL; not shown). Fourteen injections were made in CA3 (M2-04BDA; M1-92PHAL; M5-92PHAL; M9-92LPHAL; M9-92RPHAL; M11-92PHAL; M13-92PHAL; M27-92PHAL; M10-93PHAL; M1-05BDA; M5-02PHAL; M07-02BDA and M07-03PHAL; M9-93PHAL), among which three were represented (M5-02PHAL; M2-04BDA and M7-03PHAL). Eleven injections were made in CA1 (M2-92PHAL; M10-92PHAL; M28-92PHAL; M30-92PHAL; M1-93PHAL; M2-93PHAL; M9-93BDA; M8-09PHAL; M8-03BDA; M14-03BDA and M14-03PHAL) among which two were shown (M2-92PHAL and M9-93BDA). Finally, one injection was placed in CA2 (M10-93BDA). Three large injections included some parts of the subicular complex. One contained PreS, S, PaS and CA1 (M04-08BDA), and two others included PAC and EC (M04-10BDA) or PAC and EI (M06-09BDA). In all but a few cases, the tracer injections involved most layers of grey matter and did not

extend to the white matter. Furthermore, single and larger injections included different parts of the EC.

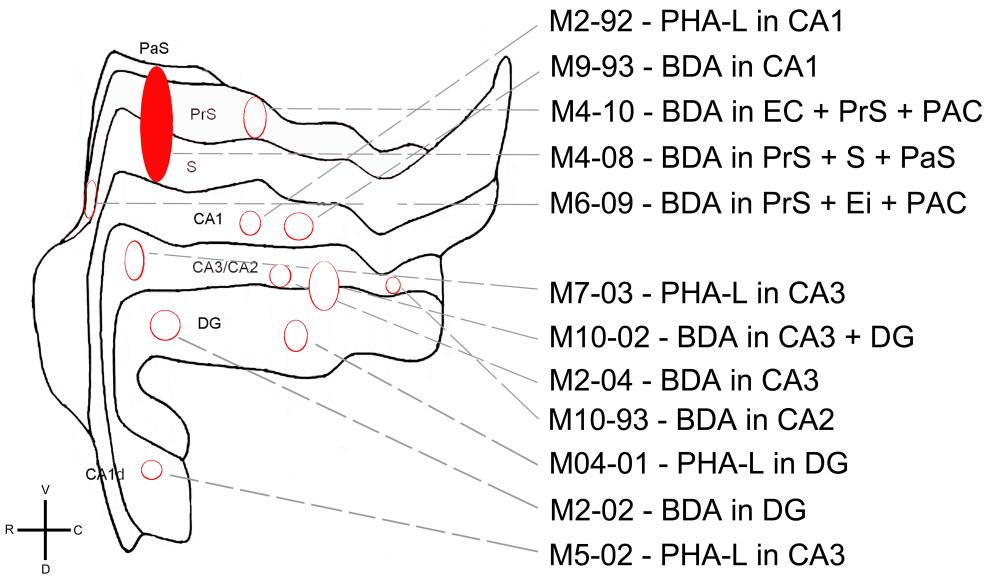

Figure 4. Topology of the injection sites in hippocampus using a relative collation of all injection sites onto a standard map of hippocampus. The ellipsoid shapes represent both the core and halo of the injection site. The ellipsoid shapes filled in red indicate the injection sites that produced anterograde labeling in VTA. The empty ellipsoid shapes indicate injection sites that did not produced labeling in VTA.

Injection sites in VTA

To confirm the projections inferred from the analysis of the anterograde labelling in VTA, retrograde tracers injections were made in or around VTA. Injections within VTA involved different adjacent nuclei and were placed at different rostro-caudal or medio-lateral levels. Out of the seven cases injected (see Methods), only three produced retrograde labelling (M2.15FB, M3.15FB and M9.9FB). Figure 5 depicts the injections sites in the VTA, as drawn coronal sections. The injections were relatively small and showed a core and a halo of deposit. Injections within VTA involved different nuclei and were placed at different rostro-caudal or medio-lateral levels.

One injection of FB was made in rostral VTA (M3.15; Fig. 5D). One injection of FB was made in the lateral aspect of the middle AP extent of VTA (M2.15; Fig. 5E). One injection of FB was made in the caudal end of VTA (M9.09 Fig. 5I). All sites were relatively small and did not spread extensively to adjacent regions.

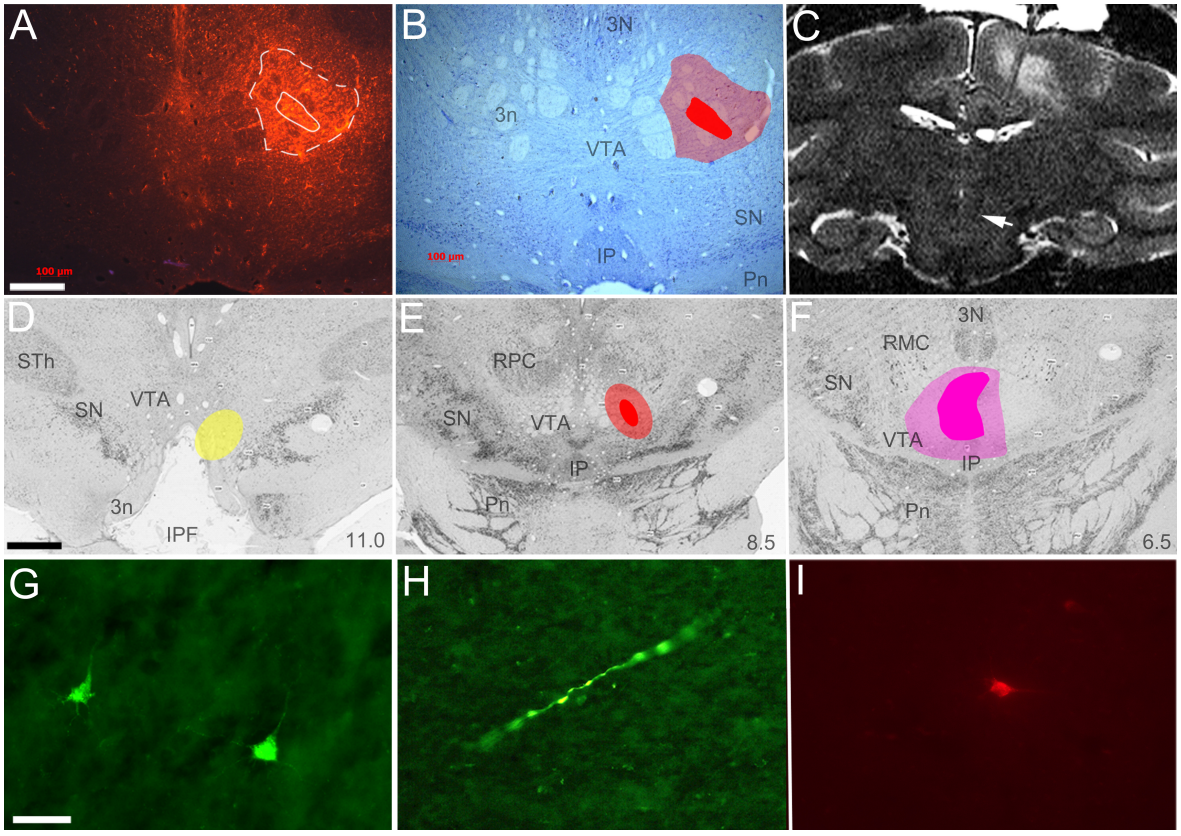

Figure 5. Photomicrographs of adjacent coronal fluorescent (A) and Nissl-stained (B) sections showing Pdex injection site in case cm28; the core and halo (circled by continuous and dashed lines, respectively) and their plots onto Nissl-stained photomicrographs of VTA, respectively. C. MRI section showing the location of the fused silica micropipette used to inject Pdex in VTA. D-F. Injection sites from cases cm018Rdex ('yellow'), cm017Rdex ('green'), cm020Rdex ('purple') and cm024Pdex ('red') depicted on a set of 3 photomicrographs through four representatives AP levels of VTA. G-I. Photomicrographs of representative retrograde (G) and anterograde (H, I) labelling produced with an injection of Rdex (G, H) or BDA (I) in VTA. Left is medial and top is dorsal. Scale bar = 150 µm (A, B), 1 mm (D-F), and 20 µm (G-I).

Anterograde labelling in VTA

Architectonic mapping of VTA.

A prerequisite to the description of the distribution of anterograde labelling in VTA is a mapping of VTA to use as a reference. Figure 6 shows an architectonic map of VTA and various neighbouring nuclei or regions of the midbrain across 4 representative anteroposterior levels of the left VTA. The absence of the mammillary nuclei at the most rostral level indicated somewhat the rostral end of VTA at approximately -10.80 mm from the antero-posterior Bregma (AP) which correspond to our level 0 in Figure 6. VTA was co-existent with and ventral to the obvious red nucleus (RN and then its magnocellular part,

RMC) throughout its almost entire rostro-caudal extent (level 1350 to 3150), and it was intermingled within the fibres of the third (oculomotor) nerve at the level of 2500. At its middle level, VTA was located dorsal to the interpeduncular fossa (IF), which, with the middle line nucleus, splitted VTA into two distinct sides. At more caudal levels, IF was replaced by the interpeduncular nucleus (IP) at (AP -14.40 mm; level 2500). The level where RM led to RMC also indicated the beginning of the tail of the VTA. The level of decussation (xscp) delimits the caudal level of the VTA that will continue further caudally until reaching AP 16.40mm (not shown).

General observation on the anterograde labelling in VTA.

All of the injections in this study produced anterograde and sometimes retrograde labelling in the VTA. Figure 7 presents examples of anterogradely labelled fibres bearing varicosities and neurons with BDA in VTA. The morphology of the labelled fibres was consistent with the presence of synaptic terminals in this region. Thicker labelled fibres of passage were found mostly around the oculomotor nucleus; that is not in VTA. Although it could be possible that some collateral of retrogradely label cells could be found, we almost did not find any retrograde labelled cells with BDA (which is sometimes both anterograde and to some extent retrograde) and found none with PHAL (almost exclusively anterograde). Moreover, labelled fibres contained varicosities and were arborized, keeping a consistent morphology of axon terminals and not collaterals (Haber et al., 2000). The size of the labelled fibres varied depending on the injection site; however the general overview showed short-medium labelled fibres segments. The number of anterogradely-labelled fibre segments in the contralateral midbrain represented barely 5 % of the number of labelled cells in the ipsilateral.

The projections within the VTA were characterized by broadly dispersed fibres mixed with clusters of denser labelling. The labelling was distributed mainly in the rostral half of the main VTA, while some labelling extended to the lateral PBP, and scarce to no labelling was seen in ventral PN or SN, with the exception of the SN pars compacta (SNc; Fig. 6) in a few cases (see below). There was no apparent medio-lateral variation in the abundance of labelling at single anteroposterior levels. There was however a dorso-ventral variation with no labelling in the ventral area confined to PN.

The abundance of labelling in VTA depended to some extent according to the exact position of the injection site within a given region. For example two injections place in BI (M7-98BDA and M1-95PHAL) produced labelling and no labelling, respectively, suggesting a complex internal topography. However, in general, the abundance of labelling mainly varied according to the localization of the injection site across the greater subdivisions HF or Amy. Most labelling in the VTA was obtained with injections made in the Basal nucleus, followed

by PL, PAC and the subicular complex. There was no labelling produced with injections in Amy's L and AB, in EC proper, or in the hippocampus with the exception of the Subiculum. In the following text we will describe the labelling from injections in Amy, EC and hippocampus, successively. When one injection included different areas of HF or EC but the same part of Amy, we compared them in terms of HF and EC.

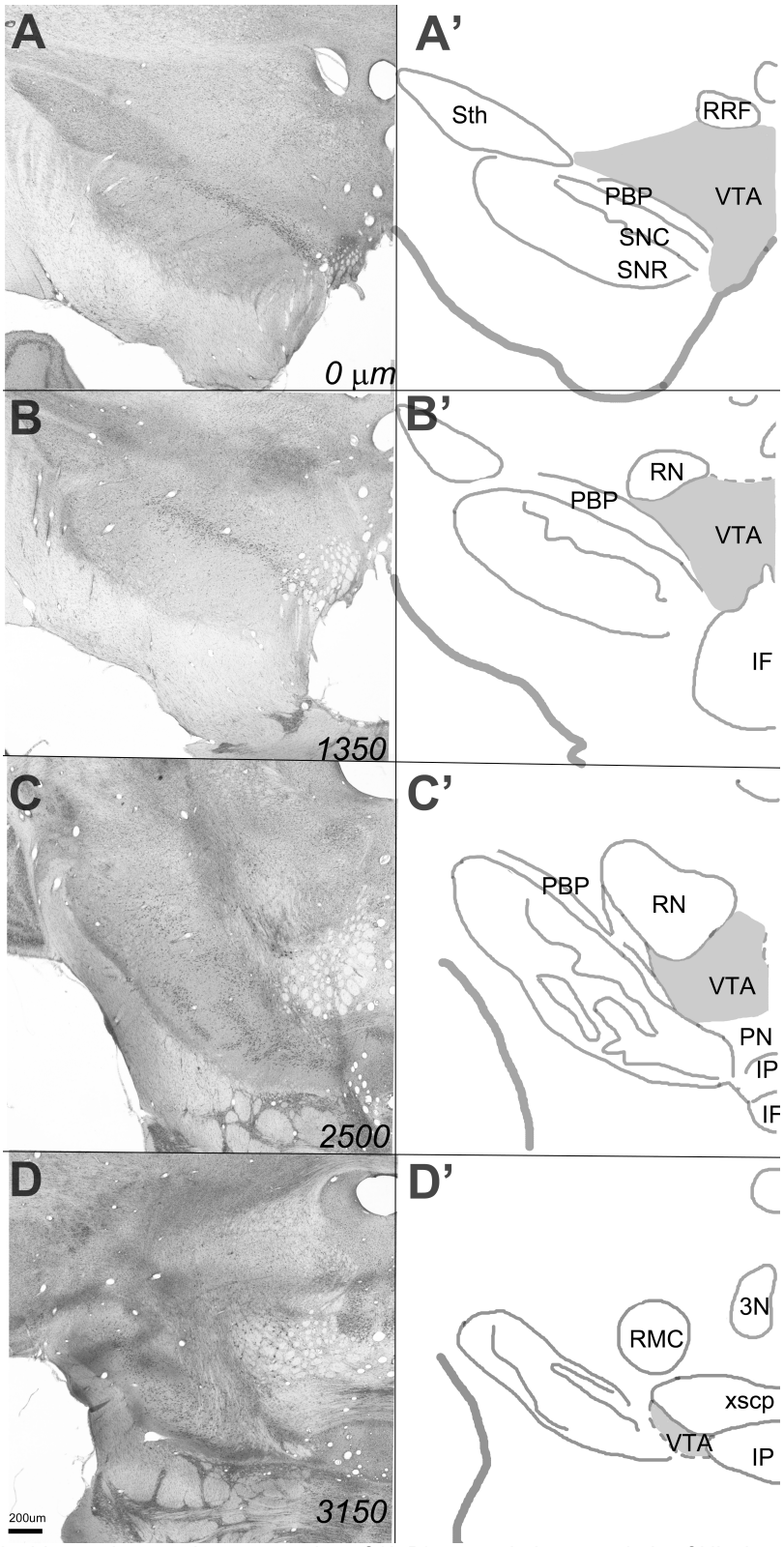

Figure 6. .Architectonic mapping on a series of (A-D) coronal photography's of Nissl and the corresponding drawing (A'-D') through the rostro-caudal axis of the VTA. STh: Hypothalamic nucleus; RRF: Retrorubral Field; PBP: Parabrachial Pigmentosus nucleus; SNC: Sustancia Nigra Compacta; SNR: Sustancia Nigra Reticulata; RN: Red nucleus; IF: Interpeduncular Fossa; IP: Interpeduncular nucleus; RMC: Red magnocellular nucleus; xscp: decussation. Scale bar 200um

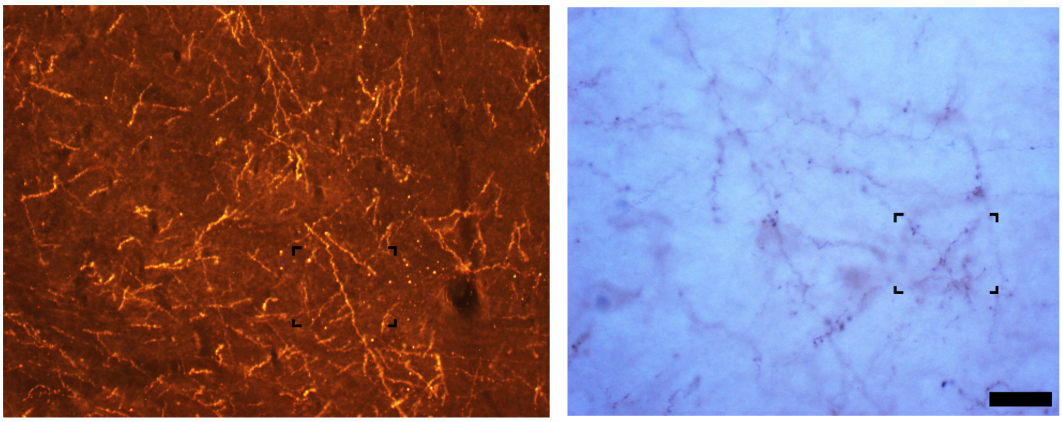

Figure 7. Photomicrographs showing examples of fibres bearing varicosities in VTA labelled with injections of BDA in the amygdala (A) and hippocampus (B). Scale bar= 1mm

Labelling from Amy injections.

Only the injections made in B and PL, and one small injection made in PAC did produce anterograde labelling in VTA (Fig. 2; filled ellipsoids). Despite repeated injections, none of the injections made in L, AB, or yet other parts of Amy produced labelling in VTA (Fig. 2; empty ellipsoids). Figure 8A-H shows the plots of anterogradely labelled fibres with varicosities in (dark red) and around (pink) VTA on consecutive coronal sections of the ventral midbrain in 8 representative cases in which an injection of BDA of PHA-L produced labelling. While labelling was obtained in several cases with injections in B, only 5 out of 15 injections in B produced labelling (Fig. 2). The three injections made in the dorsal most portion of Bmc all produced moderate labelling in VTA and in SNc (e.g., M1.03, Fig. 8A; M2-03, Fig. 8B). The more ventral injections (M4-90 and M5-95; Fig. 2) did not label VTA. Out of the 9 injections that touched Bi, only the two injections made in the centre (including one also spreading to Bmc) produced labelling in VTA (M3-95PHAL, Fig. 8E); his labelling was however scarce and mainly distributed in the lateral parts of the VTA. Only the one multiple injection (M3-95PHAL; Fig 8E) showed labelling in the VTA itself. In all cases however, the projections to the SN were very poor. None of the injections made only in Bpc showed labelling in the midbrain (M4-97BDA, M2-95PHAL; Fig. 2) but also the injections that included both Bpc and the ventral margin of Bi did not produce labelling (M11-98BDA and M2-98BDA), suggesting all together that Bpc does not project to VTA. Three out of 4 injections including PL produced labelling in VTA (M2-95PHAL; M3-98PHAL; M3-10BDA; Fig. 2 and Fig. 8G), suggesting that at least the central and medial parts of PL projects to VTA, or that the labelling originates from a subgroup of cells called the intermediate cells and that are mainly GABAergic and dispersed in between the PL and Bpc nuclei of Amy. Finally, none of the injections centred in L showed labelling in the midbrain even the ones that also

included other parts of the Amy (M5-97PHAL) (Fig. 2). Similar results were observed after single injections in ABpc (Fig. 2).

Figure 8. (A-O) Plot of anterograde labeling in the midbrain, after injections of tracers in Amy or HF.

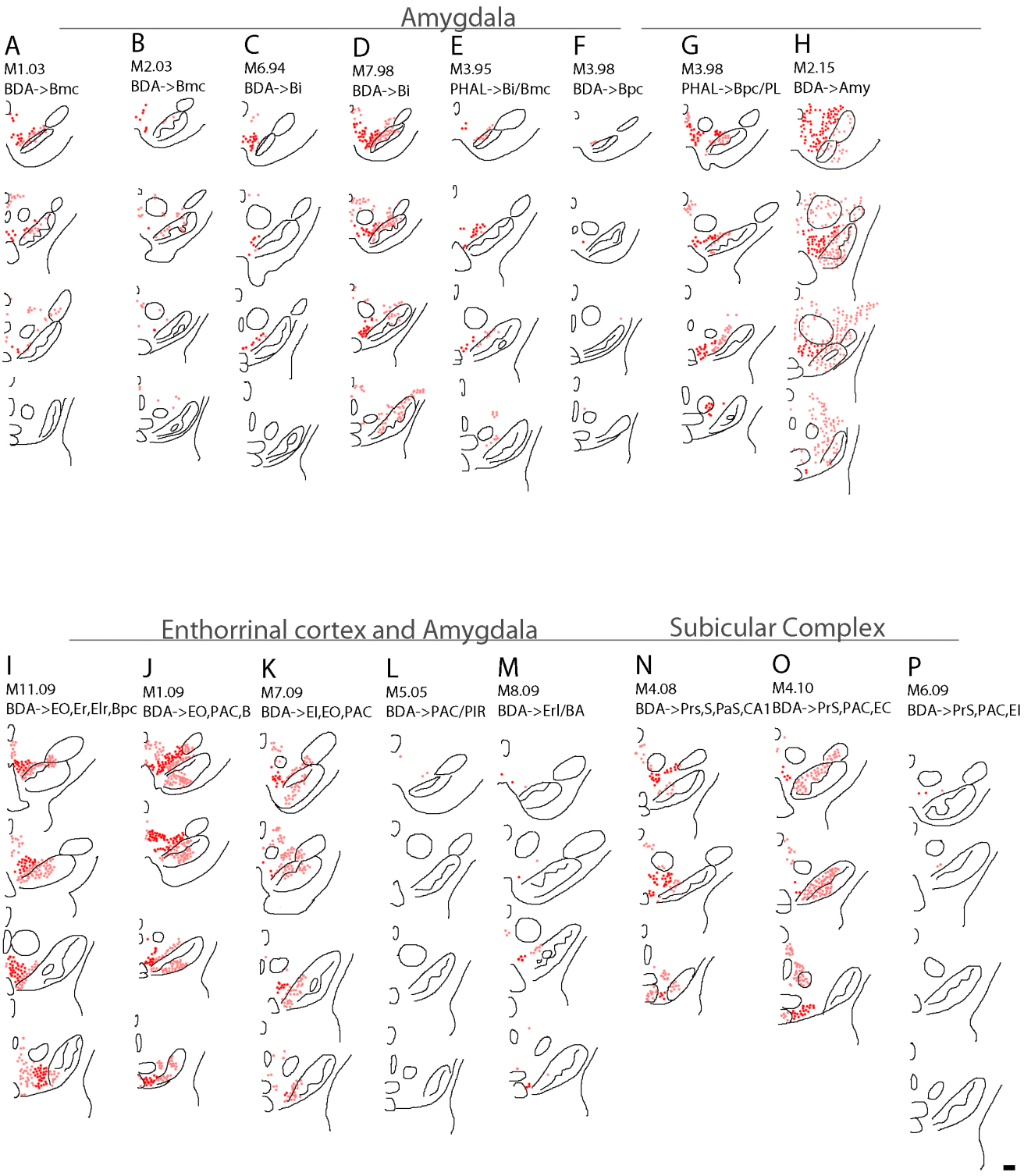

The dark red labeling corresponds to labeling in VTA. The pink labeling corresponds to labeling outside VTA. Scale bar= 1mm

Labelling from EC injections.

Among the different injections aiming EC, only the injections that spread to Amy or the Subiculum complex produced labelling in VTA (Fig. 3; Fig. 8 I-M). Injection M11-09BDA centred in E_r but spreading to other parts of the EC and Bpc produced strong labelling along the VTA that included several nucleuses (Fig. 8I). All injections made in E_o that spread to some parts of the Amy, including M1-09BDA, also produced a strong labelling in VTA and various other midbrain nuclei (Fig. 8J).

Sparse labelling was produced by an injection in E_o but with spread to PAC instead Bpc (M7-09BDA; Fig. 8K); supporting the prior observation that PAC contributes with less projections than Bpc (see above). All of the injections in E_o also spread to E_{LR} and/or E_i. However, none of the injections confined to these two EC regions produced labelling in VTA (e.g., M3-15BDA; Fig. 3). Like for E_o, only the injections in E_{RL} that spread to B (M8-09BDA) produced labelling in VTA (Fig. 8M); and one injection centred to E_l that spread to PAC and PrS also produced sparse labelling in VTA (M6-09BDA; Fig. 8P). However, none of the other injections in E_l that did not spread to Amy or HF produced labelling.

Particularly interesting is to compare the previous case mentioned before (M6-09BDA; Fig. 8P) with the case that also included PAC and PrS but E_c (M4-10BDA; Fig. 8O) that produced stronger labelling, suggesting that maybe E_c could project to VTA. However, one single injection placed in E_c that did not spread to PAC or PrS also did not produce labelling in the midbrain suggesting that the presence of fibres after larger injections in E_c were due to the PrS and/or PAC. Finally, none of the injections that included E_R, E_{Lc}or E_{CL} and that did not spread to Amy produced labelling.

Labelling from the hippocampus and Subiculum complex.

None of the injections confined to the different fields of the hippocampus proper produced labelling VTA. Only one injections that reached the Subiculum (M4-08; Fig. 4) produced moderate labelling in VTA, which is in agreement with the three cases in which labelling was produced in VTA likely because of the spread of EC-centred injections to PrS (see above and Fig. 8N-P).

Topographic distribution of the anterograde labelling

Only scant evidence or trends for a topographic were observed. For instance, in the Basal nucleus of the Amy we didn't found any topography since the density of the labelling within the Bmc changed substantially depending on the location of the injection. Moreover, one dual injection including Bmc but most of the Bi (M3-95PHAL) showed scarce labelling

mainly in the lateral portions of the VTA. Injections in PL (M3-98PHAL; M2-95BDA) produced moderate labelling in comparison with the ones mentioned before; in general this labelling was situated more into the medial than lateral parts of the VTA. One injection placed in B, without specify the subnucleus, PAC and some parts of EC (M1-09 BDA) showed the strongest labelling within the VTA with medio-lateral preference and with a presence all along VTA. However, this result is not conclusive due to the fact that we can't elucidate which area is the responsible for this projection. Three further injections that included PAC (M4-10BDA; M7-09BDA; M609BDA) showed labelling mainly in SN and some in the middle VTA, however, another injection placed in PAC (M12-91PHAL), showed no projections to the midbrain.

On the other hand, to estimate the overlap or the dispersion of the labelling produced in VTA with different Amy and HF injections; we examined dual cases, monkeys which had more than one injection with differently-coloured tracers. For example in case M2-03, injections placed in different parts of the Bmc (M2-03LBDA and M2-03RPHAL; see Fig. 2) showed that different parts of this subnuclei produced different amount of labelling (perhaps due to the different tracers) although in both cases the labelling was distributed all along the rostral and middle parts of the VTA, without apparent difference in distribution.

Retrograde labelling in HF and Amy

Figure 9-11 show plots of the retrograde labelling onto individual coronal maps of the medial temporal lobe passing through the ventral striatum in all three cases: M3-15FB (Fig. 9), M2-15FB (Fig. 10), and M9-09FB (Fig. 11). All cases showed labeling in the ventral striatum (data not shown) but only two of them showed labeling in Amy. Some isolated cells were found in the Basal, Lateral and Basal accessory nuclei cells, and a band of intercalated cells described before only from the injection placed in the rostral VTA (M3-15FB; Fig 9). Strong labelling also was found in the central, cortical and medial nuclei of the Amy from injections in the lateral VTA (M2-15FB; Fig 10). Only projections from the Subiculum and rostral entorhinal cortex showed projections, and therefore target the rostral VTA (M3-15FB; Fig 9). In contrast, caudal VTA (M9-09FB; Fig 11) showed scarce or no projections from the amygdalo-hippocampal complex, in agreement with the anterograde results observed above. However, projections from the striatum were found, but it varied greatly with the location of the injection site in VTA.

Rostral VTA.

The FB injection in rostral VTA in M3-15FB produced a relatively dense to moderate labelling in several distinct architectonic areas in the Amy. The pattern of labelling confirmed the anterograde labelling obtained in VTA with injections in the B nucleus and the Intercalated nuclei of the Amy Further projections were found arising from the Subiculum. These results confirm idea of “patchy” projections from the different subgroups of cells within the Amy.

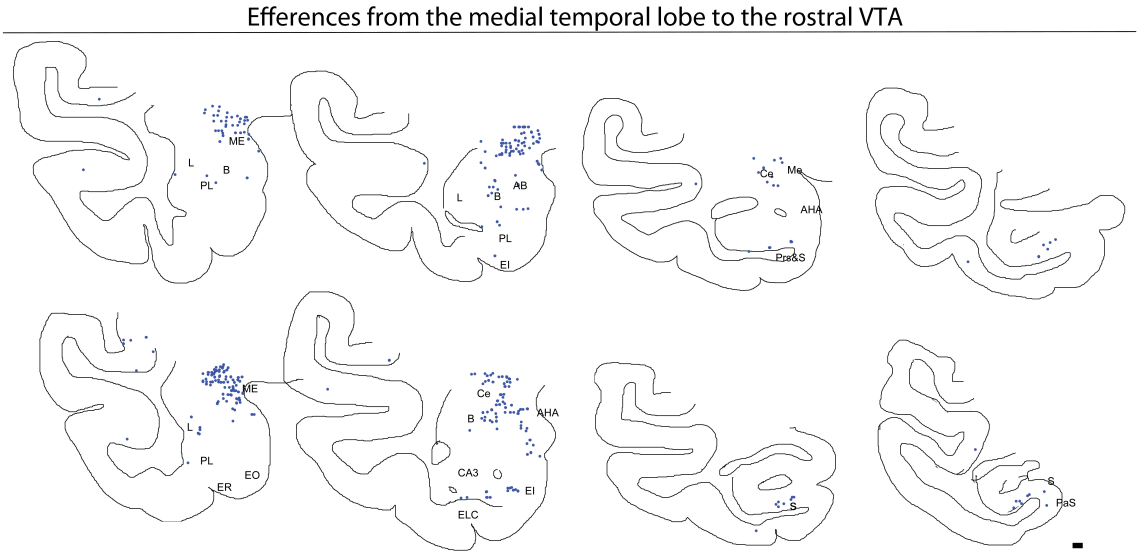

Figure 9: Plots of retrograde labeled cells in the HF and Amy from one injection placed in rostral VTA, case M3-15FB. The dots correspond to individual neurons labeled retrogradely within the medial temporal lobe. Scale bar = 1 mm

Lateral VTA.

The FB injection in lateral VTA in M2-15FB produced a relatively weak labeling in the Amy in similar architectonic areas than in case M3-15FB. The pattern of labeling confirmed the anterograde results obtained in VTA with injections in the B nucleus of the Amy. However, no projections were found from the HF suggesting that the targets to the different groups of the VTA could be topographically organized.

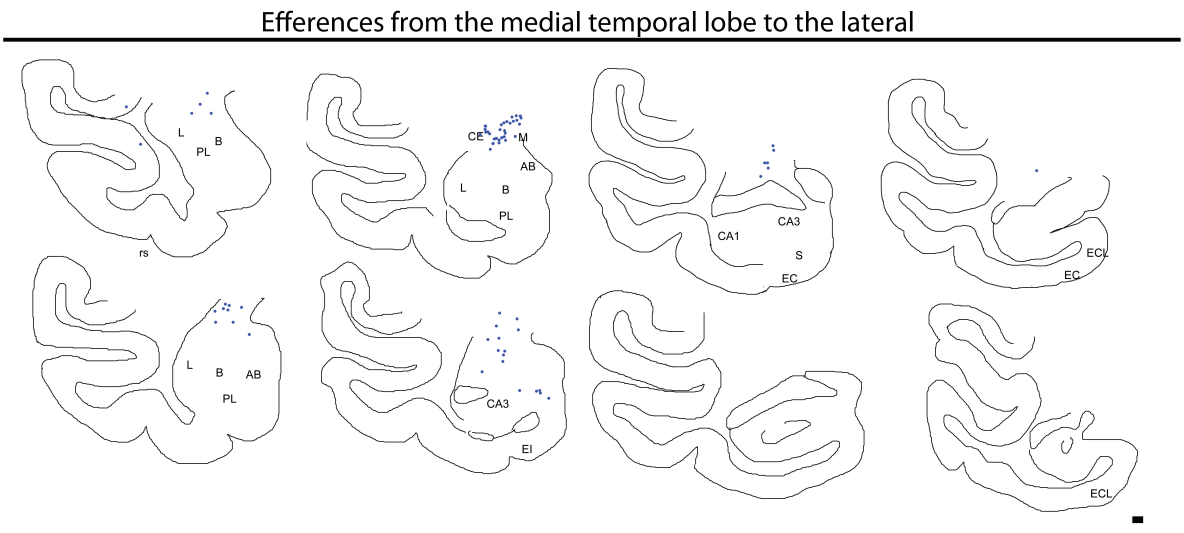

Figure 10: Plots of retrograde labelled cells in the HF and Amy from one injection placed in the lateral VTA, case M2-15FB. The dots correspond to retrograde labelling within the medial temporal lobe. Scale bar = 1 mm

Caudal VTA.

The FB injection in caudal VTA in M9-09FB produced a very scarce or no labeling in the Amy and HF, suggesting that the tail of the VTA might be modulated independently from the rostral and middle parts of the nucleus.

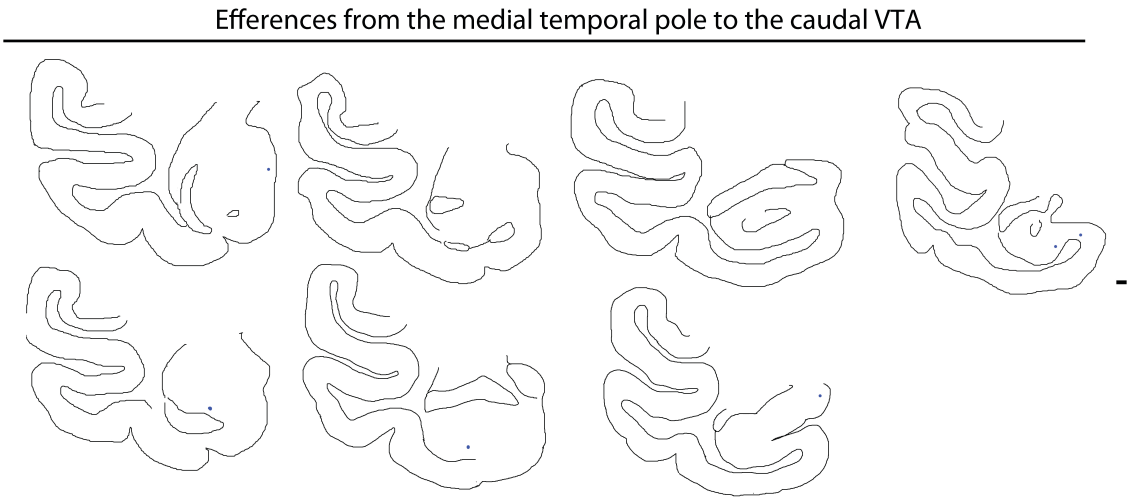

Figure 11: Plots of retrograde labelled cells in the HF and Amy from one injection placed in the caudal VTA, case M9-09FB. The dots correspond to retrograde labeling within the medial temporal lobe. Scale bar = 1 mm

DISCUSSION

Prior anatomical studies concluded that the main flow of information from Amy and HF to VTA goes through interposed nuclei (ventral pallidum, ventral striatum and medio dorsal nucleus of the thalamus) (Price et al., 2010). In the present study, we showed the existence of substantially less dense projection, than the classical mesolimbic pathway, but still very consistent direct monosynaptic projections to VTA from Amy nuclei other than CeA and from the Subiculum of the HF. In Amy, the projections generally originated from the basal nucleus with major internal variations possibly depending on the subgroup of cells implicated in the injection more than the subnuclei itself. The labelled fibres were distributed within the main VTA and in the lateral part (PBP) without any clear topography, although there was a preference for the anterior half of the VTA. In HF, the projections to rostral-middle VTA originated exclusively from the Subiculum. A careful differential analysis of the labelling produced by injections centred in other parts of HF (DG, CA1-3) and EC showed that none of these regions provides projections to the VTA Supporting this idea, studies carried out in rodents by Chandler et al., in 2014 demonstrated that the connections within the VTA are organized upon their different cell groups. Particularly, it has been found only labeled neurons in the rostral part of the VTA after placing retrograde tracers in a particular location of CA1, CA3 and DG (Swanson *et al*., 1982), and much more restricted projections from the caudal VTA (Schwab *et al*., 1978). This kind of topography is not apparent in the studies with retrograde tracers in the nonhuman primate (Amaral and Cowan, 1980; Insausti et al., 1987). However we propose a rough topography in anterograde tracer experiments in different parts of the Amy and HF.

The next paragraphs discus the present results in light of the organization of the classical polysynaptic pathways ending in VTA but also interconnecting the different structures considered in this study (e.g., HF with Amy); we indeed found that this prior anatomical insight and the models that they afforded provided the most powerful interpretational leverage for the present data.

Connections between HF and Amy

The interconnections between Amy and the hippocampus were shown by Amaral in 1986. AB and PAC have strong interconnection with CA1 and EC, Bpc with the DG/S and EC, Bmc only with EC, and L with PrS, PaS and EC. Years later Pitkänen et al. (2000) showed the topography of the connections between Amy and the different fields of EC. Injections made in Ld and Lv produced labelling all over EC except to E_{Lc} and E_c/E_{CL}. Particularly injections in Ld had more tendencies to project to E_O, E_R, and E_{lr} while Lv showed

more projections to E_R and E_I. Moreover, only injections placed in Bi/Bpc and Bpc/PL showed labelling in the E_O, E_R and E_{Lr}. Finally, the projections from the AB only rise to the E_O and E_R levels. Our results supports this idea by showing injections in Bpc/PL also produced labelling in the midbrain along with, maybe, the rostral parts of the EC (E_r and E_{Lr}), which, as we have described above, are also strongly interconnected with Bi/Bpc and PL. If the projections from E_r and E_{Lr} were true, this would suggest a possible pathway from a well-connected set amygdalo-hippocampus "partners" to the midbrain.

HF projections to VTA

So far, there exist no prior anatomical evidences of direct efferent projections from HF to the VTA. There is however one recent functional study that suggests a direct correlation between those structures (Khan et al., 2013). Earlier retrograde tracer studies in nonhuman primates suggested the existence of interconnections from the midbrain to the HF, particularly to Ammon's horn, DG, Subiculum and EC (mainly E_I and E_C) (Amaral *et al*., 1980; Insausti *et al*., 1987). In rodents, anterograde injections placed in VTA supported this idea by producing labelling in HF, particularly in the stratum oriens and molecular layer of the Subiculum, pyramidal and molecular layer of CA1, the stratum oriens of CA3 and DG (Gasbarri *et al*., 1994a). Going against the idea of reciprocal connection, our results indicate that only the Subiculum projects back to VTA.

It seems that the projections from HF are not homogeneous and arise with a particular inner topography. In 1998, Moser proposed a dorso-ventral organization within the HF in rodents, related to its inner interconnections (Swanson et al., 1977). Consistent with this idea, anatomical evidences found two performant pathways from the EC, one superior and one inferior that target the dorsal and the ventral hippocampus respectively (Fanselow et al., 2010) demonstrating that the different parts of the Subiculum might have also different interconnections. The distribution of the indirect, polysynaptic projections from the dorsal and ventral HF to the midbrain shows that the ventral hippocampus (ventral Subiculum) sends projections to VTA through the Nucleus Accumbens (NA). In parallel, the dorsal hippocampus (including CA3) sends projects to VTA, but via the Lateral Septum (Luo et al., 2011). Although in these studies did not show direct connections, they suggested the existence of topography within the Subiculum. Our results demonstrate direct projections from the Subiculum, but due to the fact that the labelling analysed here was produced with rather large injections in the Subiculum we cannot confirm the idea of the topography. Future smaller injections in different parts of this structure would be necessary to prove the topography and verify the existence of parallel pathways (direct and indirect) sharing a similar pattern of topographic organization.

Amy projections to VTA

Direct projections to the VTA from CE have been previously reported in primates, and additional projections from the ME, Co and BLA nuclei were also reported in rodents (Watabe et al., in 2012; Geiser et al., 2007). Our results show that other nuclei than CE project to VTA in the monkey. These projections come essentially from Bmc and PL, the former could correspond in part the rodent's BLA. Our study also suggests that the Amy projections are not homogeneous and arise only from particular sub-populations of projecting neurons. So far, this inhomogeneous topography has been only described for the CE, ME and stria terminalis without paying any particular attention to other parts of the brain (Price et al., 1981, Fudge et al., 2000 and 2001; Pardo et al., 2012). A review of the literature addressing the topographical organization of the Amy projections revealed that most of the neurons of origin of projections within Amy are organized in patches that have never been clearly reported or described in detail by the authors of these earlier studies. Although this patchy distribution has never been described so far (only illustrated in figures in prior papers), it is reminiscent of the patchy distribution of the Amy neurons retrogradely labelled from our injections of tracers in VTA in the present study. Identifying whether these groups of cells represent a particular class of Amy projecting neurons will be critical for our elucidation of the influence of Amy of limbic processes and on VTA.

We aimed at understanding the importance of the internal organization of the projections from different parts of Amy to the midbrain. Two main types of cells have been described in Amy: the principal (pyramidal) and secondary (inhibitory). The inhibitory cells are found mainly in PAC and Bmc, but not in PL and CE. They are mainly activated by pyramidal cells within the Amy more than from the projections from the BLA, and controlled by cortical inputs; it has been suggested that they could play a role in an inhibitory feedback loop (Smith et al., 2000). This loop is a neuronal system for adaptation to the environment in which the individual has to learn which stimuli are associated to a reward or punishment is more relevant described as sparse encoding. For one specific task, only few neurons from the population will respond to a given stimuli inhibiting the rest of the cells population in the heterogenic functional amygdala. As an example, complementary roles have been found between the B and CE during aversive stimuli and fear conditioning eliciting downstream tonic and phasic responses respectively (Knapsa et al., 2007). Another example hypothesize that phasic changes of the CE mediate tonic behaviour such as sexual and exploratory behaviours whereas plastic changes of the BLA enable phasic responses such as surveillance. It seems therefore, that the CE could enhance a tonic modulation of the VTA either by GABAergic inputs to the DA cells or through glutamatergic inputs to the GABAergic cells of the VTA to control salient behaviours. Since CE is not activated during fear

conditioning but it is the BLA, it would be really interesting to elucidate how they would regulate the behaviour dependent on the fear context.

Furthermore, despite most of the behaviours require some level of positive (reward) or negative (aversive stimuli) emotion to motivate a response, during contextual fear conditioning might also require some learning and therefore, it might be a feature in which DA midbrain neurons would sustain trough DA release the fear learning or to avoid it. Consistent with our hypothesis, in rats a disruption in the VTA and subsequently DA release has been shown to impair retrieval of previously learned fear conditioning (Nader and LeDoux, 1999, Ilango et al., 2012; Guarraci et al., 1999) highlighting the importance of direct connections within the VTA.

However, contradictory with the assumption that the DA would be released back into the Amy into CE nucleus, one of the main gateways of the Amy, studies in primates have shown that the major DA release targets are the magnocellular subdivisions of the B (Bmc) and BA (Cho et al., 2010) suggesting that the projections from the VTA to CE might be non-DA (Taylor et al., 2014). Other structures such as the M and PAC also receive projections but they are either less dense or scarce. Those observations suggest that the projections from the VTA to the Amy could be inhibitory and therefore end up the positive feedback loop of DA release into the cortex.

Along with HF, rodent BLA has been shown to play a role in the modulation of the long-term memory potentiation by emotional and motivational influence (Almaguer-Melian et al., 2003). Prior contributions proposed a polysynaptic model of projections from HF to VTA for the encoding of memory and learning (Lisman *et al.*, 2005; Lisman J, 2011). This model suggests that the connectivity within the HF-VTA circuit forms a loop in which the information about objects and their spatial location converges in EC via the perirhinal and parahippocampal cortices. Most of the stored information in the HF circuit goes through the perforant pathway, which includes many interposed structures. Inputs from layer II of the EC reaches the DG, and in step-wise fashion, to CA3-CA, where the information is compared with that arriving from layer III of the EC, and send from the S to the midbrain to enhance DA release in the VTA, and possibly memory consolidation. However, our results suggest a faster or more direct pathway from the S, presumably glutamatergic (Floresco et al., 2001; Legault et al., 2001) that receives direct inputs with novel information from the perirhinal (Kosel et al., 1983) and parahippocampal cortex (Witter et al., 2000). Another possible but not clearly supported source of projections would origin in the EC, presumably glutamatergic (Mooser et al., 2010) with spatial memory (along with the dorsal hippocampus (Tannenholz et al., 2014) (Mooser et al., 1993) that would pre-activate the VTA.

Technical limitations

The strength of the input to the VTA varied considerably across the injections from sparse to absent. Beside true anatomical variations, one of the reasons for this variation could be the viability of the PHAL injections in comparison with the BDA, and the different sizes of the injections. Another technical problem could be that some of the injections placed in EC may have not reached the deepest layers of EC, the output of the cortex and therefore from where the projections to VTA would depart (Sewards et al., 2003). Furthermore, despite our anterograde results, we observed retrograde labelled cells in the EC after placing injections within the VTA, because the FB tracer could label passing fibres, we cannot prove that those cells are projecting to the VTA. Moreover, because our study was aimed to understand subnuclei specific projections, we used small injections within the Amy, which some of them could have been too small or not reached enough principal cells to see projections in the midbrain. Despite these limitations, the high degree of reproducibility of the main data highlighted in this contribution using up to 87 injections of tracers in about 60 monkeys strongly support the viability and robustness of our finding of novel direct projections from specific parts of Amy and HF to VTA.

REFERENCES

Almaguer-Melian, W., Martinez-Marti, L., Frey, J. U., & Bergado, J. A. (2003). The amygdala is part of the behavioural reinforcement system modulating long-term potentiation in rat hippocampus. *Neuroscience*, *119*, 319-322.

Amaral DG, Cowan WM (1980). Subcortical afferents to the hippocampal formation in the monkey. J Comp Neurol. 189:573-91

Andy OJ, Stephan H (1968). The septum in the human brain. J Comp Neurol. Jul;133:383-410.

Aransay A, Rodríguez-López C, García-Amado M, Clascá F, Prensa L (2015). Long-range projection neurons of the mouse ventral tegmental area: a single-cell axon tracing analysis. Front Neuroanat. 9:59.

Blair HT, Schafe GE, Bauer EP, Rodrigues SM, LeDoux JE (2001) Synaptic plasticity in the lateral amygdala: A cellular hypothesis of fear conditioning. Learn Mem 8:229–242.

Brennan, P. A., & Kendrick, K. M. (2006). Mammalian social odours: attraction and individual recognition. Philosophical Transactions of the Royal Society B: Biological Sciences, 361, 2061-2078.

Canteras, N. S., Simerly, R. B., & Swanson, L. W. (1995). Organization of projections from the medial nucleus of the amygdala: a PHAL study in the rat. Journal of Comparative Neurology, 360, 213-245.

Canteras, N.S., and L.W. Swanson (1992) Projections of the ventral subiculum to the amygdala, septum, and hypothalamus: A PHA-L anterograde tract-tracing study in the rat. J. Comp. Neurol. 324: 180-194.

Chandler, D. J., Waterhouse, B. D., & Gao, W. J. (2014). New perspectives on catecholaminergic regulation of executive circuits: evidence for independent modulation of prefrontal functions by midbrain dopaminergic and noradrenergic neurons. Frontiers in neural circuits, 8.

Chareyron LJ, Banta Lavenex P, Amaral DG, Lavenex P (2011). Stereological analysis of the rat and monkey amygdala. J Comp Neurol. 519:3218-39.

Chergui K, Charléty PJ, Akaoka H, Saunier CF, Brunet JL, Buda M, Svensson TH, Chouvet G (1993). Tonic activation of NMDA receptors causes spontaneous burst discharge of rat midbrain dopamine neurons in vivo. Eur J Neurosci. 5:137-44.

Cho YT, Fudge JL (2010). Heterogeneous dopamine populations project to specific subregions of the primate amygdala. Neuroscience. 165:1501-18.

Eichenbaum, H., Yonelinas, A. R., & Ranganath, C. (2007). The medial temporal lobe and recognition memory. Annual review of neuroscience, 30, 123.

Fanselow, M. S., & Dong, H. W. (2010). Are the dorsal and ventral hippocampus functionally distinct structures?. *Neuron*, *65*, 7-19.

Floresco SB, Todd CL, Grace AA (2001). Glutamatergic afferents from the hippocampus to the nucleus accumbens regulate activity of ventral tegmental area dopamine neurons. J Neurosci. 21:4915-22

Floresco SB, West AR, Ash B, Moore H, Grace AA (2003). Afferent modulation of dopamine neuron firing differentially regulates tonic and phasic dopamine transmission. Nat Neurosci. Sep;6:968-73

Fudge JL, Haber SN (2000). The central nucleus of the amygdala projection to dopamine subpopulations in primates. Neuroscience.;97:479-94

Fudge JL, Haber SN (2001) Bed nucleus of the stria terminalis and extended amygdala inputs to dopamine.

Fyhn, M., Hafting, T., Treves, A., Moser, M. B., & Moser, E. I. (2007). Hippocampal remapping and grid realignment in entorhinal cortex. *Nature*, *446*, 190-194.

Gaffan, D., Murray, E. A., & Fabre‐Thorpe, M. (1993). Interaction of the amygdala with the frontal lobe in reward memory. European Journal of Neuroscience, 5, 968-975.

Gasbarri A, Packard MG, Campana E, Pacitti C (1994a). Anterograde and retrograde tracing of projections from the ventral tegmental area to the hippocampal formation in the rat. Brain Res Bull 33:445-52.

Geisler S, Derst C, Veh RW, Zahm DS (2007). Glutamatergic afferents of the ventral tegmental area in the rat. J Neurosci.27:5730-43.

Gibb, W. R., Mountjoy, C. Q., Mann, D. M., & Lees, A. J. (1989). The substantia nigra and ventral tegmental area in Alzheimer's disease and Down's syndrome. Journal of Neurology, Neurosurgery & Psychiatry, *52*, 193-200.

Guarraci, F. A., & Kapp, B. S. (1999). An electrophysiological characterization of ventral tegmental area dopaminergic neurons during differential pavlovian fear conditioning in the awake rabbit. Behavioural brain research, 99, 169-179.

Haber, S. N., Lynd, E., Klein, C., & Groenewegen, H. J. (1990). Topographic organization of the ventral striatal efferent projections in the rhesus monkey: an anterograde tracing study. *Journal of Comparative Neurology*, *293*, 282-298.

Hargreaves, E. L., Rao, G., Lee, I., & Knierim, J. J. (2005). Major dissociation between medial and lateral entorhinal input to dorsal hippocampus. *Science*, *308* (5729), 1792-1794.

Harris, G. C., Wimmer, M., Byrne, R., & Aston-Jones, G. (2004). Glutamate-associated plasticity in the ventral tegmental area is necessary for conditioning environmental stimuli with morphine. Neuroscience, 129, 841-847.

Holstege G, Meiners L, Tan K (1985). Projections of the bed nucleus of the stria terminalis to the mesencephalon, pons, and medulla oblongata in the cat. Exp Brain Res. 58:379-91.

Ilango, A., Shumake, J., Wetzel, W., Scheich, H., & Ohl, F. W. (2012). The role of dopamine in the context of aversive stimuli with particular reference to acoustically signaled avoidance learning. Frontiers in neuroscience, 6.

Insausti R, Amaral DG, Cowan WM (1987). The entorhinal cortex of the monkey: III. Subcortical afferents. J Comp Neurol. 264:396-408.

Janak, P. H., & Tye, K. M. (2015). From circuits to behaviour in the amygdala. *Nature*, *517*, 284-292.Ji, J., & Maren, S. (2008). Differential roles for hippocampal areas CA1 and CA3 in the contextual encoding and retrieval of extinguished fear. Learning & Memory, 15, 244-251.

Jin, Z., Bhandage, A. K., Bazov, I., Kononenko, O., Bakalkin, G., Korpi, E. R., & Birnir, B. (2014). Expression of specific ionotropic glutamate and GABA-A receptor subunits is decreased in central amygdala of alcoholics. Frontiers in cellular neuroscience, 8.

Johnson SW, Seutin V, North RA. (1992b) Burst firing in dopamine neurons induced by N-methyl-D-aspartate: role of electrogenic sodium pump. Science. 258:665-7

Jonas, P., & Lisman, J. (2014). Structure, function, and plasticity of hippocampal dentate gyrus microcircuits. Frontiers in neural circuits, 8, 107.

Kahn, I., & Shohamy, D. (2013). Intrinsic connectivity between the hippocampus, nucleus accumbens, and ventral tegmental area in humans. Hippocampus, 23, 187-192.

Kentner, A. C., Deslauriers, K., Parkinson, M., Fouriezos, G., & Bielajew, C. (2004). Interhemispheric involvement of the anterior cortical nuclei of the amygdala in rewarding brain stimulation. *Brain research*, *1003*, 138-150.

Kevetter, G. A., & Winans, S. S. (1981). Connections of the corticomedial amygdala in the golden hamster. II. Efferents of the “olfactory amygdala”.

Knapska, E., Radwanska, K., Werka, T., & Kaczmarek, L. (2007). Functional internal complexity of amygdala: focus on gene activity mapping after behavioral training and drugs of abuse. Physiological reviews, 87, 1113-1173.

Kosel, K. C., Van Hoesen, G. W., & Rosene, D. L. (1983). A direct projection from the perirhinal cortex (area 35) to the subiculum in the rat. Brain Research, 269, 347-351.

Krettek, J.E., and J.L. Price (1978a) Amygdaloid projections to suhcortical structures within the basal forebrain and brainstem in the rat and cat. J.Comp. Neurol. 178:225-254.

LeDoux JE, Cicchetti P, Xagoraris A, Romanski LM (1990). The lateral amygdaloid nucleus: sensory interface of the amygdala in fear conditioning. J Neurosci. 10:1062-9.

LeDoux, J. (2007). The amygdala. *Current Biology*, *17*, R868-R874.

Legault, M., & Wise, R. A. (2001). Novelty‐evoked elevations of nucleus accumbens dopamine: dependence on impulse flow from the ventral subiculum and glutamatergic neurotransmission in the ventral tegmental area. European Journal of Neuroscience, 13, 819-828.

Lisman, J. E., & Grace, A. A. (2005). The hippocampal-VTA loop: controlling the entry of information into long-term memory. Neuron, 46, 703-713.

Lisman, J., Grace, A. A., & Duze, E. (2011). A neoHebbian framework for episodic memory; role of dopamine-dependent late LTP. Trends in neurosciences, 34, 536-547.

Ljungberg T, Apicella P, Schultz W (1992). Responses of monkey dopamine neurons during learning of behavioral reactions. J Neurophysiol. Jan;67:145-63.subpopulations in primates. Neuroscience. 104:807-27.

Logothetis NK, Eschenko O, Murayama Y, Augath M, Steudel T, Evrard HC, Besserve M, Oeltermann (2010) A. Hippocampal-cortical interaction during periods of subcortical silence. Nature.

Luo AH, Tahsili-Fahadan P, Wise RA, Lupica CR, Aston- Jones G.(2011) Linking context with reward: a functional circuit from hippocampal CA3 to ventral tegmental area.Science. 333:353-7.

Majak, K., & Pitkänen, A. (2003). Projections from the periamygdaloid cortex to the amygdaloid complex, the hippocampal formation, and the parahippocampal region: A PHA‐L study in the rat. *Hippocampus*, *13*, 922-942.

Martig AK, Mizumori SJ (2011). Ventral tegmental area and substantia nigra neural correlates of spatial learning. Learn Mem. 18:260-71.

Millhouse, O. E. (1986). The intercalated cells of the amygdala. Journal of Comparative Neurology, 247, 246-271.

Moser E., Witter MP, Moser M-B (2010) Entorhinal cortex. In: Handbook of Brain Microcircuits. Shepherd GM, Grillner, S Eds. Oxford Univ Press, Oxford, UK pp175-192.

Moser, E., Moser, M. B., & Andersen, P. (1993). Spatial learning impairment parallels the magnitude of dorsal hippocampal lesions, but is hardly present following ventral lesions. The Journal of neuroscience, 13, 3916-3925.

Moser, M. B., & Moser, E. I. (1998). Functional differentiation in the hippocampus. Hippocampus, 8, 608-619.

Murray, E. A. (2007). The amygdala, reward and emotion. Trends in cognitive sciences, 11f, 489-497.

Nader, K., & LeDoux, J. (1999). Inhibition of the mesoamygdala dopaminergic pathway impairs the retrieval of conditioned fear associations. Behavioral neuroscience, 113, 891.

Pardo-Bellver C, Cádiz-Moretti B, Novejarque A, Martínez-García F, Lanuza E (2012) Differential efferent projections of the anterior, posteroventral, and posterodorsal subdivisions of the medial amygdala in mice. Front Neuroanat. 6:33.

Pitkänen A, Kemppainen S (2002). Comparison of the distribution of calcium-binding proteins and intrinsic connectivity in the lateral nucleus of the rat, monkey,and human amygdala. Pharmacol Biochem Behav. Mar;71:369-77. Review.

Pitkänen, A., Pikkarainen, M., Nurminen, N., & Ylinen, A. (2000). Reciprocal connections between the amygdala and the hippocampal formation, perirhinal cortex, and postrhinal cortex in rat: a review. Annals of the New York Academy of Sciences, 911, 369-391.

Price JL, Russchen FT, Amaral DG. (1987). The limbic region. II. The amygdaloid complex. In: Bjorklund A, Ho¨kfelt T, Swanson LW, editors. Handbook of chemical neuroanatomy. vol.5. Integrated systems of CNS. Part I. Amsterdam: Elsevier. p 279–388.

Price, J. L., & Amaral, D. G. (1981). An autoradiographic study of the projections of the central nucleus of the monkey amygdala. The journal of Neuroscience, 1, 1242-1259.

Price, J. L., & Drevets, W. C. (2010). Neurocircuitry of mood disorders. Neuropsychopharmacology, 35(1), 192-216.

Rauch, S. L., Shin, L. M., & Wright, C. I. (2003). Neuroimaging studies of amygdala function in anxiety disorders. Annals of the New York Academy of Sciences, 985, 389-410.

Rossato, J. I., Bevilaqua, L. R., Izquierdo, I., Medina, J. H., & Cammarota, M. (2009). Dopamine controls persistence of long-term memory storage. Science, 325, 1017-1020.

Russchen FT (1982). Amygdalopetal projections in the cat. II. Subcortical afferent connections. A study with retrograde tracing techniques. J Comp Neurol. 207:157-76.

Schwab, M. E., Javoy-Agid, F., & Agid, Y. (1978). Labelled wheat germ agglutinin (WGA) as a new, highly sensitive retrograde tracer in the rat brain hippocampal system. Brain research, 152, 145-150.

Sesack, S.R., A.Y. Deutch, R.H. Roth, and B.S. Bunney (1989) Topographical organization of the efferent projections of the medial prefrontal cortex in the rat: An anterograde tracct-tracing study with Phaseolus vulgaris leucoagglutinin. J. Comp. Neurol. 290:2 13-242.

Sesack, S. R., & Grace, A. A. (2010). Cortico-basal ganglia reward network: microcircuitry. Neuropsychopharmacology, 35, 27-47.

Sewards, T. V., & Sewards, M. A. (2003). Input and output stations of the entorhinal cortex: superficial vs. deep layers or lateral vs. medial divisions?. Brain Research Reviews, 42, 243-251.

Smith, Y., Paré, J. F., & Paré, D. (2000). Differential innervation of parvalbumin-immunoreactive interneurons of the basolateral amygdaloid complex by cortical and intrinsic inputs. Journal of Comparative Neurology, 416, 496-508.

Stephan H, Andy OJ (1977). Quantitative comparison of the amygdala in insectivores and primates. Acta Anat (Basel). 1977;98:130-53.

Strange, B. A., Witter, M. P., Lein, E. S., & Moser, E. I. (2014). Functional organization of the hippocampal longitudinal axis. Nature Reviews Neuroscience, 15, 655-669.

Swanson, L. W. (1982). The projections of the ventral tegmental area and adjacent regions: a combined fluorescent retrograde tracer and immunofluorescence study in the rat. Brain research bulletin, 9, 321-353.

Tannenholz, L., Jimenez, J. C., & Kheirbek, M. A. (2014). Local and regional heterogeneity underlying hippocampal modulation of cognition and mood. Frontiers in behavioral neuroscience, 8.

Turner BH, Mishkin M, Knapp M (1980). Organization of the amygdalopetal projections from modality-specific cortical association areas in the monkey. J Comp Neurol. Jun 15;191:515-43.

Van Hoesen G, Pandya DN (1975). Some connections of the entorhinal (area 28) and perirhinal (area 35) cortices of the rhesus monkey. I. Temporal lobe afferents. Brain Res. Sep 12;95:1-24.

Watabe-Uchida M, Zhu L, Ogawa SK, Vamanrao A, Uchida N (2012). Whole-brain mapping of direct inputs to midbrain dopamine neurons. Neuron. Jun 7;74:858-73.

Witter, M. P., Naber, P. A., van Haeften, T., Machielsen, W. C., Rombouts, S. A., Barkhof, F., ... & Lopes daSilva, F. H. (2000). Cortico-hippocampal communication by way of parallel parahippocampal-subicular pathways. Hippocampus, 10, 398-410.

VII. CONCLUSIONS

VII. CONCLUSIONS

1. Our results show that the *Locus coeruleus* in macaque monkey receives direct input from higher cognitive centers and limbic structures such as subiculum, amygdala, prefrontal cortex, and anterior insula. These projections target the core of the *Locus coeruleus* and are topographically organized within the nucleus.
2. The subiculum is the region of the hippocampal formation that sends the most of the projections. The entorhinal cortex might participate too, but more studies would be needed in order to confirm this projection.
3. The subiculum projects to the lateral part of the core of the *Locus coeruleus*, mostly to the rostral portion of the nucleus. Some scattered labeled axons are also distributed through the caudal extension of the nucleus.
4. Our data show that, other than the central nucleus of the amygdala, the *Locus coeruleus* receives inputs from the basal and the paralaminar nuclei.
5. Within the basal nucleus, the magnocellular division projects more than the intermediate or the parvocellular divisions. Interestingly, injections located within the same nucleus but involving different groups of neurons produced different pattern of projections, or no projection at all.
6. Subiculum and amygdala send their projections to the rostrolateral part of the *Locus coeruleus*. This suggests that the *Locus coeruleus* might have a role in modulation of memory processing under emotional conditions.
7. The current results show the existence of direct top-down projections from the medial and orbital prefrontal cortices to the core of *Locus coeruleus*. Limbic agranular and dysgranular areas (Iam, 13, 32, 24 and 25) send stronger projections than the granular areas, and directly innervate the densest part of the nucleus. This suggests a direct potent modulatory influence on the activity of the *Locus coeruleus*.
8. The areas in the prefrontal cortex that are strongly interconnected with the *Locus coeruleus* also receive strong projections from the deep layers of the entorhinal cortex. The coeruleo-cortical circuit could have a crucial role in the noradrenergic/dopaminergic modulation of memory processing in primates.

CONCLUSIONES (SPANISH)

1. Nuestros resultados muestran que el Locus coeruleus en macaco recibe proyección directa de centros cognitivos superiores y estructuras límbicas como subículo, amígdala, corteza prefrontal e ínsula anterior. Estas proyecciones llegan directamente a la parte más densa del núcleo y se organizan topográficamente dentro del mismo.
2. El subículo es la región de la formación del hipocampo que envía la mayor parte de las proyecciones. La corteza entorrinal podría participar también, pero se necesitan más estudios para confirmar esta proyección.
3. El subículo proyecta a la parte lateral de la zona más densa del Locus coeruleus, mayoritariamente a la parte rostral del núcleo. También se han encontrado axones marcados dispersos en la parte caudal del núcleo.
4. Nuestros datos muestran que, a parte del núcleo central de la amígdala, el Locus coeruleus recibe proyección de los núcleos basal y el paralaminar.
5. Dentro del núcleo basal de la amígdala, la división magnocelular envía una proyección más densa que la división intermedia o parvocelular. Además, resulta interesante destacar que inyecciones muy próximas entre sí, localizadas dentro de una misma división del núcleo basal de la amígdala, pero involucrando diferentes grupos de neuronas, producen un patrón diferente de proyección o no proyectan en absoluto.
6. Tanto subículo como amígdala envían sus proyecciones a la parte rostrolateral del Locus coeruleus. Esto sugiere que el Locus coeruleus podría participar en la modulación del procesamiento de la memoria bajo un contexto emocional.
7. Nuestros resultados muestran la existencia de proyección directa desde la corteza prefrontal medial y orbital, así como desde la ínsula anterior. Áreas límbicas agranulares y disgranulares (Iam, 13, 32, 24, 25) proyectan más densamente que las áreas granulares, e inervan directamente la parte más densa del núcleo. Esto sugiere que una potente influencia moduladora de la actividad del Locus coeruleus.
8. Las áreas de la corteza prefrontal que están fuertemente interconectadas con el Locus coeruleus, también reciben una fuerte proyección de las capas profundas de la corteza entorrinal. Así pues, el circuito coeruleo-cortical

podría tener un papel crucial en la modulación noradrenérgica/dopaminérgica del procesamiento de la memoria en el primate.